Surface Temperature Excess in Heterogeneous Catalysis

Zhu, Lianjie

Surface Temperature Excess in Heterogeneous Catalysis

Proefschrift

ter verkrijging van de graad van doctor
aan de Technische Universiteit Delft,
op gezag van de Rector Magnificus Prof. dr. ir. J.T. Fokkema,
voorzitter van het College voor Promoties,
in het openbaar te verdedigen op woensdag 16 november 2005 om 13:00 uur

door

Lianjie ZHU

Master of Science in Physical Chemistry,
Jilin University, Changchun, P.R. China

Geboren te Beizhen, P.R. China

Zhu, Lianjie
Surface Temperature Excess in Heterogeneous Catalysis
Ph.D Thesis, Delft University of Technology

To my dear parent,
husband Zhaomin,
& sisters

Contents

Chapter 1

Catalysis: homogeneous & heterogeneous

1.1 Catalysis

A catalyst is a substance that changes the rate of a chemical reaction but does not influence the thermodynamic equilibrium between the reactants and products. The catalyst changes the rate of the reactions between reactant and product molecules in the forward and reverse direction by the same factor. As a consequence, the equilibrium constant K of the overall reaction remains unchanged when a catalyst is involved to improve the reaction rate or the selectivity of the chemical process:

$$K = \frac{k_f}{k_r} = \frac{k_f^{'}}{k_r^{'}} \tag{1.1}$$

The primed rate constants in this equation are those in the presence of a catalyst. The action of the catalyst (a molecule or a site in a surface) is that it engages in the reaction by forming a temporary bond with one or more of the reactant molecules. By this, it alters the pathway that the reaction follows. On this pathway (the "reaction coordinate") there exists always one moment in which the complex of reactant, solvent and catalytic molecules has its maximum potential energy. This energy is, basically, what Arrhenius [1] called the Activation Energy E_a in his thermochemical treatment of reaction kinetics. The theory of absolute reaction rates (Eyring's "Transition State Theory" [1, 2, 3]) says, that this maximum determines the overall rate of the chemical reaction. If the maximum on the path, which involves the catalyst turns out to be lower than that on the path without it, the catalyzed reaction is faster.

For homogeneous catalysis, the catalyst is in the same phase as the reactants and participates in the reaction directly. The reaction takes place at the local temperature in the continuous medium. However, in heterogeneous catalysis, the catalyst and reactants are in different phases. Most heterogeneous catalysis is in gas-solid and liquid-solid systems. The catalyst is often the solid material, the reactants are (dissolved in) gases or liquid media. The catalyzed reactions take place between adsorbed reactant molecules. These reactants have formed a complex of some sort with active sites in the catalyst surface, *i.e.* it is the interface between the catalyst and the medium which contains both the reactants and the catalytic sites, and where the reaction takes place.

In such a heterogeneous reaction process there are several different temperatures to consider: not only those of the two phases (medium and catalyst), but also the temperature in the interface where the catalyzed reaction takes place. The temperature in the interface T^r can be the same as the temperatures T^m of the (metal) catalyst and T^g, of the surrounding (gas or liquid) medium. But that is not necessarily always the case, depending on the rates of heat generation and thermal conductivity of the materials.

If these three temperatures are different there are temperature gradients and heat fluxes in the system. This brings more difficulty to the kinetics study of heterogeneous catalysis, but this can also make the results of such studies more interesting. The differences between T^r, T^m and T^g determine the dissipation rate of the reaction enthalpy, which is set free by the chemical process. Moreover, as we shall see, that could affect the selectivity of specific heterogeneous catalysts in consecutive or parallel chemical reactions. Selectivity is a subject of great importance in industrial catalysis. Heterogeneous catalysis is extensively applied in the chemical and oil industries. These represent 20-30% of global GNP annually.

In practice, thermochemical reaction kinetics is helpful for optimization of the operation conditions in industries. As a science it was founded by Arrhenius and van 't Hoff, around 1900. Their theories allow characterization of catalysts so as to improve catalysts or design new catalysts. The activity of the catalyst can be guessed in terms of the rate constant. The activation energy of the catalytic reaction can be used to identify differences between active sites, *etc.* That is why kinetics for heterogeneous catalysis is so important in both academic and industrial laboratories. An enormous research on this subject is going on today.

It is a technological application of Arrhenius' early ideas on reaction rates of individual reactions in chemical engineering that, for two parallel reactions with different activation energies in the same reaction medium (*e.g* in a CSTR), the reaction rate

with higher activation energy should increase faster with temperature than the other. Therefore, the selectivity of the process can be optimized by picking the optimal reaction temperature. But then, in a model of heterogeneous catalysis, would this have to be the optimum value of T^r, T^m or T^g?

Around 1995, a Delft PhD student, Matthijs Soede [4], investigated the partial hydrogenation of benzene and other aromatics with ruthenium metal catalysts. Carefully measuring the relevant data he constructed a model for this reaction and for the mass transfer of reactants and products between the different phases in the reactor. Using his kinetic model he studied the selectivity of cyclohexene formation, which, contrary to his expectations, responded erratically to very small changes in the reactor temperature. He found that during hydrogenation of bezene the catalyst surface temperature is increased due to the surface reactions. The increased surface temperature changed the selectivity and yield of one of the products, cyclohexene. Because of large heats released by the surface reactions and limitations of transport, a temperature gradient is created in the stagnant fluid layer between catalyst surface and the bulk fluid. The temperature difference can be up to 10-15 K. The surface temperature influences the adsorption of the reactants and the rate constant significantly. For a parallel or consecutive reactions with different activation energies, with increasing temperature the reaction rate with higher activation energy increases faster than the others. Therefore, the selectivity of this reaction is increased. He concluded (*l.c.* page 156 [4]):

"Finally, it will be very important to investigate the influence of the temperature on the cyclohexene selectivity, and as a consequence also the heat transfer effects. It is remarkable that the cyclohexene selectivity increases when the hydrogen pressure is raised.... An increased cyclohexene desorption rate is established by an increase of the temperature of the catalyst particle, but, to the best of our knowledge, this explanation has never been observed earlier in slurry-phase reactions. Probably, the heat transfer coefficients are clearly underestimated. Nevertheless, the heat effects during the benzene hydrogenation reaction is a point of concern (about our kinetic model) and further research on this topic is necessary."

Indeed, one must reckon with considerable temperature gradients and temperature effects in this type of catalytic reaction. Relatively high temperature gradients could locally develop near the interface, because of the limitations in heat transport in the multiphase medium and the large amounts of heat, released by the catalytic surface reactions. But it remains a theoretical puzzle why Soede's observations on cyclohexene selectivity would predict reaction temperatures of up to 15 K higher (*l.c.* page 147 [4]) on the basis of the model [5], than the experimentally measured temperatures in

his reactors. Further research on this topic is indeed necessary!

Already for decades, many researchers have focussed their investigations on the temperature of active catalyst surfaces because of their importance on kinetic studies, catalyst activity and selectivity *etc.* As early as 1962, Yoshida *et al.* [6] have used numerical and graphic methods to estimate the temperature drops in a gas film next to the catalyst surface. It was found that even if the main gas stream was kept isothermal, the reaction that took place at the surface was not isothermal at all. In the case of high reaction rates and low mass velocities the temperature drops across the gas film could amount to a few hundred degrees. This led to establishing new sets of constants in kinetic models and reaction rates, using surface conditions instead of average reactor temperatures as a starting point. Later on, Cardoso and Luss [7] studied how a surface temperature depends on the reactant concentration and mass velocity. Wu *et al.* [8, 9] investigated the influence of catalyst surface temperature in calculations of catalyst effectiveness factors and reaction rates. Basile *et al.* [10, 11] observed that at very short residence times (high flow rate) relatively large temperature gradients (50-220 K) could develop in the solid-gas interphase around hot spots. This suggested heat transfer limitations: large amounts of heat produced by the exothermic reactions in combination with a low efficiency in the heat transfer through the interphase.

Basile explained these temperature differences between the solid catalyst and the gaseous reactant medium phase by considering that:

(a) Chemical reactions are largely confined to the gas-solid interface;

(b) The solid absorbs the reaction heat much better than the gas phase. Therefore he suggested that the solid can store excess enthalpy because of its high ability for heat absorption (heat capacity) compared to gases.

The excess enthalpy at the interface would then probably be responsible for the high reaction rates in moderate reactor conditions. That excess enthalpy is stored in the solid/gas interphase had originally been proposed by Weinberg and Lloyd in 1970's [12, 13].

By considering intra-particle and inter-particle transport limitations, chemical engineers have derived and discussed temperature differences between bulk fluid, catalyst surface, and catalyst interior [14, 15, 16, 17, 7]. Strategies have been devised to ensure that the largely uncontrollable effects of these temperature gradients on the observed reaction rates remain negligible [18, 19] in technological processes.

Meanwhile, in a separate development of thermodynamic theory Bedeaux and Kjelstrup derived that the coupling of flows in interfaces could be a cause for steep temperature jumps across the interface itself [20, 21, 22]. In macroscopic, three dimensional media such a coupling of processes with different vectorial characteristics

is forbidden by the Curie-Prigogine principle. But the two-dimensional character of the interface can lift this ban on the coupling of heat flows and conversion reactions in heterogeneous catalytic systems. Using irreversible thermodynamics, Bedeaux [23] gave a complete description for the thermal conditions in an interface during phase transitions. With Kjelstrup he also used this approach to investigate the thermal behaviour of electrode-electrolyte surfaces in solid oxide fuel cells.

Inspired by these authors, and intrigued by their novel results, we decided to apply the methods of irreversible surface thermodynamics to heterogeneous catalytic systems. The objective was to model the three distinct temperatures and analyze their effects on the effective temperature in the catalytic reaction at the catalyst surface. The temperature gradient between the catalyst and the medium $(T^m - T^g)$ is responsible for the transfer of the reaction heat to the reactor ambient. This temperature difference could, under circumstances, be coupled with mass transfer in a Dufour or Soret effect and give unexpected rates in transport limited reaction systems. But could a coupling between a conversion process and a thermal effect in the reaction interface itself generate a difference between the temperatures T^m and T^r, and express itself directly in kinetically controlled catalytic processes by anomalous effects in the Arrhenius equation?

In many practical situations the temperature differences between a catalyst surface and a liquid medium will remain small because the thermal conductivity is large. Therefore these differences have been generally neglected in catalytic studies on heterogeneous solid/liquid systems. However, with gases as the ambient medium, temperature differences as large as 100 K have been reported, because of the poor thermal conductivity of the gaseous phase. With these large temperature differences we have the advantage, that experimental errors in modelling or calculations remain relatively small. And indeed, considerable data are available on well executed and thoroughly analyzed experiments with heterogeneous gas-solid catalytic systems, which have been intensively used in careful kinetic studies. That is why we have selected two gas-solid systems to serve as model examples for our description of "anomalous" temperature effects in heterogeneous catalysis. One is a transport limited process. The other rate is kinetically controlled by the catalytic conversion reaction itself.

Data on hydrogen oxidation reactions, catalyzed by metal-support catalysts will be used in the first part of this thesis to demonstrate the effects of couplings between heat and mass fluxes in transport limited surface reactions. In the second part we discuss the oxidation of carbon monoxide as a kinetically controlled catalytic process and study the effects of coupling between conversion rates and thermal fluxes in the two-dimensional reaction plane in which a heterogeneous reaction does take place at

a catalytic surface.

The principle of the heterogeneous catalytic reaction cycle is shown in figure 1.1.
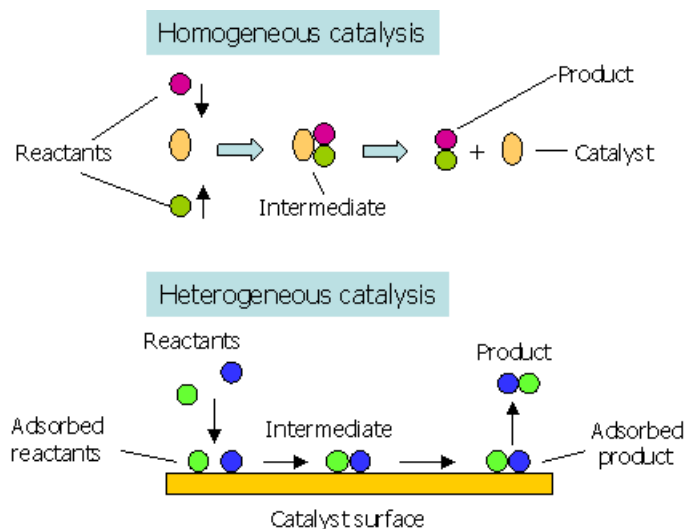
Figure 1.1: Schematic diagram of the reaction pathes in homogeneous & heterogeneous catalysis

In the first place, figure 1.1 illustrates that the involvement of a catalytic surface in the reaction changes the pathway. A number of extra steps (elementary reaction steps) is introduced when reactants A and B must first engage in the formation of an adsorbed complex at the active site of the surface. The reactants first have to adsorb on the catalyst and approach each other before they can form the intermediate which will eventually decompose into the products and the catalyst's active site.

The product molecules finally desorb from the surface and diffuse away into the medium. This transport to and from the interface because of adsorption and desorption is described by mass transfer theory in the pertinent media. It is obvious that there would be severe problems with mass transfer as a rate limiting factor if the solvent medium for the products or the reactants is a solid.

Chorkendorff and Moulijn *et al.* [24, 25] have even considered the proposition that the kinetics of a catalytic reaction at an interface can seldom be described by one single elementary reaction step. The adsorption mechanism must be brought into account as an essential aspect in heterogeneous catalysis, both as a possibly rate limiting factor and because of the energy which is involved in the adsorption of the reactants from the non-catalytic medium.

The intermediate complex of the reactants with the active site on the catalyst sur-

face does only exist in a two-dimensional surface. Its concentration (surface coverage) and other physical properties, such as heat capacity, thermal conductivity *etc.* are completely different from those in the bulk phase. We shall have to describe this in a satisfactory way when we make a quantitative model for a heterogeneous catalytic surface reaction.

1.2   Chemical kinetics

Chemical kinetics investigates rates of chemical reactions and deduces reaction mechanisms from the sensitivity of the reaction rate for changes in reactant concentration, for changes in the reaction temperature and for the catalytic effects of extra solutes or surfaces which are present in the reaction system. The expression

$$\frac{d\xi_i}{dt} = k[\text{A}]^{\text{a}}[\text{B}]^{\text{b}} \tag{1.2}$$

describes the rate of change in the extent of the reaction $d\xi_i/dt = (1/\nu_a)(d\,[\text{A}]\,/dt)$ of the process $\nu_a\text{A}+\nu_b\text{B}\rightarrow x\text{X}+y\text{Y}$. The factors [ ] indicate reactant concentrations. The exponents a and b in equation (1.2) are "reaction orders", which describe the sensitivity of the reaction rate for each separate reactant concentration. The factor k is the "rate constant" which was introduced by Arrhenius. It describes the relation of the rate with the reaction temperature.

The structure of a rate constant k is expressed by Arrhenius' equation

$$k = A\exp(\frac{-E_a}{RT}) \tag{1.3}$$

It combines an exponential - which compares the activation energy E_a with the thermal equipartition energy $\mathbf{k}T$ at the reaction temperature and a pre-exponential factor. This pre-exponential factor A takes care of dimensionality and of collision probabilities between reactant molecules in the experimental conditions. The activation energy E_a is obtained from experimental data by plotting the logarithm of the experimental rate as a function of the measured values of the reciprocal temperature $1/T$. This leads to a so called Arrhenius plot.

Arrhenius proposed all this in 1889, and reckoned that E_a and A would be characteristic constants for a reaction. According to Arrhenius' equation the reaction rate increases exponentially with the reaction temperature. Therefore, small changes in temperature can influence the reaction rate considerably. Experimentally, the activation energy E_a and the pre-exponential factor A do not change very much with the temperature over a relatively large range, like 500 K [26]. The Arrhenius plot is then

a straight line over that whole interval of experimental conditions.

Arrhenius himself did not provide a model for A and E_a. It was Henry Eyring, who later on developed the "transition state theory" for that purpose. His "Theory of Rate Processes", as the original publication was called [27], gives an expression for A and a physical meaning for E_a. But these two quantities themselves are not physical constants. They remain experimental observables in the kinetics of a reaction system. The parameters A and E_a may or may not be constant, depending on reaction conditions like the temperature and the reactant concentrations.

Individual elementary reaction steps generally follow Arrhenius law. But sometimes overall reaction rate for processes that include more than one elementary step complicate the situation. The rate determining mechanism may change from one reaction step into another, dependent on the temperature. This leads to a curved Arrhenius plot in the interpretation of the results. The experimental E_a can then only be an apparent activation energy, which reflects the transition of one rate limiting step to another as a consequence of a temperature change. In fact, these complications occur because of incomplete knowledge about the kinetic model for the reaction.

The higher a reaction's activation energy is, the bigger is the influence of temperature on the reaction rate. As we have already indicated, this property may be put to use technologically, to optimize the selectivity in the case of parallel or consecutive reaction chains with different activation energies. For two different temperatures, the Arrhenius equations for the two reactions are

$$k_{(T_1)} = A \exp(-\frac{E_a}{RT_1}) \tag{1.4}$$

$$k_{(T_2)} = A \exp(-\frac{E_a}{RT_2}) \tag{1.5}$$

Dividing eq. (1.4) by eq. (1.5), one obtains

$$\frac{k_{(T_2)}}{k_{(T_1)}} = \exp\left[\frac{E_a}{R}(\frac{1}{T_1} - \frac{1}{T_2})\right] \tag{1.6}$$

This eq. (1.6) indicates that, when the temperature increases from T_1 to T_2 for a few different reactions with different activation energies, the ratio of the rate constants $k_{(T_2)}/k_{(T_1)}$ is bigger if the activation energy E_a is bigger. The rate is more sensitive on temperature for the reactions with the higher reaction activation energies. Yield and selectivity for the reaction with the higher E_a will then be larger at higher temperatures. In this way the selectivity in Soede's experiments should have good reasons to follow the rules of the kinetic model, which it did not.

1.3   Transition state theory

The transition state theory implies that, in catalytic reactions, reactants are supposed to form some sort of intermediate complex with the catalyst. This alters the reaction path and helps to overcome the (smaller) potential energy barrier E_a, which controls the conversion rate.

This concept is described in a more rigorous way by Eyring's transition state theory [24, 2, 3]. This is a theory for the absolute rates of chemical processes. The activated complex is now, simply, the configuration of reactant molecules which has the highest potential energy along the reaction coordinate (Figures 1.2 and 1.3). Reactants and the transition complex (or activated complex) are supposed to remain in thermal equilibrium on their journey along the reaction path. In such an equilibrium the distribution of reactant along the reaction path is of the Boltzmann type. The activated complex has the smallest concentration of the reactant. A fraction (99% or so) of the concentration in the activated complex M (right at the top of the potential energy barrier) is to be converted into the product C. The rest will fall back, reversing the path along the reaction coordinate, and eventually split up again into reactants A and B. The net transmission of reactant through this narrow restriction at the top of the energy barrier determines the conversion rate.
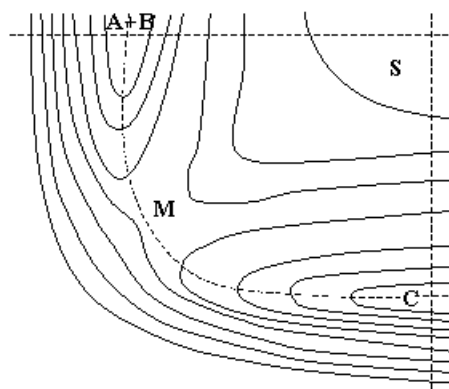
Figure 1.2: 2-D contour plot of Potential energy of a chemical reaction

A two-dimensional contour map of the potential energy for the reaction

$$A + B \overset{K^{\#}}{\rightleftharpoons} M \overset{k^{\#}}{\to} C \tag{1.7}$$

is shown schematically in figure 1.2. Reactants A and B start from some position

with a low potential energy. Moving along the dotted line (the reaction coordinate) they pass through M, where the potential energy is high. Eventually, after having crossed the energy barrier at M, they end up as the product configuration in another position with low potential energy. The dotted curved line in this diagram shows the (most probable) pathway for such a rearrangement, with the lowest potential energy. Position "S" in the diagram is out of reach altogether at the temperature for which this projection contour diagram is valid. It could be the configuration in which the reactants form a product without the catalyst interfering. There, the potential energy is very high, much higher than at the activated complex M. The probability to cross the barrier at M is then much larger.

If the dotted line in figure 1.2 is transformed into the abscissa of a plot, a reaction coordinate-potential energy diagram is drawn, as in figure 1.3. The transition state has the highest potential energy. The energy difference between reactants and the transition state is the activation energy E_a. The energy difference between reactants and products is the reaction enthalpy $\Delta_r H$ per mole of converted product. According to the transition state theory, the decomposition of complex M into the product C (*i.e* the transmission over the energy barrier) is thanks to the molecular vibrations at the reaction temperature T. These break the weak chemical bonds in the complex and make the products diffuse away along the reaction coordinate. This sets the active site free for complexation of new reactant species.
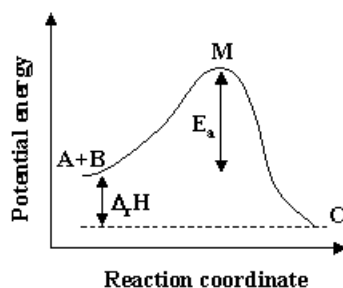
Figure 1.3: Reaction coordinate-potential energy plot

Eyring derived the quantum mechanical potential energy diagram for some simple gas reactions at high temperatures and showed how to calculate E_a from it. He derived that in the transition state

$$k = \frac{\mathbf{k}T}{h} K^{\#} \tag{1.8}$$

Page: 10

where $\mathbf{k}$ is Boltzmann constant, h Planck's constant and $K^{\#}$ the equilibrium constant for the formation of the activated complex from the reactants.

Using the relation of Gibbs free energy with the equilibrium constant K, one obtains.

$$k = \frac{\mathbf{k}T}{h} \exp(-\frac{\Delta G^{\circ \#}}{RT}) = \frac{\mathbf{k}T}{h} \exp(\frac{\Delta S^{\circ \#}}{R}) \exp(-\frac{\Delta H^{\circ \#}}{RT}) \qquad (1.9)$$

Reaction enthalpy of the transition state $\Delta H^{\circ \#}$ and entropy $\Delta S^{\circ \#}$ have constant (molecularly determined) values. Replacing the microscopic Boltzmann constant $\mathbf{k}$ by the macroscopic gas constant R, the activation energy for the macroscopic thermodynamic conversion rate is obtained as a macroscopic, experimentally measurable quantity:

$$E_a = RT^2 \frac{\partial}{\partial T} \ln k = \Delta H^{\circ \#} + RT \qquad (1.10)$$

The pre-exponential factor is obtained by writing the rate constant k in the Arrhenius form as in eq. (1.3).

$$A = \frac{\mathbf{k}T}{h} \exp(\frac{\Delta S^{\circ \#}}{R}) \qquad (1.11)$$

At low temperatures, the term RT in eq. (1.10) or $\mathbf{k}T/h$ in eq. (1.11) is rather small compared to chemical bond energies and reaction enthalpies in the corresponding equations. Therefore, temperature effects in the activation energy E_a itself and in the pre-exponential factor are negligible. That is why the activation energy and pre-exponential factor are treated as constants in logarithmic operations like constructing an Arrhenius plot. Even though they have constant values on this scale, different reactions, however, have different potential energy diagrams, different activation energies and different pre-exponential factors.

1.4 Non-equilibrium thermodynamics

How far a chemical system is away from equilibrium is determined by its remaining free energy. For a closed system in equilibrium the free energy is at the minimum value, whereas the entropy is at its maximum. In a chemical reactor the conversion reaction is one of the fluxes by which the system attempts to reach that equilibrium. Other fluxes are the heat flow, mass flow *etc.* Fresh reactants, being fed continuously into a flow reactor, keep the entropy at a lower level than it would have in equilibrium. A reaction in steady state is then mostly the result, in industry and laboratory.

That steady state represents the smallest deviation from equilibrium under given conditions. A measure for the deviation from equilibrium is the entropy production in the system. The entropy production in a steady state system is the sum of all

the fluxes, which act in that system, each of them multiplied by its conjugate force, which drives it. Non-equilibrium thermodynamics has been developed to describe the relations between these fluxes and how they interact under such steady state conditions.

We have applied that formalism - in which the overall entropy production becomes as small as possible under the given process conditions - to a two-dimensional surface instead of a reactor volume. This allows a thermodynamic treatment of the active reaction surface of a heterogeneous catalyst. In this setting, we set out in the hope to use Bedeaux' approach of irreversible surface thermodynamics for obtaining more insight in the puzzling thermal effects of some important catalytic systems. That is our program in this thesis.

Our approach to the coupling problem will be in a stepwise fashion. In the next chapter we set out to establish the machinery for a two-dimensional thermodynamic treatment of the active catalyst surface. The key aspect of Bedeaux' theory is the possibility of coupling between heat flows, mass transfer and conversion processes in heterogeneous thermodynamic systems. This is, because the dimensionality of surfaces lifts the restrictions on the thermodynamic coupling of a (scalar) chemical reaction process and a (vectorial) heat or mass flow as a response to gradients in temperature or concentration.

In heterogeneous catalysis the focus for heterogeneity is the two-dimensional catalyst surface. Coupling effects between heat and mass flows can then be found. In the case that the heterogeneous catalytic reaction is transport limited these effects will affect the rate of the process. In a transport limited reaction process the chemical conversion at the interface is fast enough to maintain local chemical equilibrium. The Gibbs free energy $\Delta_r G$, which the conversion could contribute to the overall dissipation is then zero. Therefore, chemical conversion itself does not contribute to the minimum entropy production. It only releases the amount of heat that can be transported away and the products which diffuse away from the reaction surface. Hence only heat and mass transfer are independent variables for the minimum entropy production in such a catalytic surface process. These two types of fluxes are the causes and the effect of temperature and chemical potential gradients. They produce the least possible amount of entropy for the experimental conditions set in the reactor. Based on that insight it can be derived that there is a temperature difference between the catalyst surface and the medium. The Soret effect (*i.e* the coupling of the mass flow with the heat flow into the medium) and the inverse Dufour effect are potentially important in determining the fluxes and the temperature gradients in the steady state, and, therefore, the overall reaction rate which is obtained.

The next step, to which we shall devote the rest of the thesis, addresses catalytic reaction processes, which are rate controlled by the kinetics of the reaction itself. The transport capacity exceeds the formation rate of heat and products. The processes in the reaction surface alone are then responsible for the amount of entropy production. Here, Bedeaux' approach could generate completely novel insights in interfacial heat effects and their influence in catalytic reaction kinetics.

When we apply non-equilibrium surface thermodynamics to model such a catalytic conversion we must discriminate between the temperature T^r of the reaction itself, the temperature T^m of the catalyst surface and the overall reactor temperature T^g. The difference $T^m - T^g$ is because all the heat and the products of the reaction must be transported away into the medium, through the diffusion boundary layer, under steady state conditions of the process. This is the problem in the simpler case of the transport limited surface reactions. The net transport of the heat is a kind of "thermometer" here. It allows to measure the temperature difference between the catalyst surface and the fluid if we know the thermal conductivities of both materials.

But in kinetically controlled conversion processes the Arrhenius equation for the reaction rate can be used independently to determine the reaction temperature. The experimental data on the rate of the process functions as a thermometer that indicates the temperature T^r, which exists in the two-dimensional reaction plane. This reaction plane is cast as a separate thermodynamic system, and we shall explore the distinct possibility that heat fluxes in the reaction plane couple with the conversion rate to produce a minimum entropy. The thermodynamic analysis of kinetically controlled, catalytic systems will then indicate if the temperatures T^r and T^m, of the reaction plane and the catalyst surface, respectively, are equal or not.

This difference of the temperatures T^r and T^m in heterogeneous catalysis is a completely new observation. The coupling of conversion rates and thermal effects, which causes the difference, is a specific but generally applicable thermodynamic concept for conversions involving heterogeneous catalysis.

Chapter 2

Formulism for irreversible surface thermodynamics

2.1 Non-equilibrium thermodynamics

In the study of processes involving heat transfer and multi-component mass transfer from a surface to an adjacent bulk medium it is common practice to use the film model. According to this model all the resistance for mass transfer to and from a surface is assumed to be located in a thin diffusion layer, between the surface and the medium. It is also assumed that the temperature and chemical potentials must be continuous at the surface. Any coupling of a possible heat flux to the mass flux for gases is neglected and vice versa.

But applying nonequilibrium thermodynamics within the framework of this film model we can attempt to integrate the coupling between the interdependent heat and mass fluxes in the description of the film [28, 29, 30].

Irreversible thermodynamics [23] provides a systematic method of combining heat and mass transfer. In this method the heat and mass fluxes are linearly related to the thermodynamic forces, *i.e.* the temperature and chemical potential gradients, in the system.

2.1.1 Phenomenological equations

The interdependence of the fluxes in a non-equilibrium system is made explicit when these relations are written in the form of a set of so called "phenomenological equations" (2.1). This set of equations describe all the interdependencies of fluxes and

forces, which are possible in the system.

$$\Delta(\frac{1}{T}) = r_{qq}J_q' + r_{q1}J_1 + r_{q2}J_2 + \cdots + r_{qn}J_n$$

$$-\frac{\Delta\mu_{1,T}}{T} = r_{1q}J_q' + r_{11}J_1 + r_{12}J_2 + \cdots + r_{1n}J_n$$

$$-\frac{\Delta\mu_{2,T}}{T} = r_{2q}J_q' + r_{21}J_1 + r_{22}J_2 + \cdots + r_{2n}J_n$$

$$\vdots \qquad\qquad \vdots$$

$$-\frac{\Delta\mu_{n,T}}{T} = r_{nq}J_q' + r_{n1}J_1 + r_{n2}J_2 + \cdots + r_{nn}J_n \tag{2.1}$$

The resistance coefficients can be written in one matrix

$$\begin{pmatrix} r_{qq} & r_{q1} & r_{q2} & \cdots & r_{qn} \\ r_{1q} & r_{11} & r_{12} & \cdots & r_{1n} \\ r_{2q} & r_{21} & r_{22} & \cdots & r_{2n} \\ \vdots & \vdots & \vdots & \ddots & \vdots \\ r_{nq} & r_{n1} & r_{n2} & \cdots & r_{nn} \end{pmatrix} \tag{2.2}$$

Here J_q' is the measurable heat flux and J_i the molar flux of component i and r matrix is resistance coefficients. The resistance coefficients r include the film thickness and are subject to Onsager reciprocity. Furthermore, $\mu_{i,T}$ is the chemical potential of the component i and the subscript T signifies that the gradient is evaluated at constant temperature. The direction of the heat and the mass transfer is normal to the catalyst surface.

The diagonal elements in the resistance coefficient matrix represent the well-known Fourier and Fick processes whereas the non-diagonal elements represent cross effects such as the Dufour and the Soret effects.

An equivalent set of expressions for conjugate fluxes and forces is

$$J_q' = l_{qq}\Delta\left(\frac{1}{T}\right) - \frac{1}{T}l_{q1}\Delta\mu_{1,T} - \frac{1}{T}l_{q2}\Delta\mu_{2,T} - \cdots - \frac{1}{T}l_{qn}\Delta\mu_{n,T}$$

$$J_1 = l_{q1}\Delta\left(\frac{1}{T}\right) - \frac{1}{T}l_{11}\Delta\mu_{1,T} - \frac{1}{T}l_{12}\Delta\mu_{2,T} - \cdots - \frac{1}{T}l_{1n}\Delta\mu_{n,T}$$

$$J_2 = l_{q2}\Delta\left(\frac{1}{T}\right) - \frac{1}{T}l_{21}\Delta\mu_{1,T} - \frac{1}{T}l_{22}\Delta\mu_{2,T} - \cdots - \frac{1}{T}l_{2n}\Delta\mu_{n,T}$$

$$\vdots$$

$$J_n = l_{qn}\Delta\left(\frac{1}{T}\right) - \frac{1}{T}l_{n1}\Delta\mu_{1,T} - \frac{1}{T}l_{n2}\Delta\mu_{2,T} - \cdots - \frac{1}{T}l_{nn}\Delta\mu_{n,T} \tag{2.3}$$

and the corresponding conductivity coefficient matrix is

$$
\begin{pmatrix}
l_{qq} & l_{q1} & l_{q2} & \cdots & l_{qn} \\
l_{1q} & l_{11} & l_{12} & \cdots & l_{1n} \\
l_{2q} & l_{21} & l_{22} & \cdots & l_{2n} \\
\vdots & \vdots & \vdots & \ddots & \vdots \\
l_{nq} & l_{n1} & l_{n2} & \cdots & l_{nn}
\end{pmatrix}
\tag{2.4}
$$

2.1.2 Effective phenomenological l-coefficients

We can describe mass transfer by introducing effective mass transfer coefficients instead of the full set of coefficients l_{ij} in eq. (2.3). In such a representation the mass transfer process is described only by the diagonal terms of the phenomenological equations in which the effective conductivities incorporate the coupling effects between various molar fluxes. The effective diagonal mass transfer coefficients are no longer materials properties, but will depend on the process conditions. Using the effective mass transfer coefficients $l_{i,eff}$ the flux-force equations are simplified as

$$
J_q' = l_{qq}\Delta\left(\frac{1}{T}\right) - \frac{1}{T}l_{q1}\Delta\mu_{1,T} - \frac{1}{T}l_{q2}\Delta\mu_{2,T} - \cdots - \frac{1}{T}l_{qn}\Delta\mu_{n,T}
$$

$$
J_1 = l_{q1}\Delta\left(\frac{1}{T}\right) - \frac{1}{T}l_{1,eff}\ \Delta\mu_{1,T}
$$

$$
J_2 = l_{q2}\Delta\left(\frac{1}{T}\right) - \frac{1}{T}l_{2,eff}\ \Delta\mu_{2,T}
$$

$$
\vdots
$$

$$
J_n = l_{qn}\Delta\left(\frac{1}{T}\right) - \frac{1}{T}l_{n,eff}\ \Delta\mu_{n,T}
\tag{2.5}
$$

and the conductivity coefficient matrix becomes

$$
\begin{pmatrix}
l_{qq} & l_{q1} & l_{q2} & \cdots & l_{qn} \\
 & l_{1,eff} & 0 & 0 & 0 \\
 & & l_{2,eff} & 0 & 0 \\
 & & & \ddots & 0 \\
 & & & & l_{n,eff}
\end{pmatrix}
\tag{2.6}
$$

where only half of the l-coefficients are given because of the Onsager symmetry.

To find the expressions for the l-coefficients we introduce Fick's effective diffusion

coefficient $D_{i,eff}$ and write the flux-force equation as [31]

$$J_i = -D_{i,eff} \frac{dc_i}{dx} \tag{2.7}$$

Substituting the chemical potential μ_i in eq. (2.5) with the relation,

$$\mu_i = \mu_i^\circ + RT \ln \frac{c_i}{c} \tag{2.8}$$

assuming the ideal gas law and comparing eq. (2.5) to the integral of eq. (2.7), one obtains

$$l_{i,eff} = \frac{x_i D_{i,eff} \; p}{\delta R^2 T} \tag{2.9}$$

The Fick's effective diffusion coefficient is calculated by [32, 31]

$$\frac{1}{D_{i,eff}} = \sum_{\substack{j=1 \\ j \neq i}}^{n} \frac{x_j}{\mathrm{Ð}_{ij}} \left(1 - \frac{x_i J_j}{x_j J_i}\right) \tag{2.10}$$

For a surface reaction the flux ratios J_j/J_i are constant in the thin film and related to the ratios of stoichiometric coefficients of the chemical reaction. In fact, this is why this description is so useful here. The conductivity heat transfer coefficient l_{qq} is calculated by

$$l_{qq} = \frac{\lambda_m T^2}{\delta} \tag{2.11}$$

This relation can be obtained by comparing eq. (2.5) to Fourier's law.

The coupling conductivity coefficients are related to the heats of transfer in the following derivation. When the temperature difference is zero, eqs. (2.5) become

$$\begin{cases} J_q' = -\dfrac{1}{T} \sum_i l_{qi} \; \Delta\mu_{i,T} \mid_{\Delta T=0} \\[2mm] J_i = -\dfrac{1}{T} \; l_{i,eff} \; \Delta\mu_{i,T} \mid_{\Delta T=0} \end{cases} \tag{2.12}$$

Comparing these two equations, one obtains

$$\left(J_q'\right)_{\Delta T=0} = \sum_i \frac{l_{qi}}{l_{i,eff}} \left(J_i\right)_{\Delta T=0} \tag{2.13}$$

When the temperature difference in the thin film is zero, the heat flux due to the molar flux is also written as

$$\left(J_q'\right)_{\Delta T=0} = \sum_i Q_i^* \left(J_i\right)_{\Delta T=0} \tag{2.14}$$

where Q_i^* is the heat of transfer carried by the component i. Comparing eq. (2.13) to (2.14) the heat of transfer Q_i^* is obtained

$$Q_i^* = \frac{l_{qi}}{l_{i,eff}} \qquad (2.15)$$

which is similar to the definition given by Kjelstrup and Bedeaux [33] for a binary component system.

When the molar flux of the component i vanishes, namely $J_i = 0$, which means that the chemical potential difference is caused only by the thermal diffusion, the equation for mass transfer in eqs. (2.5) is rewritten as

$$l_{qi} \ \Delta \left(\frac{1}{T} \right) = \frac{1}{T} \ l_{i,eff} \ \Delta\mu_{i,T} \ |_{J_i=0} \qquad (2.16)$$

Replacing l_{qi} with eq. 2.15 and rewriting eq. (2.16), one obtains

$$\Delta\mu_{i,T} = -Q_i^* \frac{\Delta T}{T} \ |_{J_i=0} \qquad (2.17)$$

Comparing eq. (2.17) to eq. (3.9) in chapter 3, one obtains the expression for heat of transfer

$$Q_i^* = \sum_{\substack{j=1 \\ j \neq i}}^{n} \frac{x_j R \ T}{Ð_{ij}} \left(\frac{D_i^T}{\rho_i} - \frac{D_j^T}{\rho_j} \right) \qquad (2.18)$$

Non-equilibrium thermodynamic theory opens a door to a consistent and complete description of mass and heat transfer through the film around the catalyst particle and subsequently from the film to the surface where the reaction takes place. As we shall show, the surface features as an "additional film" with its own rates of generating heats and products. As it is often enough to use a thin film approximation in the bulk phase, which is most easy to implement, we shall follow this procedure for estimating the resistance coefficients in experimental model systems. This could make the similarity between the alternative descriptions of the catalytically active plane as a thin film or as an abstract two-dimensional Gibbs dividing surface more apparent.

2.2 Heterogeneous reaction systems

The next issue is to account for the heterogeneity in a catalytic system. Following Gibbs [34] we begin by introducing the interface between the phases of catalyst and medium as a separate thermodynamic system. This is done by defining a dividing

plane (between the two homogeneous bulk phases). All the extensive properties, which distinguish the heterogeneous system from the two phases, are assigned to this hypothetical interface.

One phase is the medium. The other is the catalyst. Either phase has a constant composition everywhere, up to the dividing surface. The dividing plane is located, following Gibbs' convention [34], where one referent component (in this case the major component of the medium) has zero excess concentration assigned to the dividing surface. All other components will then automatically acquire excess concentrations (positive or negative adsorption), which are assigned to the 2-dimensional dividing plane to make up for the differences in contents of the complete system with the summed contents of the two bulk phases. All the thermodynamic properties of the surface are fixed then. For all the extensive thermodynamic properties the dividing plane has excess values assigned to it. It has excess densities of mass for the individual components, of heat, of entropy and of energy. With these properties it becomes a separate, two-dimensional thermodynamic system. This is independent of the state of the interface. It may be in equilibrium or not, but Gibbs' definition ensures that the usual thermodynamic relations apply to the excess values of the dividing plane, like in a homogeneous, three dimensional system.

2.2.1   Thermodynamic variables for a surface

When excess surface densities are defined in the manner of Gibbs, the normal thermodynamic relations, like the first and the second law and derived relations, apply for the densities [34]. For a surface in equilibrium, the Gibbs equation for the total excess internal energy, U^{s}, becomes:

$$dU^{\mathrm{s}} = TdS^{\mathrm{s}} + \sum_{i=1}^{n} \mu_i dN_i^{\mathrm{s}} \qquad (2.19)$$

where S^{s} and N_i^{s} are the total excess entropy and the total excess number of moles of the component i. Furthermore T and μ_i are the temperature and the chemical potential of component i, respectively. Using the extensive nature of U^{s}, S^{s} and N_i^{s} we can integrate this equation and obtain

$$U^{\mathrm{s}} = TS^{\mathrm{s}} + \sum_{i=1}^{n} \mu_i N_i^{\mathrm{s}} \qquad (2.20)$$

The Gibbs-Duhem's equation for the surface follows by differentiation of Eq. (2.20) and subtracting Eq.(2.19):

$$0 = S^{\mathrm{s}}dT + \sum_{i=1}^{n} N_i^{\mathrm{s}}d\mu_i \qquad (2.21)$$

To describe the properties in the $y-z$-plane we shall need local variables, given in units per surface area. These are the excess internal energy density $u^{\mathrm{s}} = U^{\mathrm{s}}/\Omega$, the adsorptions $\Gamma_i = N_i^{\mathrm{s}}/\Omega$ of components in the interface and the excess entropy density, $s^{\mathrm{s}} = S^{\mathrm{s}}/\Omega$ where Ω is the interface area. When these variables are introduced into Eqs.(2.19) and (2.20), we obtain Gibbs equation with local surface properties

$$du^{\mathrm{s}} = Tds^{\mathrm{s}} + \sum_{i=1}^{n} \mu_i d\Gamma_i \qquad (2.22)$$

and the surface excess internal energy density

$$u^{\mathrm{s}} = Ts^{\mathrm{s}} + \sum_{i=1}^{n} \mu_i \Gamma_i \qquad (2.23)$$

The Gibbs-Duhem's equation is then

$$0 = s^{\mathrm{s}}dT + \sum_{i=1}^{n} \Gamma_i d\mu_i \qquad (2.24)$$

We see that the Gibbs dividing plane is, indeed, described as an additional thermodynamic system, which is, of course, connected to the two adjacent phases by processes of mass and heat transfer.

Bedeaux and Kjelstrup [23] have described the interface between a liquid and a vapour phase in this way. For our chosen model systems we need experimental data for gas-solid catalytic systems, but the principle of the thermodynamic procedure to analyse these data is the same and will be repeated here.

In our equations we shall define the dividing surface by its normal and choose the x-axis perpendicular to it. The resulting $y-z$ surface can then be regarded as a two-dimensional thermodynamic system. The logical choice of the reference component, which defines the location of the dividing plane, is the carrier gas.

The alternative, less abstract, description would be as a three-dimensional thin film, with properties of gradients in the thickness that can be integrated out in the x-direction and are given per surface area. The dependence of local properties on the coordinates y and z remains. For the usual catalytic surface the thickness is not more than a few nanometers. In the application of the above methods using excess

densities and fluxes there is no reason to restrict oneself to surfaces that are so thin, however.

The three-dimensional interphase with its finite real thickness δ may be treated as one additional film in transport equations at interfaces. Whereas in the Gibbs approach this complete interphase with thickness δ is contracted into the abstract, essentially two-dimensional, dividing surface between the phases.

2.2.2 Local equilibrium and its consequences

Local equilibrium implies that all the usual thermodynamic relations are valid locally. This applies to the catalyst and the medium, but also to the dividing surface. In eq. (2.22), the intensive thermodynamic variables for the surface, indicated by superscript s, are given by the derivatives

$$T^{\mathrm{s}} = \left(\frac{\partial u^{\mathrm{s}}}{\partial s^{\mathrm{s}}}\right)_{\Gamma_j} \text{ and } \mu_j^{\mathrm{s}} = \left(\frac{\partial u^{\mathrm{s}}}{\partial \Gamma_j}\right)_{s^{\mathrm{s}}, \Gamma_k} \tag{2.25}$$

The temperature and chemical potentials in the dividing surface, defined in this manner, depend only on the surface excess variables, not on the value of bulk variables close to the surface. Molecular dynamics simulations support the validity of the assumption of local equilibrium for surfaces [35].

The assumption of local equilibrium, as formulated above, means that all macroscopic thermodynamic functions retain their meaning locally. It does not imply local chemical equilibrium at the reacting surface [36]. In the special case of a chemical equilibrium in the interface and a steady state process, *e.g.* in a surface reaction with a transport limited rate, the Gibbs energy of the reaction itself would be zero. All the other excess densities in the dividing surface have time independent values whenever the reaction is in steady state. We notice, however, that by introducing these definitions the surface is allowed to have a different temperature or chemical potential from the adjacent homogeneous systems.

An essential and surprising consequence of the local equilibrium assumption for the surface and the adjacent homogeneous phases is, that the temperature and chemical potentials on both sides of the interface may differ. Not only from each other, but also from the values for the reaction surface or dividing plane in the heterogeneous process.

2.3 The excess entropy production rate for the surface

2.3.1 Balance equations

If an excess molar density of a component j takes part in some transport or chemical conversion process at the interface, the mass balance for this component would be

$$\frac{d}{dt}\Gamma_j = J_j^{\mathrm{i}} + \nu_j \Re \qquad (2.26)$$

where J_j^{i} is the molar flux into the surface and ν_j the stoichiometric coefficient of component j, while $\Re$ is the reaction rate per unit of surface area. The stoichiometric coefficients are taken negative for the reactants and positive for the products. The first law (conservation of energy) tells, that in the surface (as a thermodynamic system)

$$\frac{du^{\mathrm{s}}}{dt} = J_e^{\mathrm{i}} - J_e^{\mathrm{o}} \qquad (2.27)$$

The change of the excess internal energy density of the reaction surface is given by the energy flux into the surface from the left, J_e^{i}, minus the energy flux out of the surface to the right, J_e^{o}. Both the molar and the energy fluxes in the above equations should be taken in a frame of reference in which the surface is at rest. The energy fluxes in the i and the o phases are related to the physical heat fluxes J_q' by

$$J_e^{\mathrm{i}} = J_q'^{\mathrm{i}} + \sum_j h_j^{\mathrm{i}} J_j^{\mathrm{i}} \quad \text{and} \quad J_e^{\mathrm{o}} = J_q'^{\mathrm{o}} \qquad (2.28)$$

where h_j^{i} is the partial enthalpy density of component j in the i-phase. The measurable heat fluxes are independent of the frame of reference [36].

2.3.2 The rate of excess entropy production

Now, let us consider a reaction surface s as a separate thermodynamic system sandwiched between the two phases i and o. We take the origin of the x-axis to coincide with the surface s. Phase i is located on the left of the surface, $x < 0$, whereas phase o is on the right of the dividing surface, $x > 0$. In our model systems i is the gas phase in which the diffusion takes place. The phase o is the solid catalyst in which only heat flux may exist. The change of the entropy in a surface area element is a result of the flow of entropy into, J_s^{i}, and out of, J_s^{o}, the surface element, and of the entropy production rate, σ^{s}, by the processes inside the reaction plane. The entropy

production in this reaction plane is given by

$$\frac{d}{dt}s^s = J_s^i - J_s^o + \sigma^s \qquad (2.29)$$

Both fluxes should be taken in a frame of reference in which the surface is at rest. Thermodynamics demands that the excess entropy production rate in equation 2.8 is positive: $\sigma^s \geq 0$. In a heterogeneous reaction we shall have to develop explicit expressions for σ^s by combining (a) mass balances, (b) the first law of thermodynamics, and (c) the local form of the Gibbs equation.

In the derivation of the excess entropy production rate for this kind of system we shall not do anything new. The thermodynamic procedures from references [28, 29, 30] will directly be applied to our problem. The entropy production rate σ^s in the system can be written as the product sum of thermodynamic fluxes with their conjugate forces. We shall identify the relevant conjugate fluxes and forces and model the two catalytic systems, in which the conversion rate is controlled by limitations in the transport of mass to the reaction surface, for the first case, and the surface reaction rate is the rate-limiting step in the second case.

The entropy fluxes in the i and the o phases are related to energy fluxes by the equations [33]

$$J_s^i = \frac{1}{T^i}\left(J_e^i - \sum_{j=1}^{n}\mu_j^i J_j^i\right) \quad \text{and} \quad J_s^o = \frac{1}{T^o}J_e^o \qquad (2.30)$$

Whreas the time derivative of the entropy density is given by the Gibbs equation in its local form:

$$\frac{ds^s}{dt} = \frac{1}{T^s}\frac{du^s}{dt} - \frac{1}{T^s}\sum_{j=1}^{n}\mu_j^s\frac{d\Gamma_j}{dt} \qquad (2.31)$$

By introducing eqs.(2.26) and (2.27) into eq.(2.31), and comparing the result to the entropy balance Eq.(2.29), we must obtain the excess entropy production rate in the surface

$$\sigma^s = J_e^i(\frac{1}{T^s} - \frac{1}{T^i}) + J_e^o(\frac{1}{T^o} - \frac{1}{T^s}) + \sum_{j=1}^{n}J_j^i\left[-(\frac{\mu_j^s}{T^s} - \frac{\mu_j^i}{T^i})\right] + \Re\left[-\frac{\Delta_r G^s}{T^s}\right] \qquad (2.32)$$

where $\Delta_r G^s = \sum \nu_j \mu_j^s$ is the Gibbs energy for the surface reaction. This quantity vanishes in the case of a chemical equilibrium in the interface.

2.4   Steady state conditions

The experimental data in our gas/solid model systems were obtained in steady state conditions. In the steady state of a heterogeneous reaction, the net energy flux into the thin interfacial layer must be zero, since no internal energy is accumulating in the surface during the process. The surface excess energy density remains constant. This implies that

$$J_e^{\mathrm{i}} - J_e^{\mathrm{o}} = 0 \tag{2.33}$$

Both J_e^{i} and J_e^{o} are constant throughout the i and the o phases. This relation will be used later to simplify the calculations.

The excess entropy production, eq. (2.32) can be written as

$$\sigma^{\mathrm{s}} = J_e^{\mathrm{i}} \Delta_{\mathrm{i,s}}\!\left(\frac{1}{T}\right) + J_e^{\mathrm{o}} \Delta_{\mathrm{s,o}}\!\left(\frac{1}{T}\right) + \sum_{j=1}^{n} J_j^{\mathrm{i}} \left[-\Delta_{\mathrm{i,s}}\!\left(\frac{\mu_j}{T}\right) \right] + \Re\left[-\frac{\Delta_r G^{\mathrm{s}}}{T^{\mathrm{s}}} \right] \tag{2.34}$$

In the last equality we introduced $\Delta_{\mathrm{i,s}}$ or $\Delta_{\mathrm{s,o}}$ as a short hand notation for the difference of a variable. In steady states the molar fluxes, J_j^{i}, are constant throughout the diffusion layer while the total energy flux, J_e, is constant everywhere. It follows using eqs.(2.26), (2.28) and (2.33) that

$$J_j^{\mathrm{i}} = -\nu_j \Re \quad \text{and} \quad J_e^{\mathrm{i}} - J_e^{\mathrm{o}} = J_q'^{\mathrm{i}} + \sum_j h_j^{\mathrm{i}} J_j - J_q'^{\mathrm{o}} = 0 \tag{2.35}$$

When the energy fluxes are eliminated in eq. (2.34) and replaced by the measurable heat fluxes, using eq.(2.28) and the thermodynamic identity $\partial(\mu_j/T)/\partial(1/T) = h_j$, one obtains after some algebra

$$\sigma^{\mathrm{s}} = J_q'^{\mathrm{i}} \Delta_{\mathrm{i,s}}\!\left(\frac{1}{T}\right) + J_q'^{\mathrm{o}} \Delta_{\mathrm{s,o}}\!\left(\frac{1}{T}\right) + \sum_{j=1}^{n} J_j \left[-\frac{\Delta_{\mathrm{i,s}} \mu_{j;T}(T^{\mathrm{s}})}{T^{\mathrm{s}}} \right] + \Re\left[-\frac{\Delta_r G^{\mathrm{s}}}{T^{\mathrm{s}}} \right] \tag{2.36}$$

In this expression the subscript T implies that the pertinent difference is calculated at a constant temperature, which in this case is given by T^{s}.

2.5   The "reaction surface" in heterogeneous catalytic systems

There is an excess entropy assigned to the Gibbs dividing plane. If there is an irreversible process going on in that surface, like in heterogeneous catalytic reactions,

then it is logical that such a surface is the locus of excess entropy production. The stage for the conversion reaction is the Gibbs dividing surface and the adsorbed reactant molecules in their excess concentrations have been assigned to play their roles in this process. This identifies the two-dimensional dividing plane as the "reaction surface" with its own thermodynamic properties. Like in any surface of its kind, the temperature, the conversion rate and the entropy production may differ from those in the separate bulk phases of the heterogeneous system.

Having obtained the entropy production rate for a catalytic model reaction we can identify the relevant fluxes and forces. For this we make use of the linear phenomenological relations. Excess entropy productions, like that given in eq.(2.34) can then be expressed by the relations

$$\Delta_{\mathrm{i,s}}(\frac{1}{T}) = r_{ee}^{\mathrm{s,i}} J_e^{\mathrm{i}} + \sum_{k=1}^{n} r_{ek}^{\mathrm{s,i}} J_k + r_{er}^{\mathrm{s,i}} \Re$$

$$\Delta_{\mathrm{s,o}}(\frac{1}{T}) = r_{ee}^{\mathrm{s,o}} J_e^{\mathrm{o}} + r_{er}^{\mathrm{s,o}} \Re$$

$$-\Delta_{\mathrm{i,s}}(\frac{\mu_j}{T}) = r_{je}^{\mathrm{s,i}} J_e + \sum_{k=1}^{n} r_{jk}^{\mathrm{s,e}} J_k + r_{jr}^{\mathrm{s,e}} \Re$$

$$-\frac{\Delta_r G^{\mathrm{s}}}{T^{\mathrm{s}}} = r_{re}^{\mathrm{s,i}} J_e^{\mathrm{i}} + r_{re}^{\mathrm{s,o}} J_e^{\mathrm{o}} + \sum_{k=1}^{n} r_{rk}^{\mathrm{s,e}} J_k + r_{rr}^{\mathrm{s,e}} \Re \qquad (2.37)$$

while the excess entropy production given in eq.(2.36) results in the linear relations

$$\Delta_{\mathrm{i,s}}(\frac{1}{T}) = r_{qq}^{\mathrm{s,i}} J_q'^{\mathrm{i}} + \sum_{k=1}^{n} r_{qk}^{\mathrm{s,i}} J_k + r_{qr}^{\mathrm{s,i}} \Re$$

$$\Delta_{\mathrm{s,o}}(\frac{1}{T}) = r_{qq}^{\mathrm{s,o}} J_q'^{\mathrm{o}} + r_{qr}^{\mathrm{s,o}} \Re$$

$$-\frac{\Delta_{\mathrm{i,s}}\mu_{j;T}(T^{\mathrm{s}})}{T^{\mathrm{s}}} = r_{jq}^{\mathrm{s,i}} J_q'^{\mathrm{i}} + \sum_{k=1}^{n} r_{jk}^{\mathrm{s,q}} J_k + r_{jr}^{\mathrm{s,q}} \Re$$

$$-\frac{\Delta_r G^{\mathrm{s}}}{T^{\mathrm{s}}} = r_{rq}^{\mathrm{s,i}} J_q'^{\mathrm{i}} + r_{rq}^{\mathrm{s,o}} J_q'^{\mathrm{o}} + \sum_{k=1}^{n} r_{rk}^{\mathrm{s,q}} J_k + r_{rr}^{\mathrm{s,q}} \Re \qquad (2.38)$$

The resistance matrices in these sets satisfy the Onsager symmetry relations. There are therefore $5 + n(n+5)/2$ independent resistance parameters. The resistances in

Page: 26

these matrices are related by

$$r_{ee}^{s,i} = r_{qq}^{s,i} \quad , \quad r_{ek}^{s,i} = r_{qk}^{s,i} - h_k^i r_{qq}^{s,i} \quad , \quad r_{er}^{s,i} = r_{qr}^{s,i}$$
$$r_{ee}^{s,o} = r_{qq}^{s,o} \quad , \quad r_{er}^{s,o} = r_{qr}^{s,o}$$
$$r_{jk}^{s,e} = r_{jk}^{s,q} - h_k^i r_{jq}^{s,i} - h_j^i r_{qk}^{s,i} + h_k^i h_j^i r_{qq}^{s,i} \quad , \quad r_{jr}^{s,e} = r_{jr}^{s,q} - h_j^i r_{rq}^{s,i}$$
$$r_{rr}^{s,e} = r_{rr}^{s,q} \tag{2.39}$$

This follows from eq.(2.28) in combination with the thermodynamic identity $\partial(\mu_j/T)$ $/\partial(1/T) = h_j$. Expressions for some of these resistances have been obtained with kinetic model for a liquid-vapour interface [37, 38, 39, 40]. But for a gas-solid catalytic surface, there seem to be no relevant data in the literature for the resistance coefficients in our kind of kinetically controlled surface process. In a kinetically controlled heterogeneous catalytic reaction, the surface reaction is the most important thing and hence the relevant coupling between reaction and heat transfer. In a diffusion limited reaction, the coupling effect between heat and mass transfer, which is quantified by these resistance parameters, can become important, as we shall show in the next chapters.

2.6   The film model for transport limited reactions

To model catalyst surface temperatures or concentrations from the experimental data in transport limited processes we have used a thin film model. Between catalytic surface and bulk gas phase there is a diffusion boundary layer, in which the heat and mass transfer take place. If this diffusion boundary layer is regarded as a thin layer of gas, the film model can be applied.

The derivation of the entropy production in such a film has been discussed in many places, see for instance [41, 31]. Here, we shall only refer the results in the form that is most convenient for our present purpose (see also [33]:

$$\sigma^i = J_e^i \left(\frac{\partial}{\partial x} \frac{1}{T} \right) + \sum_{j=1}^{n} J_j^i \left(-\frac{\partial}{\partial x} \frac{\mu_j}{T} \right) \tag{2.40}$$

Let us consider an active metal catalyst on a solid support and with the reactants and the products in a gaseous ambient. The conversion reaction takes place in the reaction surface, between adsorbed species. The temperature T^m of the catalyst surface is equal to the temperature on the right hand boundary of the surface. At the interface between metal catalyst and the support there is no reaction and no mass

transfer. The only possible process is a heat flux, which continues until the support has risen in temperature to T^m. The entropy production at this interface can then be written as

$$\sigma^{\mathrm{m,s}} = J_e^{\mathrm{o}} \left(\frac{\partial}{\partial x} \frac{1}{T} \right) \tag{2.41}$$

The interface can be described as an interphase with a finite but small thickness $\delta^{\mathrm{m,s}}$. This interphase behaves as a solid film with unknown composition.

In a stationary state the energy and the molar fluxes are constant, like in the previous discussion. This makes it possible to integrate the entropy production in the x-direction, over the film volumes of the catalyst and the boundary layer in the gas atmosphere. This results in

$$\int \sigma^{\mathrm{f}} dx = J_e^{\mathrm{i}} \Delta_{\mathrm{f}} \left(\frac{1}{T} \right) + \sum_{j=1}^{n} J_j^{\mathrm{i}} \Delta_{\mathrm{f}} \left(-\frac{\mu_j}{T} \right) \tag{2.42}$$

$$\int \sigma^{\mathrm{m,s}} dx = J_e^{\mathrm{o}} \Delta_{\mathrm{m,s}} \left(\frac{1}{T} \right) \tag{2.43}$$

for the boundary layer and the catalyst, respectively. In these expressions the notation $\Delta_{\mathrm{f}} (...)$ or $\Delta_{\mathrm{m,s}} (...)$ means: "the difference of a quantity across the thickness" in a thin gas, or metal-support, film.

The resulting phenomenological equations are the linear expressions

$$\Delta_{\mathrm{f}} \left(\frac{1}{T} \right) = r_{ee}^{\mathrm{f}} J_e^{\mathrm{i}} + \sum_{k=1}^{n} r_{ek}^{\mathrm{f}} J_k^{\mathrm{i}}$$

$$-\Delta_{\mathrm{f}} \left(\frac{\mu_j}{T} \right) = r_{je}^{\mathrm{f}} J_e^{\mathrm{i}} + \sum_{k=1}^{n} r_{jk}^{\mathrm{f,e}} J_k^{\mathrm{i}} \tag{2.44}$$

which relate fluxes and forces in the gas film. The matrix of resistances r satisfies the Onsager symmetry relation. The analogous expression for the other side of the thin interphase of catalyst material is

$$\Delta_{\mathrm{m,s}} \left(\frac{1}{T} \right) = r_{ee}^{\mathrm{m,s}} J_e^{\mathrm{o}} = r_{qq}^{\mathrm{m,s}} J_q^{\prime \mathrm{o}} \tag{2.45}$$

To be able relating the resistances r in these expressions to experimental data of the model reaction we express the resistances in terms of the more familiar coefficients from the film theory. The energy flux in eq.(2.42) is replaced by the measurable heat

flux, $J_q'^{i}$ (as in Fourier's law), using eq.(2.28). This gives:

$$\int \sigma^{f} dx = J_q'^{i} \Delta_{f} \left(\frac{1}{T}\right) + \sum_{j=1}^{n} J_j^{i} \left[\Delta_{f}\left(-\frac{\mu_j}{T}\right) + h_j^{f} \Delta_{f}\left(\frac{1}{T}\right)\right] \qquad (2.46)$$

Here h_j^{f} are the average specific enthalpies in the film. The film thicknesses are between 0.1 and 1.0 mm for a gas film [31]. In writing eq.(2.46) we did assume that the film thickness is small. Therefore, the variation of the specific enthalpies across the box is also small and can be neglected. In practice a choice is made for the film thickness to fit the experimental data.

Using a thin film approximation, one could also write eq.(2.46) in the form

$$\int \sigma^{f} dx = J_q'^{i} \Delta_{f} \left(\frac{1}{T}\right) + \sum_{j=1}^{n} J_j^{i} \left(-\frac{\Delta_{f}\mu_{j,T}(T^{g})}{T^{g}}\right) \qquad (2.47)$$

where $J_q'^{i}$ is the heat flux in the gas film and $\Delta_{f}\mu_{j,T}(T^{g})$ is the difference of the chemical potential across the film at the constant temperature T^{g}, which is the bulk temperature of the gas in the reactor. This expression leads to the linear relations

$$\Delta_{f}\left(\frac{1}{T}\right) = r_{qq}^{f} J_q'^{i} + \sum_{k=1}^{n} r_{qk}^{f} J_k$$

$$-\frac{\Delta_{f}\mu_{j,T}(T^{g})}{T^{g}} = r_{jq}^{f} J_q'^{i} + \sum_{k=1}^{n} r_{jk}^{f,q} J_k \qquad (2.48)$$

for the driving forces and the flows in the gas film. The resistance coefficient matrix satisfies again the Onsager symmetry relations. The relation between the two sets of resistance coefficients in eqs.(2.44) and (2.48) is

$$r_{ee}^{f} = r_{qq}^{f}$$
$$r_{ek}^{f} = r_{qk}^{f} - h_k^{f} r_{qq}^{f}$$
$$r_{jk}^{f,e} = r_{jk}^{f} - h_k^{f} r_{jq}^{f} - h_j^{f} r_{qk}^{f} + h_k^{f} h_j^{f} r_{qq}^{f} \qquad (2.49)$$

In chapter 3, we will show how to calculate these resistance coefficients in the gas film.

There are a number of different situations in which the thermodynamic machinery of this chapter is useful for the analysis of heterogeneous catalytic systems. Force-flux equations for the diffusion boundary layer can be applied to calculate the catalyst surface temperature from the gas temperature for a mass transfer limited heterogeneous

reaction. In that case the catalysed conversion rate in the reaction plane is throttled by the transport rate. The surface is in a local chemical equilibrium and only the heat and mass transfer in the gas film can be important. The experimental resistance coefficients will indicate the relative values of these coupled fluxes, which, together, generate the least possible entropy in the steady state of the catalytic process.

The case of the kinetically controlled reaction is more interesting, though. In a heterogeneous system there is the, largely unexplored, possibility that the conversion rate is coupled with heat fluxes in the two-dimensional reaction surface. This extra coupling opportunity, as such, may force an effective temperature T^r on the two-dimensional reaction plane in the heterogeneous catalyst, which could be more than 10 K, positive or negative, relative to the temperature T^m of the catalyst itself.

The question to be answered is, whether the Arrhenius equation will reflect this special property of temperature in a heterogeneous catalysis. If there is a difference between T^m on the catalyst surface and T^r in the reaction plane, will it give a value to the rate constant k for the heterogeneous reaction process that corresponds with the reaction temperature T^r and not with the measured catalyst temperature T^m. In this way the reaction kinetics would predict unexpected selectivity and conversion rates in experiments with heterogeneous catalytic processes.

Chapter 3

Heat of transfer and resistance coefficients in coupled processes

3.1 Coupling of fluxes

In irreversible thermodynamics the phenomenological equations connect the fluxes in a linear way to the thermodynamic forces. This is described in physical laws like Ohm's law for an electrical current, Fick's law for diffusion transport, Fourier's law for heat conduction, and so on. For fluxes like heat and mass flow the conjugate driving forces are the temperature and chemical potential gradients in the system. The magnitude of the flow depends on the resistance coefficients r in the experimental system under investigation.

The phenomenological equations also suggest that a flux J_i is sometimes changed by additional effects which are driven by other forces $(X_{j,k,l})$ than the conjugate force X_i. Examples of such cross effects are: thermal diffusion (the Soret effect) where diffusion of molecules J_1 in a concentration gradient X_1 according to Fick's law is increased or decreased by extra flows of molecules, driven by a temperature gradient X_2; or the Dufour effect, which is a heat flux J_2, driven by a gradient in the chemical potential X_1. It is clear that these extra effects must be avoided by experimental skill, or that they must explicitly been taken into account in the description of experimental rates of flow or chemical conversions. If these coupling effects are ignored, the measured values of temperature, concentration or reaction
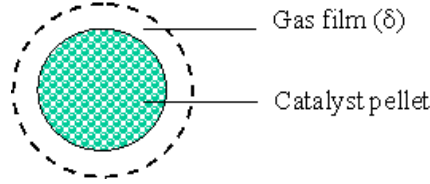
Figure 3.1: Schematic diagram of a catalyst pellet and the gas film around the surface

rate would be too large or too small. Sometimes, as we shall demonstrate for a heterogeneous catalytic system the necessary corrections are tens of percents!

To investigate the importance of Soret and Dufour effects we shall study a heterogeneous catalytic reaction whose rate is limited by the resistance of the system for mass transfer.

The model is sketched in Figure 3.1. The basis of the film model is the assumption that all the resistance to transfer fluxes lies within a hypothetical layer next to the interface, where the sole transfer mechanism is (molecular or thermal) diffusion [31]. The film thicknesses for mass transfer and for heat transfer are different, and a symmetric matrix of δ's could be used to describe that. However, in our case the use of one film thickness is sufficient. Inside this film, there are temperature and concentration gradients, because of the surface reaction. Outside the film, the catalyst is assumed a homogeneous solid. The medium is assumed to be a homogeneous, stirred bulk phase, which contains the reactants and absorbs the products.

The catalyst is a single pellet, as has been extensively studied by Maymo and Smith [42]. It is surrounded with a gas film of thickness δ in which the mass and heat transfer to and from the gaseous medium takes place. Temperature and concentration gradients are assumed to exist only in this thin film, which functions as a diffusion boundary layer. The heat of transfer for the processes in this thin film is a measure for the strength of the fluxes that participate in the heat or mass transfer processes at the interface between medium and catalyst.

The boundary conditions in our analysis are twofold. On the pellet side, the mass fluxes are related by the chemical reaction rate and the mass balance, whereas the heat flux is equal to the reaction heat per unit external surface area of the catalyst particle. No reaction is taking place in the film, hence all the fluxes are constant, all through the film. On the other side of the boundary layer the gas concentrations and temperature are those in the gas bulk phase. In the gas outside the film, conditions approached ideal stirred tank conditions with known gas concentrations and temperature.

If we focus on the coupling processes in the gas film and evaluate the heats of

transfer, this is sufficient to assess the relative importance of the Dufour and the Soret effects in the overall transfer of products and heat from the catalyst surface to the medium.

The Dufour and Soret effects are given by the non-zero cross coefficients r_{qi} of the resistance and proportional with the concentration gradient and the temperature gradient, respectively. These resistance coefficients can be expressed in terms of heats of transport for the individual effects. Many methods are presented in the literature [43, 44, 45, 46, 47, 48, 49, 50] to measure or predict the heat of transport in liquid solutions, solids, liquid-vapour interfaces, *etc*. Here we shall use an expression for the heat of transfer analogous to the one by Taylor and Krishna for the continuous case [31], see also [23].

To find the expression for heat of transfer we start with the phenomenological equation (2.1). It shows the relation of the driving forces, temperature and chemical potential gradients on the left side, and corresponding fluxes, heat and mass fluxes, on the right side for hydrogen oxidation reaction.

$$\Delta(\frac{1}{T}) = r_{qq}J_q' + r_{qH}J_H + r_{qO}J_O + r_{qW}J_W$$

$$-\frac{\Delta\mu_{H,T}}{T} = r_{Hq}J_q' + r_{HH}J_H + r_{HO}J_O + r_{HW}J_W$$

$$-\frac{\Delta\mu_{O,T}}{T} = r_{Oq}J_q' + r_{OH}J_H + r_{OO}J_O + r_{OW}J_W$$

$$-\frac{\Delta\mu_{W,T}}{T} = r_{Wq}J_q' + r_{WH}J_H + r_{WO}J_O + r_{WW}J_W \tag{3.1}$$

The resistance coefficients can be written as a matrix

$$\begin{pmatrix} r_{qq} & r_{qH} & r_{qO} & r_{qW} \\ r_{Hq} & r_{HH} & r_{HO} & r_{HW} \\ r_{Oq} & r_{OH} & r_{OO} & r_{OW} \\ r_{Wq} & r_{WH} & r_{WO} & r_{WW} \end{pmatrix} \tag{3.2}$$

Here J_q' is the measurable heat flux, J_i the molar flux of component i and r the resistance coefficients. In a catalyzed oxidation of hydrogen the component i represents H_2, O_2 and H_2O, respectively. The resistance coefficients include the film thickness and are subject to Onsager reciprocity. Furthermore, μ_i is the chemical potential of the component i and the subscript T signifies that the gradient is evaluated at constant temperature. The direction of the heat and the mass transfer is normal to the catalyst surface. The diagonal elements in the resistance coefficient matrix are related to the well-known Fourier and Fick processes whereas the non-diagonal

elements represent cross effects such as the Dufour and the Soret effects.

The diffusion thermoeffect or Dufour effect is the heat flux caused by a chemical potential gradient. The Dufour effect is usually significant for gaseous systems as has, for instance, been discussed by Sawford *et al* [51] and more recently by Hort *et al* [52]. A very interesting phenomenon was described by Linz [53], who found significant temperature variations in binary gas mixtures when a time-dependent external concentration gradient was applied. In several studies [54, 51, 55] it was found that the Dufour effect can induce a temperature difference up to 4 K depending on the initial composition and pressure.

The reciprocal process, thermal diffusion or the Soret effect, is the diffusional flux induced by a temperature gradient. De Groot gave a theoretical prediction of the Soret effect in 1945 [56], which arose considerable interest. Many experiments [57, 58, 59, 60] on this effect were performed in liquid solutions and electrolytes. Convection can be induced in some cases by a large Soret effect [61, 62, 63]. In a chemical vapour deposition reactor, the deposition rate was found to be changed up to 20% due to the Soret effect for some systems [64] while it was negligible for other systems [65].

In solid-gas catalytic systems both the Dufour effect and the Soret effect are potentially important because significant concentration and temperature gradients are expected between the surface and the gas bulk phase due to the surface reaction. Ignoring the Dufour and Soret effects in catalytic systems may lead to erroneous predictions for the surface reaction rate, the driving forces for heat and mass transfer, and the surface temperature.

3.2 The heat of transfer, Q_i^*

Thermodynamic cross effects like the Dufour and the Soret effect involve heats of transfer Q_i^*. Values for this quantity can not often be found in the literature for a specific chemical process. To calculate the heats of transfer in our hydrogen oxidation model system we can use a relation given by Taylor and Krishna [31], which expresses a heat of transfer in terms of the thermal diffusion coefficients D_i^T

$$Q_i^* = \sum_{\substack{j=1 \\ j \neq i}}^{n} \frac{x_j R\ T}{Ð_{ij}} \left(\frac{D_i^T}{\rho_i} - \frac{D_j^T}{\rho_j} \right) \tag{3.3}$$

In the literature thermal diffusion coefficients are usually given in units of mass per meter second. We need to divide these data by the mass densities ρ_i. Furthermore,

x_i represents the mole fraction of component i, R is the gas constant, and $Đ_{ij}$ are the Maxwell Stefan diffusion coefficients. Because the measurable heat fluxes are invariant to a change in the velocity of the frame of reference, heats of transfer obey the following relation

$$\sum_i c_i Q_i^* = 0 \tag{3.4}$$

where c_i are molar concentrations. This relation can be used as a test on the obtained values of Q_i^*.

There are two operational methods to obtain the expression of Q_i^*. In both treatments the heats of transfer are found as a ratio of two phenomenological coefficients. Since the heat of transfer is only involved in cross effects, the coupling effects should be considered separately. Therefore the basic condition we are going to use in these two methods is that only the thermal diffusion causes the molar flux or the chemical potential gradient. This is the pure Soret effect. The comparable parameters for other cross terms in the phenomenological equations can be obtained via analogous lines of reasoning, by expressing them by experimentally accessible quantities.

In the first method one starts with the Maxwell-Stefan eqs. [66] for an isothermal mass transfer of a multi-component mixture

$$\nabla \mu_{i,T} = -RT \sum_{\substack{j=1 \\ j \neq i}}^{n} \frac{x_j (u_i - u_j)}{Đ_{ij}} \qquad i = 1, 2 \cdots n \tag{3.5}$$

in which $u_i \equiv J_i / c_i$ is the velocity of the diffusing component i and the chemical potential gradient in the film is $\nabla \mu_{i,T} = \Delta \mu_{i,T} / \delta$. When large temperature gradients exist, the thermal diffusion contribution to the molar fluxes should be taken into account. Eq. (3.5) can then be augmented [66, 41] as

$$\Delta \mu_{i,T} = -RT \delta \sum_{\substack{j=1 \\ j \neq i}}^{n} \frac{x_j \left(u_i^T - u_j^T\right)}{Đ_{ij}} \qquad i = 1, 2 \cdots n \tag{3.6}$$

where u_i^T is the augmented species velocity. It includes the contribution of the thermal diffusion, which is [66]

$$u_i^T = u_i + \left(\frac{D_i^T}{\rho_i}\right) \frac{\Delta T}{\delta T}, \qquad i = 1, 2, \cdots, n \tag{3.7}$$

The thermal diffusion coefficients D_i^T in this expression have been defined in the manner of Hirschfelder *et al* [67]. $\rho_i \equiv c_i M_i$ is the mass density of the component i.

c_i and M_i are the concentration and the molar mass of the gas component i.

The species velocity due to the thermal diffusion (the pure Soret effect) is

$$u_i^T = \left(\frac{D_i^T}{\rho_i} \right) \frac{\Delta T}{\delta T}, \qquad\qquad i = 1, 2, \cdots, n \qquad (3.8)$$

Replacing u_i^T in eq. (3.6) with eq. (3.8), we obtain the chemical potential difference caused by the thermal diffusion as

$$\Delta\mu_{i,T} = -\sum_{\substack{j=1 \\ j \neq i}}^{n} \frac{x_j \; R \; \Delta T}{\Bbb{D}_{ij}} \left(\frac{D_i^T}{\rho_i} - \frac{D_j^T}{\rho_j} \right) \qquad i = 1, 2 \cdots n \qquad (3.9)$$

If the temperature difference across the film is negligible, the first of eqs. (3.1) reduces to

$$J_q' = -\sum_{i=1}^{n} \frac{r_{qi}}{r_{qq}} J_i \qquad\qquad (3.10)$$

where the heat flux is completely driven by the concentration gradients. The heat flux due to the molar flux can also be written by

$$J_q' = \sum_{i=1}^{n} Q_i^* J_i \qquad\qquad (3.11)$$

where Q_i^* is the heats of transfer by the component i. Comparing eqs. (3.10) to (3.11) one obtains the expression for the heat of transfer, expressed in terms of the resistance coefficients for the pertinent fluxes

$$Q_i^* = -\frac{r_{qi}}{r_{qq}} \qquad\qquad (3.12)$$

This is the same expression as derived by Bedeaux in [23].

Starting with the phenomenological expression for mass transfer of the component i in eqs.(3.1) and rewriting it by introducing the equation for heat transfer in it, together with eq. (3.12), one has

$$-\frac{\Delta\mu_{i,T}}{T} = -Q_i^* \; \Delta \left(\frac{1}{T} \right) + \sum_{j=1}^{n} (r_{ji} - \frac{r_{jq}r_{qi}}{r_{qq}}) J_j \qquad\qquad (3.13)$$

The chemical potential difference caused by the thermal diffusion is then

$$\Delta\mu_{i,T} = -Q_i^* \frac{\Delta T}{T} \qquad\qquad (3.14)$$

Comparing eqs. (3.9) to (3.14), one obtains the expression for the heat of transfer (eq. (3.3)). According to Taylor and Krishna it is related to experimentally accessible data.

In the second method we start with eq. (3.13) to obtain the expression for the heat of transfer Q_i^*. Using the definition of resistance coefficients R_{ij} given by Bedeaux [23]

$$R_{ij} = R_{ji} = r_{ji} - \frac{r_{jq}r_{qi}}{r_{qq}} = -\frac{\delta R}{c Đ_{ij}} = -\frac{\delta R^2 T}{p\ Đ_{ij}} \qquad \text{for} \qquad i \neq j \quad (3.15)$$

for the case of ideal gases. The thermodynamic eq. (3.13) becomes

$$-\frac{\Delta \mu_{i,T}}{T} = -Q_i^* \Delta \left(\frac{1}{T}\right) + \sum_{j=1}^{n} R_{ij} J_j \qquad (3.16)$$

For $\Delta \mu_{i,T} = 0$, this equation reduces to

$$-Q_i^* \Delta \left(\frac{1}{T}\right) + \sum_{j=1}^{n} R_{ij} J_j = 0 \qquad (3.17)$$

Using phenomenological equation for mass transfer in eq. (2.3) one obtains an expression for a molar flux J_i^T caused by the thermal diffusion.

$$J_i^T = l_{qi} \Delta \left(\frac{1}{T}\right) \qquad (3.18)$$

Replacing J_i in eq. (3.17) with eq. (3.18) gives

$$Q_i^* = l_{qi} \sum_{j=1}^{n} R_{ij} \qquad (3.19)$$

In this expression R_{ij} can be replaced with eq. (3.15). Then one can obtain an expression for the heat of transfer by component i using the relation of $\sum_{i=1}^{n} c_i R_{ij} = \sum_{i=1}^{n} c_i R_{ji} = 0$

$$Q_i^* = \sum_{j=1}^{n} \frac{c_j R\ \delta}{c\ Đ_{ij}} \left(\frac{l_{qj}}{c_j} - \frac{l_{qi}}{c_i}\right) \qquad (3.20)$$

The molar flux due to the thermal diffusion can be also written as

$$J_i^T = u_i^T c_i \qquad (3.21)$$

Substituting u_i^T with eq. (3.8) and c_i with the density $\rho_i \equiv c_i M_i$, this molar flux becomes

$$J_i^T = \left(\frac{D_i^T}{M_i}\right) \frac{\Delta T}{T\ \delta} \qquad (3.22)$$

Comparing eqs. (3.22) and (3.18), one obtains

$$l_{qi} = -\frac{T\ D_i^T}{\delta\ M_i} \qquad (3.23)$$

as an expression for the coupling conductivity coefficient.

Now we can again obtain the eq. (3.3) by replacing l_{qi} and c_i in eq. (3.20) with eqs. (3.23) and $\rho_i \equiv c_i M_i$, respectively. The Maxwell-Stefan diffusion coefficient is calculated by [68]

$$Đ_{i,j} = \sqrt{\frac{2}{\pi^3} \frac{(RT)^{3/2}}{N_A\ p\ d_{i,j}^2} \left(\frac{1}{M_i} + \frac{1}{M_j}\right)^{1/2}}, \qquad d_{i,j} = \frac{d_i + d_j}{2} \qquad (3.24)$$

where N_A is the Avogadro constant, p the total pressure of the gas mixture and d_i the diameter of the gas molecule i.

3.3 Calculated heats of transfer

We are now in a position to calculate heats of transfer and resistances for fluxes in an experimental system. Our first example will be the catalytic oxidation of hydrogen on a Pt/Al$_2$O$_3$ catalyst [42]. It is represented by the film model of Figure 3.1. The components, which participate in the conversion are H$_2$, O$_2$ and H$_2$O. Some relevant literature data about these three components are given in table 3.1.

Table 3.1: Molar mass, radius and thermal conductivity of the components

Components	H$_2$	O$_2$	H$_2$O
M_i (kg/mol)	0.002	0.032	0.018
r$_i$ ($\times 10^{-10}$ m)	0.64	1.46	1.37
λ_i ($\times 10^{-3}$ W/K m)	211.8	32.2	24.2

Under the conditions of the experiment, which was carried out with great care by Maymo and Smith [42] the conversion rate is limited by the mass transport. The

oxidation processes were carried out at 1 atm pressure and for well controlled temperatures of the reactor. The mole fraction of water is 0.023 and the mole fractions for hydrogen and oxygen are chosen in the range of 0.966-0.772 and 0.011-0.205, respectively. Under these conditions the concentration dependence of the heats of transfer are evaluated.

Maxwell-Stefan diffusion coefficients for the components could be calculated using eq. (3.24), and the molecular properties given in table 3.1. The thermal diffusion coefficients are evaluated using a computer program by Kleijn and Dorsman [69] based on Hirschfelder's method [67].

3.3.1 Concentration dependence of the heats of transfer for reactants

First we calculated heats of transfer at a constant reactor temperature of $T^g = 415$ K for various mole fractions of the gases, using eq. (3.3). Since the results indicated that the coupling between heat and mass fluxes differs for the different compounds, oxygen transferring the largest amount of heat per mole among these three gases, we did calculate the heats of transfer of the three gases keeping the mole fraction of water vapour constant and varying the mole fractions of oxygen. The thermal diffusion coefficient is an important parameter for the process of the heat of transfer. Its concentration dependence is presented as well.

It appears from these plots that non-linear relations exist between the thermal diffusion coefficients and the mole fraction of oxygen. The thermal diffusion coefficients are positive for oxygen and negative for hydrogen. The oxygen thermally diffuses away from the hot catalyst surface to the cold gas bulk phase by a negative Soret effect. The hydrogen thermally diffuses towards the hot surface.

The thermal diffusion coefficients for oxygen and hydrogen increase smoothly with mole fraction until they reach a maximum at $x_O \approx 0.15$. At higher oxygen concentrations they begin to decrease somewhat. Water vapour thermally diffuses away from the hot catalyst surface to the surrounding bulk of gas phase as long as the mole fraction of oxygen remains below 0.2. This is judged in terms of its positive thermal diffusion coefficients. But when the mole fraction of oxygen in the gas is higher than that, water vapour tends to move towards the hot surface by a thermal diffusion effect, diminishing the net transport of the reaction product to the medium. This reversal in the direction of the thermal transport of the reaction product would lead to a lower reaction rate at the catalyst surface.

The heats of transfer and the thermal diffusion coefficients for the fluxes of oxygen, hydrogen and water in figure 3.2 vary with the mole fraction of oxygen. The heats of
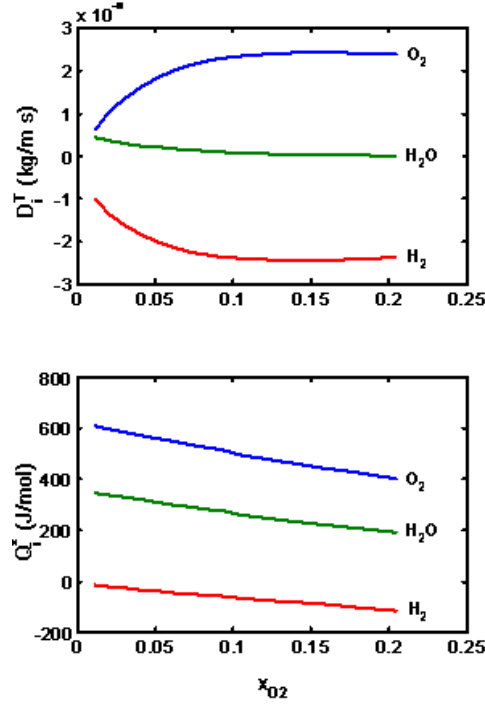
Figure 3.2: Concentration dependences of heats of transfer and thermal diffusion coefficients for O_2, H_2 and H_2O

transfer by oxygen and water vapour are positive and by hydrogen negative, which means oxygen and water vapour release heat while hydrogen takes up heat during the thermal diffusion. Heats of transfer by each mole of a component satisfy the relation $Q_O^* > Q_W^* > |Q_H^*|$. The heats of transfer by oxygen and water vapour decrease with increasing mole fraction but the absolute value increases in case of the hydrogen. Approximate linear relations hold between the heats of transport and the mole fractions of oxygen for each of the three gases. The maximum deviations of these linear plots are $+9\%$ for hydrogen, $+4\%$ for oxygen and $+2\%$ for water vapour, respectively.

An interesting phenomenon is, that the calculated heat of transfer by water and its thermal diffusion coefficient decrease with the mole fraction of oxygen, even when the mole fraction of the product (water) is kept constant. This implies that the heat of transfer for one component not only depends on its own concentration but also on the concentrations of the other components in the system. It demonstrates that

different components in a multi-component system interact with each other. This makes the system more complex than for a binary reaction system.

Finally, our calculated heats of transfer here are comparable to values obtained by Mill *et al* [49] in experiments for a liquid mixture (In the work by Mill *et al* the definition of the heats of transfer are a factor R, 8.314 J/mol, different from ours).

3.3.2   The dependence of the heats of transfer on the temperature in the medium

Heats of transfer and thermal diffusion coefficients have also been calculated for fixed concentrations of the components, but for different temperatures. The temperatures were varied from 350 K to 700 K and the calculated results were obtained at several constant combinations of reactant mole fractions. A representative result, obtained for mole fractions $x_H = 0.955$, $x_O = 0.0212$, $x_W = 0.0238$ is shown in figure 3.3.

The absolute values for the heats of transfer in each component flux are seen to increase with increasing temperature. The heat of transfer by oxygen changes by an order of magnitude in this temperature range. The variation speed is about 2 J/(mol.K).

Approximately linear relations exist in these plots, both for the calculated heats of transfer and for the thermal diffusion coefficients as a function of the reactor temperatures. Linear plots for these data would only give a maximum deviation of +2.5%. The maximum deviation from the linearity for the thermal diffusion coefficients is -5.5% for hydrogen and less than 0.5% for oxygen and water.

The signs of the deviations for the heats of transfer and the thermal diffusion coefficients differ for the three components. In absolute terms the heats of transfer by the oxygen and the water increase faster than the heat of transfer by the hydrogen that is a primary reactant in the catalytic system. This effect seems to be caused by the fact that the thermal diffusion coefficients for oxygen and water increase more slowly with the temperature than they decrease for the hydrogen.

Observations like these, derived from the calculated heats of transfer and thermal diffusion coefficients could have technological implications for better running of the processes for catalytic hydrogen oxidation - like in batteries and fuel cells. But the objective of our calculations has been different from that. The derivations and calculations for heats of transfer and thermal diffusion coefficients were undertaken because they are key factors for the coupling effects in heterogeneous catalytic reactions and the coupling effects are very important for the accurate surface temperature predictions. Measured data from Maymo's carefully executed experiments on catalytic hydrogen oxidation have only been used here as a specific example to illustrate the ac-
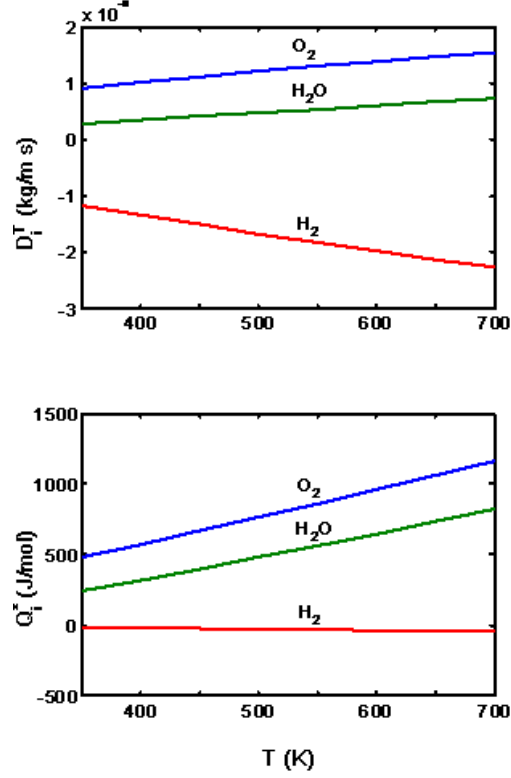
Figure 3.3: Temperature dependences of the thermal diffusion coefficients and heats of transfer for H_2, O_2 and H_2O

curacy of our model. Now, to investigate the coupling effects between mass and heat fluxes and how they will affect the surface temperature of the catalyst, we shall proceed and calculate the resistance coefficients for the coupled fluxes in that particular model system.

3.4 Calculated resistance coefficients

For calculating resistance coefficients we shall again refer to the film model, as sketched in figure 3.1. We have assumed in the derivation of the method for obtaining resistance coefficients that there is good conduction at the surface of the pellet, so that the surface temperature and the pellet temperature are equal to the gas temperature in the film near the surface. This may deviate somewhat from the real experimental

situation in the described experiment, but the discrepancies seem of minor impact on the results. We shall focus on the temperature difference across the gas film and neglect a possible temperature difference between the surface and the center of the pellet. This is sufficient to assess the importance of the Dufour and the Soret effects.

Two reciprocal methods are available to relate the fluxes and thermodynamic forces in the thin film by sets of phenomenological equations. The first is expressing the differences in temperature and chemical potentials across the film in terms of resistance coefficients

$$
\begin{cases}
\Delta \left(\dfrac{1}{T} \right) = r_{qq} J_q' + \displaystyle\sum_{i=1}^{n} r_{qi} J_i \\
-\dfrac{\Delta \mu_{i,T}}{T} = r_{iq} J_q' + \displaystyle\sum_{j=1}^{n} r_{ij} J_j
\end{cases}
\tag{3.25}
$$

The second alternative expresses the fluxes in terms of the temperature and chemical potential differences across the film using conductivity coefficients. Then, following Kubota's [32] reasoning, the mass transfer coefficients can be simplified into effective coefficients $l_{i,eff}$. Consequently, we only have diagonal effective mass transfer coefficients in our phenomenological equations, but these have become dependent on process conditions. Nevertheless, this reduces the mathematical burdens considerably, because all the the non-diagonal elements for mass transfer are zero. Therefore we write:

$$
\begin{cases}
J_q' = l_{qq} \Delta \left(\dfrac{1}{T} \right) - \dfrac{1}{T} \displaystyle\sum_i l_{qi} \Delta \mu_{i,T} \\
J_i = l_{qi} \Delta \left(\dfrac{1}{T} \right) - \dfrac{1}{T} l_{i,eff} \ \Delta \mu_{i,T}
\end{cases}
\tag{3.26}
$$

Essentially, eqs. (3.25) and (3.26) are the same as the eqs. (2.1) and (2.5) in chapter 2, respectively, but written in different forms.

In the film model we shall study the combination of heat and mass transfer and only use one film thickness of 0.1000 mm to simplify the mathematics (even though usually the film thickness is assumed to be different for heat and for mass transfer).

This choice was made after an investigation of the sensitivity of calculated concentrations and surface temperatures for the thickness δ of the boundary layer in our transport model. Among the range of possible film thicknesses for normal technological conditions, given by Taylor and Krishna [31] we calculated the surface temperatures and the mole fractions of oxygen near the surface of the catalyst and found that the calculated surface temperature and mole fraction of oxygen near the surface will both vary linearly with the film thickness, as seen in Figure 3.4.

When the film thickness is chosen as 0.0935 mm, the calculated surface temperature is exactly the same as the measured surface temperature, 390.7 K. However,
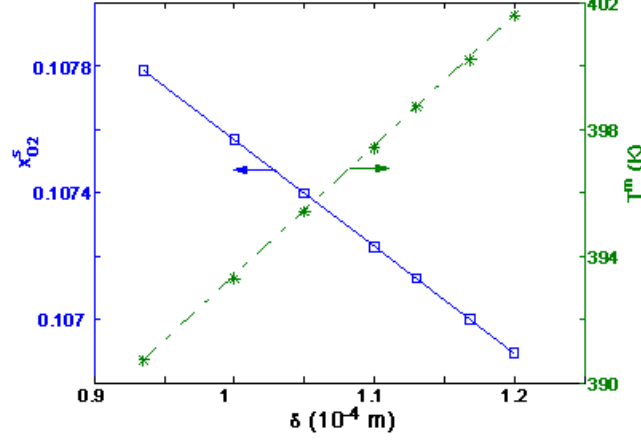
Figure 3.4: Calculated catalyst surface temperature and mole fraction of oxygen near the surface when various thicknesses of the thin film are chosen

the calculated mole fraction of oxygen near the surface is much larger than the given value under these conditions. With an increased film thickness of 0.120 mm, the calculated surface temperature becomes 401.6 K, which is not so close to the measured value any more. The calculated mole fractions of oxygen near the surface are exactly equal to the given value by Maymo [42] for a thickness δ=0.1168 mm. However, the corresponding surface temperature of 400.2 K is much higher than the measured value.

The real experimental film thicknesses must lie in the range between 0.0935 and 0.1168 mm. For our model calculations we have, accordingly, chosen $\delta = 0.1000$ mm. This keeps the combination of calculated surface temperatures and mole fractions close to the measured values. Otherwise, the film thickness could become a sensitive parameter in our theoretical predictions. Any discrepancy between calculated and measurable results can be minimized by a slight adaptation of the gas film thickness.

In a calculation of the temperature and the concentrations near the active catalyst surface, the coefficients in the equations (3.25), (3.26) need to be determined. The resistance coefficients are calculated by using the method given by Bedeaux and Kjelstrup [23]. The heat transfer resistance coefficient r_{qq} is related to the thermal conductivity of the gas mixture λ_m as

$$r_{qq} = \frac{\delta}{\lambda_m T^2} \tag{3.27}$$

where δ is the thickness of the layer. The resistance cross coefficients are

$$r_{qi} = r_{iq} \equiv -r_{qq} \ Q_i^* \tag{3.28}$$

Maxwell-Stefan diffusion coefficients are related to the resistance coefficients by

$$R_{ji} = R_{ij} = r_{ji} - \frac{r_{jq} r_{qi}}{r_{qq}} = -\frac{\delta R}{c \DJ_{ij}} = -\frac{\delta R^2 T}{p \ \DJ_{ij}} \qquad \text{for} \qquad i \neq j \tag{3.29}$$

where we use the ideal gas law and p is total pressure of the gas mixture. The diagonal coefficients are obtained by using the relation

$$\sum_{i=1}^{n} c_i R_{ij} = \sum_{i=1}^{n} c_i R_{ji} = 0 \tag{3.30}$$

The mass transfer resistance coefficients can now be obtained from the expression

$$r_{ij} = R_{ij} + \frac{r_{iq} \ r_{qj}}{r_{qq}} \tag{3.31}$$

Taking the conditions from the chosen model experiment on the kinetics of hydrogen oxidation by Maymo $et \ al$ [42] we have calculated the transport in the gas film around a catalyst pellet of 2.149 g with a diameter of 1.86 cm. The gas mole fractions are 0.857 for H_2, 0.111 for O_2 and 0.032 for H_2O, respectively. The average temperature in the gas film was 373.6 K. Under these conditions, the average rate of the conversion reaction was 140.5×10^{-6} mol/s per gram of catalyst. The total pressure was 1 atm. The thermal conductivity of the gas mixture is calculated with the relation $\lambda_m = \sum_i x_i \lambda_i$. The thermal conductivities of three gases at temperature of 374 K are taken from ref. [70] and are shown in table 3.1.

The resulting resistance coefficient matrix in SI units is then given by

$$\begin{pmatrix} r_{qq} & r_{qH} & r_{qO} & r_{qw} \\ & r_{HH} & r_{HO} & r_{Hw} \\ & & r_{OO} & r_{Ow} \\ & & & r_{ww} \end{pmatrix}$$

$$= \begin{pmatrix} 3.855 \times 10^{-9} & 2.407 \times 10^{-7} & -1.632 \times 10^{-6} & -7.853 \times 10^{-7} \\ & 1.103 \times 10^{-2} & -6.771 \times 10^{-2} & -6.061 \times 10^{-2} \\ & & 6.102 \times 10^{-1} & -3.034 \times 10^{-1} \\ & & & 2.676 \end{pmatrix}$$

The matrix obeys Onsager symmetry. Therefore we have presented only half the number of the actual values for resistance coefficients in the modelled process. These resistance values will be needed for the calculation of the surface temperature T^m of the catalyst in this heterogeneous, transport limited catalytic reaction.

Chapter 4

The catalyst surface temperature T^m in a transport limited catalytic reaction

The film model, as sketched in figure 3.1, is used again for the calculation of the temperature at a catalyst surface. The calculated resistance coefficients of the coupled transport fluxes in this model form a description of the transport limited conversion process. We continue the irreversible thermodynamics approach and proceed to calculate the catalyst temperature T^m during the catalytic hydrogen oxidation reaction which we have selected from the literature as a qualitatively excellent experimental example. Strong Dufour and Soret effects are expected because of the large temperature gradients in the gas film, which surrounds the active catalyst particles. These gradients span the temperature range between the bulk gas temperature T^g and the surface temperature T^m of the external catalyst surface, which is often measured. It is regarded as the reaction temperature by most experimentalists. This assumption seems correct for a transport limited process, but it remains questionable in other types of reaction kinetics, where the reaction temperature T^r and the catalyst temperature T^m are related to the reaction rate and the heat transport processes, respectively. But with the chosen experiment we have good experimental data for a transport limited reaction and we can compare these with model predictions, based on coupled heat and mass transfer fluxes at the catalytic interface.

In the gas outside the film reactant concentrations, partial pressures of the gases and the temperature T^g are known under conditions, which approach an ideal stirred tank. The reaction rates, the catalyst surface temperatures as well as the oxygen surface concentrations were given in the chosen model experiment. These data can be used in our analysis and compared with predicted values. In this respect the oxygen concentration at the surface is of special interest, because we have seen the special properties of the gas in thermal diffusion processes as an outcome of the thermodynamic analysis in Chapter 3.

That temperature and concentration gradients are assumed only to exist in a thin film around the catalyst pellet, is somewhat different from the real conditions in the experiment. The assumption is that the condensed material of the catalyst has a better heat conduction up to the surface of the pellet. In that case the surface temperature T^m and the pellet temperature are equal, and presumed equal to the temperature in the gas film near the surface.

The possibility of a temperature profile inside the catalyst is worth some consideration. The conversion may also be active inside the pores of the porous catalyst pellet. The solid catalyst is a porous material with very low thermal conductivity, which has been determined experimentally. The measured value of 0.26 W/(K.m) is only marginally higher than the thermal conductivity of the gas mixture itself, which was 0.21 W/(K.m).

Inside such a porous pellet the net energy is still constant in the steady state. No extra energy will be accumulated in the pellet or at the surface. This is only possible if all the generated energy of the conversion is transported away. The temperature inside a porous catalyst pellet will inevitably be higher than the surface temperature T^m at its external surface if there are catalytic conversion rates inside the catalyst pores and the low thermal conductivity of the porous material. Some layer of the catalyst material, inward from its external surface, behaves as an extension of the gas film around the catalyst surface. That additional part of the film generates a big percentage of the overall reaction heat. The direction of the net heat fluxes inside the catalyst can only be from inside to the external surface, since all heat generated by reactions inside the pores and at the surface of the catalyst particle must eventually pass through the external surface and into the gas phase. The transfer is, of course, through the gaseous boundary layer which is part of our idealized film model.

Therefore, the following relation holds for the effective fluxes into the medium

$$J_e = J_q^{'} + J_H H_H + J_O H_O + J_W H_W = J_q^{'} - \Re^{'} \Delta_r H / a = 0 \qquad (4.1)$$

But in a porous catalyst, the process inside the narrow pores is starved from reactants.

It is even more severely limited in rate by the vanishingly low transfer of reactants compared with the outside surface of the catalyst. Its contribution to the overall fluxes in the boundary layer are negligible.

The net heat flux J_q' can be written as the product of the reaction heat and the integrated reaction rate in the catalyst. The catalytic process in our model is assumed to be a pure surface reaction.

$$J_q' = \frac{\Re' \Delta_r H}{a} \tag{4.2}$$

where H_i is the molar enthalpy of component i and $\Delta_r H$ the reaction enthalpy, 244.34 kJ/mol, at 374 K.

Focussing on the temperature difference across the gas film and not considering a temperature difference between the surface and the center of the pellet is sufficient to assess the importance of the Dufour and the Soret effects. The differences in temperature and chemical potentials across the film are expressed in terms of resistance coefficients for the fluxes, see also eq. (3.25) in Chapter 3.

$$\begin{cases} \Delta\left(\dfrac{1}{T}\right) = r_{qq}J_q' + \displaystyle\sum_{i=1}^{n} r_{qi}J_i \\ -\dfrac{\Delta\mu_{i,T}}{T} = r_{iq}J_q' + \displaystyle\sum_{j=1}^{n} r_{ij}J_j \end{cases} \tag{4.3}$$

4.1 Surface temperatures and concentrations

In the steady state of the catalytic conversion reaction, the molar fluxes for the three components are related by stoichiometry of the chemical reaction. The transport through the gas film is also related to the reaction rate in the catalyst surface, which is, in our case, determined by the mass transport fluxes as a limiting factor. The direction of the molar flux to the surface is defined positive. Therefore:

$$J_H = 2J_O = -J_W = \frac{\Re'}{a} = J \tag{4.4}$$

where $\Re'$ is the average surface reaction rate and a the external surface area of the catalyst pellet. Since no reaction takes place in the gas film the energy flux is continuous and constant throughout.

4.1.1 Calculated and experimental results

The experimental data give measured values for the reaction rate of the hydrogen oxidation. The mole fraction of oxygen near the surface are also given. We can use

either of these two parameters in our model calculations and compare one result with the experimental value of the other. Let us start with the experimental reaction rate and calculate the surface temperature and mole fractions near the surface. To prove the working of the model we shall also follow the alternative route and investigate the difference between the measured and the theoretical conversion rates for this transport limited catalytic process.

In the model experiment the conversion rate of the hydrogen $\Re^{''}$ was 140.5×10^{-6} mol/s per gram of catalyst for an external surface area of the catalyst $a = 3.368 \times 10^{-6}$ m^2. The gas temperature T^g for this rate is given as 356.6 K. The total gas pressure was 1.0 atm, with mole fractions of hydrogen, oxygen and water of 0.857, 0.111 and 0.032 respectively. Using eq. (4.3) and referring to the values of the resistance coefficients for this condition, which were calculated for this system in the previous chapter, we can calculate the surface temperature of the catalyst and the concentrations of the reactants near the surface, which would give this conversion rate in the film model.

The measured temperature difference across the thin gas film was found to be ΔT = 34.1 K in this experiment, and the mole fraction of the oxygen at the surface of the catalyst was given to be $x_O^s = 0.107$, which is 0.004 smaller than the mole fraction of the oxygen in the ambient gas.

The results of the model calculations are presented in Table 4.1.

Table 4.1: The surface temperatures and mole fractions by using reaction rate

	Measured	Calculated		Prediction error
		Dufour effect	**no Dufour effect**	
T^m(K)	390.7	393.3	393.3	2.6
		Soret effect	**no Soret effect**	
x_H^s	–	0.8576	0.8559	–
x_O^s	0.107*	0.10757	0.10901	0.5%
x_W^s	–	0.0350	0.0352	–

1

It demonstrates that the reaction rate can be used to predict the surface temperature of the catalyst within experimental error. It could, therefore, be used as a reliable "thermometer" for the temperature T^r in the reaction plane for this catalytic system. Of course, in a transport limited heterogeneous system the temperatures T^m of the catalyst and T^r of the reaction plane are expected to be equal. But in other heterogeneous reactions this is not necessarily so.

Quantitatively, the contributions of the Dufour effect to the heat flow and of the

---
[1] *, value given in the paper [42]

Soret effect to the mass transfer in the thin gas film are rather small. We have concluded this from the comparison of the calculated data with the cross effects included (eq. (4.3)) and without them. The temperature and the mole fractions listed in table 4.1 are those in the gas film near the catalyst surface. They appear not to be very different in the two cases.

However, the relative deviations from the measured data in temperature and in the mole fraction of oxygen across the thin gas film, (ΔT=34.1 K and Δx_O=0.004, respectively) are quite large. The relative deviation for the calculated surface temperature is then 8%. Considering the Soret effect, the relative deviation in the predicted mole fraction of the oxygen near the surface is 14%. This relative deviation becomes extremely large (50% or so) if the calculations were made without considering the Soret effect. A prediction for the mole fractions near the surface without considering the Soret effect is, therefore, unreliable. The large temperature difference ΔT=34.1 K is the driving force for the thermal diffusion or the Soret effect which is rather significant for our model system.

This conclusion becomes even clearer if the calculation is made the other way around. In that case we use the given mole fraction of oxygen near the catalytic surface as the input for the model and calculate the catalyst temperature.

We start replacing J_q', J_i and μ_i in eq. (4.3) with eqs. (4.2), (4.4) and relation of $\mu_i = \mu_i^0 + RT \ln x_i$, and find expressions for the molar flux and the surface temperature

$$
\begin{cases}
J \left(r_{qO} \, \Delta_r H + r_{OH} + \frac{1}{2} r_{OO} - r_{OW} \right) = R \ln \dfrac{x_O^g}{x_O^s} \\
\dfrac{1}{T^m} - \dfrac{1}{T^g} = J \left(r_{qq} \, \Delta_r H + r_{qH} + \frac{1}{2} r_{qO} - r_{qW} \right)
\end{cases}
\tag{4.5}
$$

We discovered, using these expressions, that the surface temperature and the reaction rate are very sensitive for small changes in the mole fractions near the surface. Like in a fuel cell, the reaction rate at the catalytic hydrogen electrode is limited by the molar fluxes through the thin film, and by the oxygen transport in particular.

We have calculated the molar fluxes in the thin gas film for two slightly different mole fractions of oxygen near the surface. The value given in the model system was $x_O^s = 0.107$. The other value, $x_O^s = 0.10757$ is our calculated result in Table 4.1 with the Soret effect included.

In these two cases the calculated oxygen molar fluxes were 0.1624 mol/(m^2 s) and 0.1390 mol/(m^2 s), respectively. Again, a small difference of 0.5% for the mole fractions of oxygen near the surface corresponds to a 14% deviation in the prediction of the mole fractions across the film and about 17% difference in the predicted molar flux of oxygen. Therefore, we conclude that the mole fraction of oxygen near the surface

of a hydrogen fuel cell electrode and its surface temperature T^m must probably be controlled very accurately, to obtain a predictable and reliable functioning of the catalytic reaction process.

This is also made clear and explicit in table 4.2, where we have calculated the temperature T^m and the reaction rate for these two slightly different amounts of available oxygen reactant. The availability of the reactant is controlled by the overall oxygen flux in the gas film. It seems important to investigate the role of the Dufour and Soret fluxes of heat and chemical components in the functioning of the oxidation process.

Table 4.2: The surface temperature and reaction rate by using oxygen mole fraction near the surface

		Meas.	Calculated		
			Dufour & Soret	no Soret	no Dufour
x_O^s=0.107	T^m (K)	390.7	400.25	440	400.26
	$T_{cal.}^m - T_{meas.}^m$(K)	–	**9.6**	**49**	**9.6**
	$\Re''(\times 10^{-6}$mol/s g$_{cat.}$)	140.5	164.1	285.2	164.2
	Pred. error for $\Re''$	–	**17 %**	**103 %**	**17 %**
x_O^s=0.10757	T^m (K)	390.7	393.31	426	393.32
	$T_{cal.}^m - T_{meas.}^m$(K)	–	**2.6**	**35**	**2.6**
	$\Re''(\times 10^{-6}$mol/s g$_{cat.}$)	140.5	140.4	244.1	140.5
	Pred. error for $\Re''$	–	**0 %**	**74 %**	**0 %**

Again, the Dufour effect turns out to be negligible, but the Soret effect is very significant. With this calculation method the surface temperature and the reaction rate are predicted very well. This is especially so, when the starting point is the mole fraction of oxygen x_O^s=0.10757. This value was obtained from the model by introducing the measured reaction rate at the catalyst surface. The outcome of the calculation here is a surface temperature T^m, which is only 2.6 K different from the measured value. This is probably within the experimental error. But in view of its large contribution to the concentrations of the reacting species we conclude that it is necessary to include the Soret effect in the fluxes of the thin film model to obtain reliable values of the surface temperature and the reaction rate.

4.1.2 Water vapour mole fractions

The mole fraction of the water vapour at the entrance of the reactor or the inlet value was 0.023 in the experiments [42]. We used this value for the mole fraction of water in the gas phase. In steady state, the mole fraction of the reaction product water in

the gas phase, which was not measured, will be higher than the inlet value.

To assess the importance of this effect we have used various values of the water vapour concentration to calculate the surface temperature in our model. With the varying water vapour mole fractions the resistance coefficients vary as well. The effect of the water mole fraction in the gas phase on the surface temperature prediction is shown in figure 4.1.
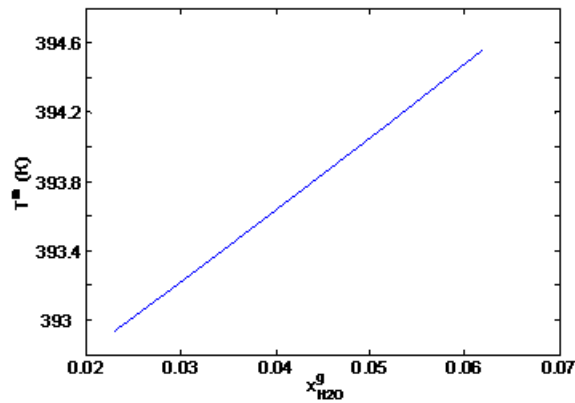

Figure 4.1: Catalyst surface temperature dependence on the water mole fraction keeping x_{O_2} constant in the bulk gas phase

Calculated catalyst surface temperature varies linearly with the water mole fraction. However, the variations are smaller than the errors in our calculated values. We conclude that in a reasonable range the chosen value of the water vapour mole fraction in the reactor does not influence the reliability of the calculated surface temperature.

4.1.3 Thermal diffusion effects

An interesting observation is that the mole fraction of hydrogen near the surface is a little bit higher than that in the gas bulk phase although the hydrogen is consumed by the surface reaction. The simple reason is that the hydrogen thermally diffuses to the surface and the pure mass transfer rate plus the thermal diffusion rate is larger than the consumption rate by the conversion reaction at the catalyst surface.

In our model reaction the thermal diffusion effect is found to reduce the reaction rate about 74%. The positive thermal diffusion coefficient implies that the oxygen tends to thermally diffuse away from the reacting surface and back into the gas bulk phase. The Soret effect has a considerable influence on the net oxygen supply for the reaction. This theoretical observation is in line with results by Jenkinson and Pollard

[64], who discovered in a chemical vapour deposition reactor with large temperature gradients at the solid/gas interface, that the deposition rate could be lowered or raised up to 20% by the effects of the multi-component thermal diffusion.

The effective surface reaction rates which are affected by thermal diffusion cross effects between the fluxes will also influence the temperature T^r in the reaction surface itself. This follows from our results, but such an effect had not yet been calculated before. In the modelled heterogeneous, transport limited, exothermic catalytic hydrogen oxidation the reaction rate is strongly reduced. The negative thermal diffusion effect of the oxygen will, therefore, directly affect the activity and the selectivity of the catalyst. In such a conversion process the Soret effect produces a lower temperature T^r in the two-dimensional reaction plane and reduces the conversion rate in accordance with Arrhenius' Law. Here, T^r is equal to T^m because of the transport limited conditions, whereas these two temperatures may differ when the conversion rate is limited by the kinetics of a catalytic reaction.

4.2   Effective conductivity coefficients

In Chapter 2 we introduced Kubota's concept to use effective phenomenological constants in a set of flux-force equations for the description of overall process. In order to investigate the validity of this proposition we calculated the effective conductivity coefficients $l_{i,eff}$ for our experimental model system and predicted the surface temperature and mole fractions from these parameters. We expressed again the fluxes in terms of the temperature and chemical potential differences across the film, and conductivity coefficients l, see also eq. (3.26):

$$\begin{cases} J_q' = l_{qq}\Delta\left(\dfrac{1}{T}\right) - \dfrac{1}{T}\sum_i l_{qi}\Delta\mu_{i,T} \\ J_i = l_{qi}\Delta\left(\dfrac{1}{T}\right) - \dfrac{1}{T}l_{i,eff}\,\Delta\mu_{i,T} \end{cases} \tag{4.6}$$

Using Kubota [32, 31] 's approximation the mass transfer coefficients were reduced to the effective coefficients $l_{i,eff}$. These effective mass transfer coefficients are of a purely diagonal character and the non-diagonal elements for mass transfer are zeros.

Fick's effective diffusion coefficients of the three gas components are calculated by using eq. (2.10) (in Chapter 2) in SI units for $T = 373.6$ K, $x_{H_2} = 0.857$, $x_{O_2} = 0.111$ and $x_{H_2O} = 0.032$. The values are

$$\begin{pmatrix} D_{H,eff} & D_{O,eff} & D_{W,eff} \end{pmatrix} = \begin{pmatrix} 7.872 \times 10^{-4} & 2.123 \times 10^{-4} & 2.758 \times 10^{-4} \end{pmatrix}$$

The phenomenological l-coefficients are calculated by using eqs. (2.9), (2.11) and (2.15)

$$\begin{pmatrix} l_{qq} & l_{qH} & l_{qO} & l_{qW} \\ & l_{H,eff} & 0 & 0 \\ & & l_{O,eff} & 0 \\ & & & l_{W,eff} \end{pmatrix}$$

$$= \begin{pmatrix} 2.594 \times 10^8 & -1.653 \times 10^3 & 3.915 \times 10^2 & 7.054 \times 10^1 \\ & 2.647 \times 10^1 & 0 & 0 \\ & & 9.244 \times 10^{-1} & 0 \\ & & & 3.463 \times 10^{-1} \end{pmatrix}$$

which are used for the calculations of the surface temperature and concentrations near the surface.

Rewriting the flux-force equations (4.6) using the relation of $\mu_i = \mu_i^0 + RT \ln x_i$, one obtained

$$\begin{cases} J_q' = l_{qq} \left(\dfrac{1}{T^m} - \dfrac{1}{T^g} \right) - R \sum_i l_{qi} \ln \dfrac{x_i^s}{x_i^g} \\ J_i = l_{qi} \left(\dfrac{1}{T^m} - \dfrac{1}{T^g} \right) - R \, l_{i,eff} \, \ln \dfrac{x_i^s}{x_i^g} \end{cases} \quad (4.7)$$

which are used to repeat the calculations for the surface quantities. The results from these operations were compared with values, which had been calculated with the full matrix of resistance coefficients for the process. The two methods were found to be practically equivalent. The calculated catalyst surface temperature is 393.35 K. Therefore, the maximum discrepancy between the calculated results in these two methods was as small as 0.01%.

It turns out that effective conductivity coefficients are a reliable tool for such model calculations. The effective l-coefficients for mass transfer do include in their values the contributions from the coupling between various molar fluxes. Effective conductivity coefficients can be transformed into effective Fick diffusion coefficients in a stagnant gas film. Heats of transfer can be defined in two ways by using the resistance coefficient for heat transfer and the effective conductivity coefficients for mass transfer, respectively. Both methods are working very well.

4.3   Conclusions

Irreversible thermodynamics for conjugate fluxes and forces is a systematic way to evaluate coupling between seemingly independent processes, like the heat and mass

transfer in a diffusion boundary layer in front of a catalyst surface.

An interesting and unexpected observation about the transport limited oxidation of hydrogen is, that at the catalyst surface, because of thermal diffusion, the mole fraction of hydrogen near the surface remains higher than that in the gas bulk phase. The Soret effect overcompensates the consumption of hydrogen by the surface reaction.

From the experimental rate of the catalytic reaction we have been able to calculate the surface temperature T^m of the catalyst. This temperature is strongly affected by the Soret cross effects. Whereas the Dufour effect is negligible under the experimental circumstances. It was discovered that the Soret effect or the thermal diffusion considerably influences the mole fractions of reactants near the surface.

It is for the first time that such a Soret effect is found to significantly influence the surface temperature and, therefore, the reaction rate at a catalyst surface. The calculated surface temperature T^m is lowered by 39 K as a result of the negative Soret effect. Thermodiffusion co-determines the mole fraction of the reactive oxygen near the surface because it creates a flux of oxygen that diffuses away from the hotter catalytic surface. The surface temperature of the catalyst, and, consequently the rate of the chemical conversion in the reaction plane are significantly reduced by this cross effect.

Chapter 5

The 2-D reaction temperature excess, $\Delta \mathbf{T} = \mathbf{T}^r \text{-} \mathbf{T}^m$

5.1 Heterogeneous reaction mechanisms

In kinetic models for heterogeneous catalysis the reaction path consists (at least) of a chain with five different types of kinetic steps [71, 72]. Each of these steps could, under the right conditions, become the limiting factor in the conversion rate.

For a heterogeneous conversion mechanism in the surface of a catalyst it is needed that:

(1) Reactant molecules and the dissipated heat of the reaction must be exchanged between the ambient bulk phase and the external and internal surface of the catalyst by the available transport (diffusion, convection *etc.*) in the medium.

(2) Reactant molecules chemisorb at the active sites on the catalytic surface. An adsorption isotherm determines the available concentration of chemisorbed species in the interface. The heat of chemisorption affects the potential energy and the stability of the adsorbate molecules.

(3) Reactant molecules are converted into products by a chemical reaction at the active sites. The conversion rate is related to the temperature in the reaction plane by the Arrhenius equation.

(4) Product molecules desorb from the catalyst surface. This makes catalytic sites available again for chemisorption of the next reactant molecule.

(5) Products and generated heat diffuse away from the catalyst surface and into the ambient medium.

The steps (1) and (5) are processes of heat and mass transfer, like those which

were analyzed in Chapters 3 and 4. Near an interface there can be coupled fluxes of heat and mass transfer processes, as described by Fourier's and Fick's laws together with the Soret and Dufour cross-effects.

Steps (2), (3) and (4) involve chemisorbed molecules in a 2-dimensional (Gibbs', "dividing") space. Properties of that plane must be described in terms of "surface excess quantities", like adsorbed amounts, extra entropy, enthalpy of the surface etc. The heterogeneous catalytic effect of the surface is described as a "surface excess rate" in that plane.

The excess rates in steps (2) and (4) are determined by the thermodynamics and kinetics of chemisorption. The excess rate in step (3) is a chemical conversion rate. Adsorbed reactant molecules are converted into other, equally adsorbed products. The dependence of the reaction rate on the temperature is described by the Arrhenius equation.

Each step on the reaction path sets the stage for the next elementary step in the conversion. And each elementary reaction step could, under circumstances, become rate limiting in the catalytic conversion of reactants to products. Whether it will be the slowest step in the chain depends on the reactant concentrations and on the operation conditions in the experiment. The overall rate of the conversion is controlled by this slowest elementary step in the chain of events which constitutes the pathway of the reaction along the reaction coordinate. All the faster elements in the chain of elementary steps retain equilibrium values for beginning and final configurations.

The character of the rate determining mechanism can be guessed from the temperature dependence of the reaction rate. Three regimes can often be distinguished for the same catalytic reaction. When the temperature of the reactor rises [73], conversion rates may successively become limited by the chemical kinetics of the catalyzed process, by internal diffusion inside the porous catalyst and by external mass transfer of reactants and products. At low temperatures the reaction rate is very low. The diffusion rate of molecules is then relatively larger than the reaction rate. In these situations the conversion (step (3) limits the overall rate of the process right at the source of the products. The measured overall rates of the catalytic process are then determined by the kinetics of the chemical reactions at the surface. The experimental activation energy E_a is the true activation energy of these surface reactions. It is of the order of 100 kJ/mol, the energy involved in making and breaking chemical bonds in molecules.

With increasing temperatures the diffusion coefficients of reactant and product molecules will increase in a linear fashion, whereas the rates of the chemical reactions grow exponentially. At the higher temperatures catalytic sites remain available inside

the porous catalyst structure. But because of hindered diffusion through a porous material these sites may easily become starved of chemisorbed reactant species. Both the rapid chemical reaction which consumes the reactants, and the internal diffusion in the catalyst, which must deliver reactants to the active sites are temperature dependent. With some types of catalyst materials this interplay between rate limiting mechanisms can result in a non-linearity of the Arrhenius plots [74, 75]. The effectively measured activation energies in such situations with porous heterogeneous catalysts give apparent values no more than half of the "real" activation energy for the conversion reaction itself.

At even higher temperatures the mass transfer in the diffusion boundary layer around the catalyst particles will eventually limit the overall rate of the process. It restricts the mass transfer by diffusion between the catalyst and the ambient. In that case the effectively measured conversion rate is equal to the mass transfer rate. It is sensitive for intensive stirring or higher flow rates. The apparent activation energy is that for diffusion, which is typically in the order of 10 kJ/mol.

Rates which are controlled by the mass transfer steps (1) and (5) depend on diffusion coefficients and flow rates, and, sometimes, on porosity and tortuosity (inner surface) of the catalysts. Rate limitations, which are due to these steps can easily be identified, because of the sensitivity for flow rate and non-sensitivity for temperature. Their temperature dependence is through heat conductivity and diffusion coefficients – which explains the low apparent activation energies of these processes.

Rates of chemisorption processes will normally increase with the temperature, at least in terms of the Turn Over Number per active site. But this effect is often obscured by the lower amounts of reactant molecules, which remain chemisorbed at more elevated temperatures. This adsorption effect limits the conversion rates, since fewer reactant molecules will then be available in the reaction plane. Van de Runstraat et al. claim that this effect alters the reaction order [76].

There are several telltale criteria for "kinetically controlled" chemical reaction processes in the literature on heterogeneous catalysis:

(a) The conversion rate is not sensitive to the flow rates in the reactor.

(b) The conversion rate increases quickly (exponentially) with increasing temperature.

(c) The experimental activation energy is of the order of 100 kJ/mol.

For experiments on study of chemical kinetics and the mechanisms of these systems one uses differential "thin layer" flow reactors. In that type of reactor conversion rates can be kept very low compared to the transport rates. When adsorption and desorption are not rate-limiting, the availability of reactant and product molecules

remains close to saturation in all the elementary steps of the types (1), (2), (4) and (5). Only the conversion step is focussed upon under these chosen conditions. The activation energy and the temperature dependence of the overall process are determined by the type (3) chemical reaction step at the catalytic surface.

5.2 Heat storage and heat flux as thermal effects in a 2-D catalytic reacting surface

An essential aspect of heterogeneous compared with homogeneous catalysis is, that the chemisorption and the conversion itself are limited to the adsorbed monolayer at the interface between the catalyst and the fluid. That a kinetically controlled catalytic conversion reaction can only take place in this interface brings special thermodynamic consequences for the rates of conversion and their relation to heat dissipation. In particular, the 2-dimensional space for a surface reaction is a separate thermodynamic system. In such a system there exists the possibility of a thermodynamic coupling between the conversion and the heat transfer processes, because of the Onsager relations. In a homogeneous three-dimensional volume this coupling between a (scalar) chemical conversion process and a (vectorial) heat flux would be forbidden by the Curie-Prigogine principle. But in an anisotropic system like an interface the coupling could be allowed. A question would then be, how to describe a heat capacity in such a two-dimensional reaction plane. The interface should, somehow, be capable of storing an excess quantity of heat and then generating a heat flux, driven by the temperature difference in the reacting plane. Like in the previous chapter, the relation between the flux and the driving force would define a resistance coefficient for the thermal effect in the diffusion boundary layer.

The special properties of the monolayer can be discriminated from those of the two adjacent bulk media (catalyst and fluid) in terms of thermodynamic excess quantities. An excess amount of adsorbed reactant, an excess enthalpy, etc. are then assigned to the hypothetical two-dimensional plane in which the catalytic conversion takes place. In fact the conversion rate itself is an excess rate. It is very large, compared with the rates of the uncatalyzed reactions in the two bulk phases.

The location of this geometrical plane (a "Gibbs dividing surface") was chosen – at will, for convenience – somewhere in the interfacial region where the reactants participate in the reaction. This choice, however, has fixed all the values of all the excess quantities, which must be assigned to this essentially 2-dimensional reaction space. One excess quantity is the stored energy or enthalpy in the interface. By being fixed at the adsorbed monolayer of reactant molecules the reaction plane also acquires

an excess amount of heat, and, as a consequence, a 2-dimensional surface temperature. The heat capacity is responsible for storing the latent excess heat at the temperature T^r of the reaction plane. It can be thought of as a percentage of the adsorbed product molecules, which are still in the excited state. These excited product molecules retain the bond energies that are set free by breaking up the activated complex. They return to the ground state and release their excess energy as heat to the two-dimensional system. This release of the reaction heat is the thermal process that is coupled with the chemical conversion rate.

The temperature of the reaction plane will, therefore, differ from the temperatures of the catalyst material and of the medium with the reactants.
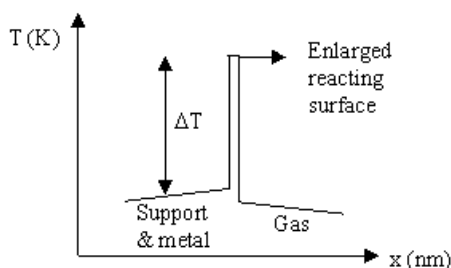

Figure 5.1: Schematic diagram of reaction temperature at 2-D catalytic surface for an exothermic reaction

Focussing here on gas-solid catalytic systems, the medium is a gas atmosphere. Three different temperatures can be distinguished in figure 5.1. Each of them plays a role in the interpretation of experiments with heterogeneous catalysis. The gas temperature T^g of the medium, which contains the unadsorbed reactant molecules, is set by the reactor conditions. During a reaction process the temperature of the catalyst particles T^m differs from T^g. This difference creates the temperature gradient, which drives the (proportional) flow that transports the dissipated reaction heat from the catalyst material to the medium. We have described this in the previous chapter: in a steady state T^m can be obtained from T^g based on experimental data - using irreversible thermodynamics to describe the coupled heat and mass fluxes.

But in heterogeneous catalysis we also have to consider a third temperature, T^r. This is the temperature in the two-dimensional reaction plane. This temperature T^r has to be assigned to the 2-dimensional plane where a chemical process occurs. The temperature T^r in the locus plane of the reaction process differs from the temperature T^m of the catalyst particles by a difference ΔT. This temperature difference ΔT is kept up by the heat, which is set free in the reaction. It is the heat flux in

Page: 61

the reaction plane that can couple thermodynamically to the conversion rate of the catalytic surface reaction.

5.3   Arrhenius plots for surface reactions

The temperature $T^r = T^m + \Delta T$ is also the effective temperature in thermochemical kinetics of the reaction at the catalyst surface. The assigned value ΔT arises as a consequence of the thermodynamic coupling between the conversion rate and the thermal effects in the reaction plane. The temperature difference $\Delta T = T^r - T^m$ may acquire positive as well as negative values. It could, or rather should, depend on the reaction rate and the reaction enthalpy (positive for absorbing heat or negative for releasing heat). The coupling is, because the 2D-thermodynamic system at the active interface relaxes to a minimum in the entropy production by the coupled chemical and thermal processes under the conditions of the experiment. In a steady state this requirement of minimum entropy production will set the quantitative values for the separate flows of heat, mass and catalytic conversion which are, all together, driven by the imposed affinity for the chemical conversion in the reaction surface.

In the thermochemical kinetics of the catalyzed reaction our third temperature T^r will affect the overall conversion rate of the catalytic process. Conversion rates in the reaction plane are always described by the experimental data in the Arrhenius equation for the rate constant k:

$$k = Ae^{-\frac{E_a}{RT^r}} \tag{5.1}$$

The activation energy E_a in this equation may still be understood, in a two dimensional thermodynamic system, in terms of Eyring's transition state theory for reaction processes. It is determined by the potential energy landscape of the reactant configuration along the reaction path. As such, the activation energy E_a should be a quantity of a quantum mechanical nature, and independent of the temperature.

It has become common practice to construct "Arrhenius plots" for obtaining these activation energies E_a for chemical reactions. Indeed, there are many of these Arrhenius plots in the literature on chemical kinetics, which are linear and indicate constant activation energies for the (homogeneous) reactions in gases or liquid media.

But in the 2-dimensional space for a heterogeneous reaction the abscissa $(1/T)$ of an Arrhenius plot should relate the reaction rates to the surface reaction temperature T^r, and not to the other temperatures, T^g or T^m, which are set by the design of the reactor and by the heat transfer properties, respectively.

We come to the proposition that the two-dimensional surface reaction temperature

T^r is then a separate, measurable property of the reaction plane in heterogeneous catalysis. If it must affect the rate of the conversion because it is the real reaction temperature, it can, in principle, after calibration, be obtained from the experimental conversion rates of kinetically controlled chemical reactions at the interface.

Indeed, reconsidering available experimental data we hope to discover non-linearities in the Arrhenius plots for heterogeneous catalytic reactions. Most often, such deviations from the expected patterns tend to be massaged away with uncontrollable *ad hoc* assumptions for the special case of the reaction that is studied, such as the case by van de Runstraat *et al* [76].

Our explanation for non- linear Arrhenius plots would be of a more general, thermodynamic nature. To explain curved Arrhenius plots in heterogeneous catalysis the experimental kinetic data would have to be re-plotted, in terms of T^r instead of T^m or (even worse) T^g. Upward or downward curvatures would then be indicative of positive or negative ΔT, which contribute to the real temperature in the reaction plane.

Now, still assuming that a pure E_a of a rate determining reaction step should be independent of the temperature, one could easily correct this situation and straighten the Arrhenius plots. The ordinates would still represent the experimentally observed reaction rates. But the abscissa $(1/T)$ of the Arrhenius plot has been altered, by adding the temperature excess ΔT in the reaction plane on top of the catalyst temperature T^m. Introducing the reaction temperature T^r instead of T^m would stretch the abscissa and straighten the curves in the Arrhenius plot.

By measuring the reaction rates and using their temperature dependence as a sensor one would gain independent experimental access to the reaction temperature T^r. The measured reaction rates are then used as a temperature sensor, a thermometer in the two-dimensional reaction plane of the catalyst! This method should establish the effects of the two-dimensional surface temperatures and of the coupling between reaction rate and heat flows at catalytic reacting surfaces. In Chapter 6 and Chapter 7, this method will be applied to heterogeneous catalytic CO oxidations with kinetically controlled rates.

Chapter 6

Experimental evidence for a 2-D reaction temperature excess in heterogeneous catalysis

Chemical reaction rates increase exponentially with temperature, as is described by the Arrhenius equation. If the rate of a conversion is limited by the catalytic reaction at the surface, as the rate determining step it will, characteristically, have the true activation energy of that chemical reaction. As mentioned in Chapter 5, the measured reaction rates could then be used as a rather sensitive temperature sensor, a thermometer in the two-dimensional reaction plane of the catalyst.

For the reinterpretation of Arrhenius plots in terms of T^r, the temperature in the reaction plane, we will consider examples of simple surface reactions which are kinetically limited in their rates. We have searched the literature for well-researched catalytic systems of this type, with their temperature dependence and the magnitude of their activation energy E_a as selection criteria.

6.1   Curved Arrhenius plots

According to the theoretical derivation of the Arrhenius equation from the transition state theory

$$k = \frac{k_B T}{h} \exp(\frac{\Delta S^{\#}}{R} - \frac{\Delta H^{\#}}{RT}) = A \exp(-\frac{E_a}{RT}) \qquad (6.1)$$

there is no evident reason why the activation energy E_a for a kinetically determined reaction rate should depend on the temperature. In that case the logarithm of the reaction rate, plotted against $1/T$ (the "Arrhenius plot") is a straight line. The activation energy is obtained from the slope of the plot. Indeed, we found many straight Arrhenius plots for kinetically controlled chemical reactions in the literature.

But for some catalytic systems the Arrhenius plot has an upward or downward curvature (*e.g.* the system described in Figure 6.1). This would suggest that E_a is a function of the reaction temperature. Other examples from the literature are found at Liu *et al.* [74], who investigated the n-pentane isomerisation over PtHMordenite catalyst in the temperature range of 462-523 K and found that the activation energy decreases gradually with temperature. Lei *et al.* [75] observed the similar phenomenon for a neopentane hydrogenolysis and isomerisation reaction over a Pt/HMordenite catalyst. Belessi *et al.* [77] reported curved Arrhenius plots for NO+CO reaction.

As we have already observed there is a tendency to account for observations of this kind by postulating some *ad hoc* property, *e.g.* a changeover between competing kinetic mechanisms as the temperature rises. Such a transition would then be accompanied by a change in the effective activation energy for the overall process.

The many *ad hoc* explanations for curved Arrhenius plots can be lumped together in a small number of categories:

(1) Because of increasing temperature there will be a transition from the kinetically controlled regime at low temperatures to the mass transfer limited at high temperatures (see above).

(2) The rate-determining step itself is altered [78] with rising temperatures, such as, changing from a desorption-limited rate in low temperatures to adsorption as the limiting step in high temperature.

(3) Gradual transitions, like from single-file diffusion limited rate of the process to the kinetically limited rate, which is characteristic for a micro-porous, one-dimensional, zeolite catalysts [75, 74]. In low temperature, because of diffusion difficulties only the catalytic sites near the outer surface are active. But at more elevated temperatures the internal surface of the catalyst becomes available. The apparent activation energy decreases gradually to a lower value.

(4) Changes in surface coverage and reaction order. The activation energy seems to decrease with the reactor temperature in terms of the Arrhenius plot. But, rather than the energy barrier in the potential energy diagram undergoes a change, it is, in fact, the surface coverage of the reactive intermediates, which diminishes as a function of

the temperature and gradually changes the order of the reaction [76].Van de Runstraat *et al.* [76] have demonstrated such a mechanism for the thermochemical kinetics of a catalytic n-hexane isomerization. When all the existing acid sites in the surface of a zeolite catalyst were taken into account she found non-linear Arrhenius plots for the reaction. But only counting the sites which were occupied by an alkoxy (which is an identifiable intermediate of the reaction) she obtained the normal, straight Arrhenius plot and, indeed, a constant activation energy for the active acid sites.

Of course, there may sometimes be unexpected complications in a heterogeneous reaction system. Apparently non-linear Arrhenius plots for specific cases can indeed be the result of complications in the chain of elementary reaction steps. We accept that there exist gradual transitions to other types of rate limitation when the reaction temperature is altered. But, in general, we believe that each kinetically limited reaction step should have its own, specific, temperature independent activation energy. And in many cases this same step remains rate determining over a considerable temperature range. In all those cases we think that the activation energy does not change with temperature, but that the real reaction temperature is different from the temperature, which has been measured in the experimental reactor.

The temperature difference which we have introduced as a surface reaction temperature excess, $\Delta T = T^r - T^m$, between a 2-dimensional reaction plane and the catalyst surface, leads to one more, and more generally applicable reason for non-linear Arrhenius plots in heterogeneous catalysis. A fifth possibility to account for such observations is the notion that the real temperature in the reaction plane, T^r, must be established for the construction of these Arrhenius plots. We maintain that the real activation energy of a surface reaction should, normally, be independent of the temperature, even when a measured Arrhenius plot appears to be non-linear. The plot becomes non-linear because the inverse of the real reaction temperature $1/T^r$ should have been used as the abscissa, and not a value of $1/T^m$ or $1/T^g$.

6.2 Experimental systems with curved Arrhenius plots

A promising candidate to investigate our hypothesis that curved Arrhenius plots reflect a temperature difference between the catalyst surface and the reaction plane is the catalytic oxidation of carbon monoxide (CO). Many authors, investigating the reaction kinetics using different catalysts, saw the activation energies for CO oxidation increase gradually with the temperature. These phenomena have been observed

with Pd/Al$_2$O$_3$-catalysts [79, 80], a single crystalline Pt (100) surface [81] and with a Pd/SiO$_2$ catalyst [82].

In all these experiments the Arrhenius plots had an upwards curvature like Figure 6.1. The slope of the plot is steeper at the high temperature end. It seems that the activation energy E_a of the catalytic surface reaction increases with the temperature.
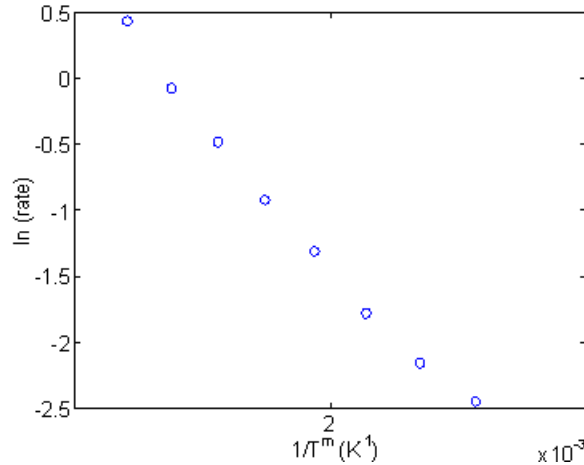

Figure 6.1: Arrhenius plot for CO oxidation in conventional heating system. This plot is reproduced using data in figure 7 of paper by Perry *et al* [79]

From the numerous reports on curved Arrhenius plots for CO-oxidation we have selected two particularly well-executed experiments and re-interpreted the raw experimental data with the idea of a surface reaction temperature T^r in mind.

One set of data is from Perry *et al.* [79] using 5 wt% Pd/γ-Al$_2$O$_3$ catalyst. The other experiment is done by Wei *et al.* [83] using 10 wt% V-TUD-1 catalyst.

Differential reactors were used in both cases. This enables direct measurement of the conversion rate from the experiments and minimizes the uncertainties because of temperature and concentration gradients along the reactor. A differential reactor is also known as a "thin layer reactor" since very small amounts of catalyst, only a thin layer, are used and the corresponding conversion is very low. Normally, the conversion in a differential reactor is a small percentage, below 10%. In such a low conversion regime the temperature and concentration gradients along the reactor are negligible and the reaction rate in the catalyst thin layer is assumed uniform.

From Perry's experimental data we calculated the activation energies from the curved Arrhenius plot, Fig. 6.1 for CO oxidation. This Arrhenius plot presents the data in Perry's paper as a conventional thermo-kinetic experiment. In the temper-

Page: 68

ature range of 482-544 K the apparent activation energies E_a were calculated from the tangent lines at the original experimental points. The temperature dependent activation energy E_a which is obtained in this procedure is shown in Fig. 6.2.
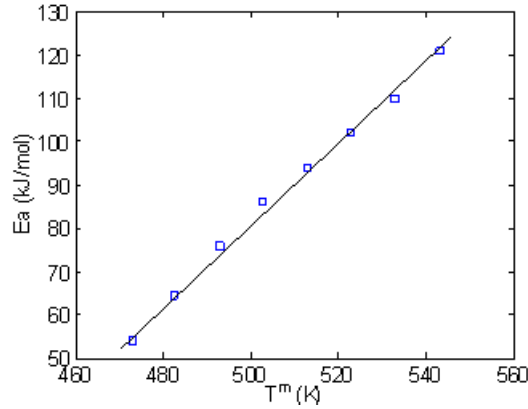

Figure 6.2: Temperature dependence of the reaction activation energy for CO oxidation catalyzed by Pd/γ-Al$_2$O$_3$

From the values of these activation energies it is confirmed that reaction kinetics is in the kinetically controlled regime over the whole temperature range. Why would we say that? First, the reaction system could not be external mass transfer limited because the apparent activation energy is much higher than the diffusion activation energy of around 10 kJ/mol. Secondly, there is no change in the rate limiting mechanism to some internal diffusion controlled limitation as temperatures increase. In this experiment the activation energy does not decrease with temperature, but seems to increase. According to Figure 6.2 the apparent activation energy would increase rather drastically with measured catalyst temperature. The measured temperature T^m in Figure 6.2 is the surface temperature of catalyst particle. It was measured by a thermocouple, embedded in the active catalyst material.

There is no realistic way around assuming that we know the reaction temperature to obtain the activation energy directly from an experiment. But also, there is no logical reason why the activation energy for a reaction should not remain constant with increasing temperature. Then, in our chosen experiment, the measured temperature of the thermocouple can not be the real reaction temperature. As we have analyzed above, the reaction temperature T^r in an active heterogeneous catalyst should probably be different from the solid surface temperature T^m that we know from the experiment.

It turns out that the exponential of Arrhenius' expression for rate constants, $k = Aexp(-E_a/RT)$, has, in fact, not one, but two independent experimental variables, E_a and T^r. The traditional interpretation of the plot is that the activation energy can be calculated from measured temperatures and reaction rates or rate constants. But let us assume, that we knew the value of E_a from some theory, experiment or assumption, then we might just as well calculate the temperature in the reaction plane T^r from the available data.

If we make the assumption that the activation energy E_a must be independent from the reaction temperature there is a direct, albeit rather crude method to obtain the real reaction temperature T^r from the data shown in Figure 6.1. This is done in Figure 6.3.
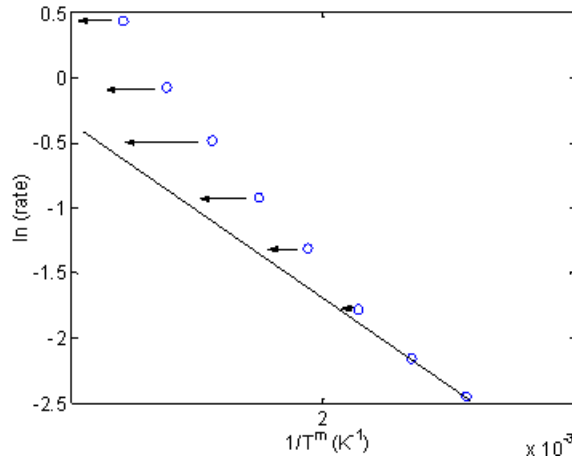
Figure 6.3: Temperature shift from the measured catalyst T^m to the real reaction T^r by assuming constant activation energy of the surface reaction (circles correspond to T^m and the line represents T^r)

At the low temperature end of the Arrhenius plot the reaction rate vanishes. The reaction temperature is then not much different from the measured catalyst temperature, or from the temperature of the ambient gas atmosphere. At this starting point, with a negligibly small reaction rate all the temperatures in the system are equal ($T^g = T^m = T^r$) and equal to the "reactor temperature T^o.

Extrapolating the tangent in $1/T^o$ of the measured Arrhenius plot, we obtain a straight line, a plot, which represents the reaction rates at different temperatures, in the case that they should all be determined by the (constant) activation energy E_a at T^o. The reaction rates on this straightened plot have now shifted to other, lower values

Page: 70

of $1/T$ compared with the original plot in Figure 6.1. But the higher temperatures $T^r > T^o$ in the new plot are the real reaction temperatures which correspond to the experimental reaction rates.

6.3 Surface reaction temperature

The assumption in our interpretation of Figure 6.3 is, that the measured temperature T^m is equal to the reaction temperature T^r when the reaction takes place at the lowest measurable temperature T^o. The pre-exponential factor in the rate expression is assumed independent of the ambient temperatures. Taking the activation energy E_a at T^o on the original curved Arrhenius plot as the really constant activation energy for the reaction, T^r is directly obtained from the experimental data.

Using expression

$$\ln \frac{\Re(T^r)}{\Re(T^o)} = -\frac{E_a}{R} \left(\frac{1}{T^r} - \frac{1}{T^o} \right) \tag{6.2}$$

we calculated the real reaction temperatures, T^r, that should correspond to the measured reaction rates. The lowest reaction temperature, T^o, and its corresponding reaction rate, $\Re(T^o)$, are used as reference values in eq. (6.2). The temperature difference, $\Delta T = T^r - T^m$ shows the relation between the "measured" and the "real" temperatures T^m and T^r in Fig. 6.3. In this heterogeneous system the real reaction temperature T^r is always higher than the experimentally determined temperature T^m of the catalyst material. This is shown in Figure 6.4.
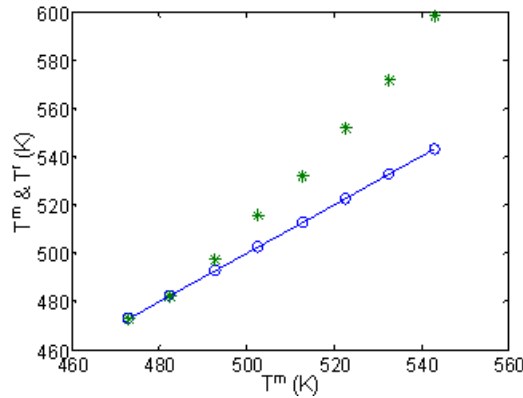

Figure 6.4: Relation of the measured temperature (circles) and the corresponding calculated reaction temperature (stars) for CO oxidation catalyzed by $Pd/\gamma\text{-}Al_2O_3$

T^m is the surface temperature of the catalyst. It is, as we have seen in the

previous chapters, determined by the heat flow into the medium. The difference $\Delta T = T^r - T^m$ increases with the temperature of the reactor T^g, and, therefore, with the experimental reaction rate. To obtain the Arrhenius plot, however, one should represent data in terms of T^r, not of T^m.

Upon increasing the reactor temperature, the reaction rate is increased. This produces more heat, $Q = \Re^{'} \Delta_r H$, in the 2-D reaction surface. Q is the heat per second that is released in the exothermic conversion reaction, $\Re^{'}$ the catalytic surface reaction rate and $\Delta_r H$ the reaction enthalpy.

This does affect the temperature excess ΔT in the reaction plane. The model is that the surplus in bond energy is stored in excited state energy levels of the product molecules when the activated complex is broken up. The next step in the process is that these product molecules relax to the ground state and the temperature T^m. This is a process that may take some time and converts the reaction enthalpy in molecular kinetic energy. The temperature difference ΔT is related to the reaction rates in two different ways: as an additional term which describes the difference between T^r and T^m, and as the driving force for the thermal effects in the reaction plane itself. The relaxation of the product molecules to the ground state can be described as a heat flow in the reaction plane, which eventually transports all the generated heat into the catalyst surface and the ambient medium.

Therefore, we have shown the experimental values of ΔT in Fig. 6.5. The temperature difference $\Delta T = T^r - T^m$ can become as high as 56 K at the highest measured conversion rate in Perry's catalytic experiment. It is seen to increase in a non-linear fashion with the catalyst temperature and also increases with the reaction rate. This is shown clearly in Fig. 6.5. We also notice that the curvatures in the two plots of Fig. 6.5 are different. This may reflect the exponential Arrhenius relation between temperatures and reaction rates.

6.4   Parallel observations with another catalyst

Now the question is "Can we reproduce similar phenomena if another type of catalyst is employed for CO oxidation?". Are there similar values of experimental parameters like the activation energy and the temperature difference $\Delta T = T^r - T^m$?

To answer this question, we performed a similar set of calculations, using the experimental data from Wei *et al.* [83], who used a 10 wt% V-TUD-1 meso-porous catalyst for a kinetic study of CO oxidation in a differential reactor. The slightly curved Arrhenius plot and temperature dependent activation energies E_a which would follow from his measurements are shown in Fig. 6.6 and Fig. 6.7.

Figure 6.5: Temperature differences between surface reaction temperature and measured catalyst temperature increase with the reactor temperature and the reaction rate for CO oxidation catalyzed by Pd/γ-Al$_2$O$_3$
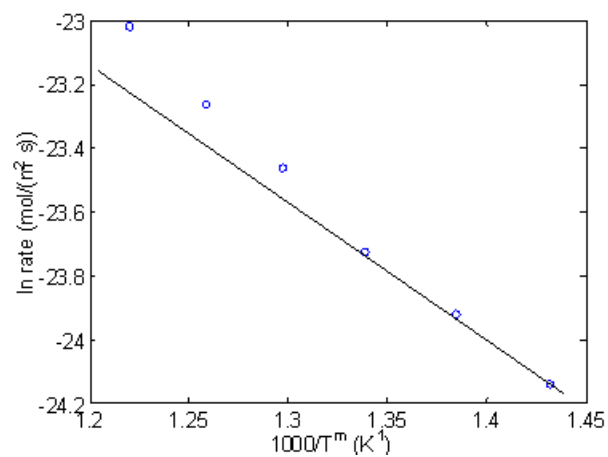
Figure 6.6: Arrhenius plot for CO oxidation catalyzed by V-TUD-1
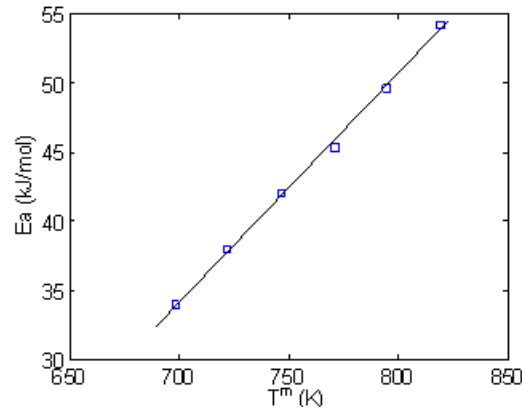
Figure 6.7: Calculated activation energies in various measured temperatures for CO oxidation catalyzed by V-TUD-1

As in Perry's experiments we see the activation energy increase linearly with the reactor temperature. With this Vanadium catalyst much lower apparent activation energies are obtained. Because the activated complex of the reactant molecules and the catalytic site has a different chemical bond strength, there is a different potential energy to overcome in the reaction. The temperature difference $\Delta T = T^r - T^m$ is positive again and the largest temperature difference is about 44 K in this case.

Figure 6.8: Relation of the measured temperatures (circles) and the corresponding reaction temperatures (stars) for CO oxidation catalyzed by V-TUD-1

The conversion rates in Wei's experiments are much smaller, the temperatures are much higher and the reaction temperature excess ΔT has less impact on the
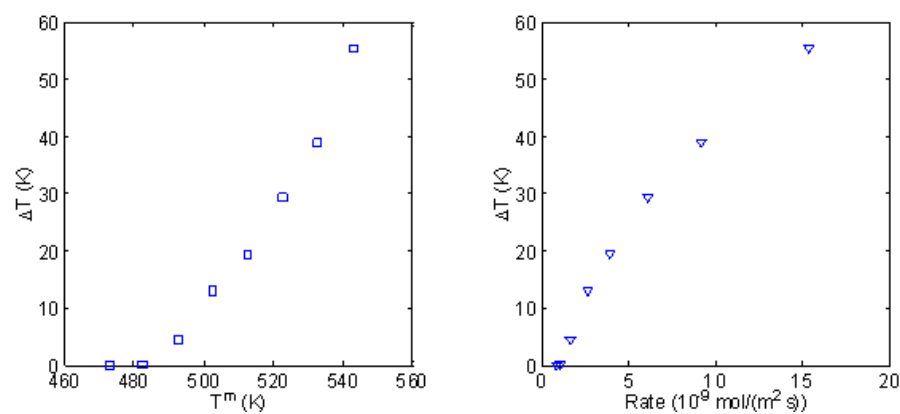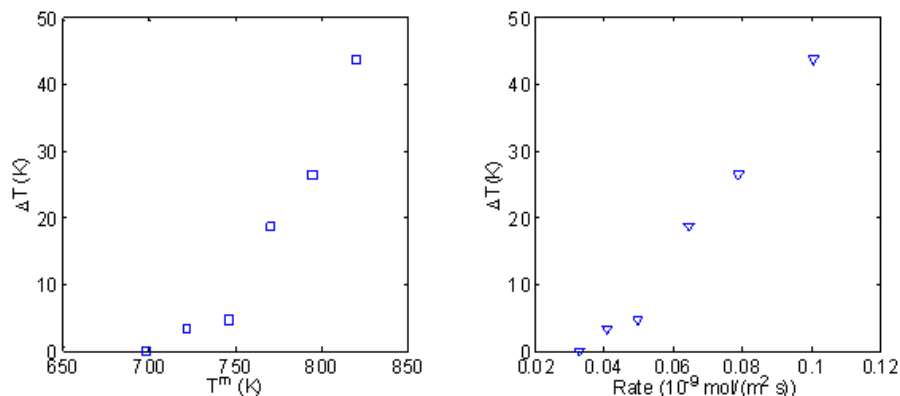
Figure 6.9: Temperature differences between surface reaction temperature and measured catalyst temperature increase with the reactor temperature and the reaction rate for CO oxidation catalyzed by V-TUD-1 catalyst
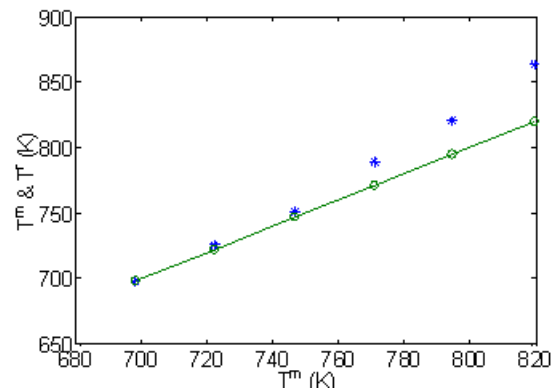
conversion rates with this catalyst. But the qualitative aspects that were observed in Perry's experiment are reproduced with Wei's different catalyst materials. And this may lead to a better understanding of the thermal effects in the reaction plane and their thermodynamic coupling with the conversion rate in heterogeneous reactions like the catalytic oxidation of CO.

6.5 Proof of Principle

In this Chapter we have introduced a new principle for treating heterogeneous catalytic reactions. We started with the assumption that the Arrhenius plots for such systems should be straight. Therefore, there is a discrepancy between the temperature T^r in the two-dimensional reaction surface and the temperature T^m of the catalyst. If this discrepancy ΔT is positive it augments the reaction rate at the surface. Thermodynamically, the two-dimensional reaction plane is a separate system. It can be also analyzed in terms of fluxes and the corresponding forces which drive them. The temperature gradient in the reaction plane could be responsible for a thermal effect, which leads to the dissipation of the reaction heat in the system. As a heat flux, such a thermal effect will be proportional with the temperature excess ΔT which drives it. The heat flux as such may be coupled thermodynamically with the chemical conversion rate, which is another flux in the two-dimensional reaction plane. But according to Arrhenius the conversion rate is an exponential function of the temperature in the reaction plane. And the heat that is generated by the conversion reaction must all

be dissipated through the thermal effects in the reaction plane. This is only possible if the surface temperature excess ΔT is found to be an exponential function of the reaction temperature T^r. If that is the case, it proves that straightening the curved Arrhenius plot is not an arbitrary action, but a meaningful operation, which exposes the temperature excess ΔT in the two-dimensional reaction plane. Therefore, in Fig. 6.10 we have plotted the logarithms of the ΔT values, which were obtained in our analyses of the Perry and the Wei data, as a function of the corresponding temperatures T^r.
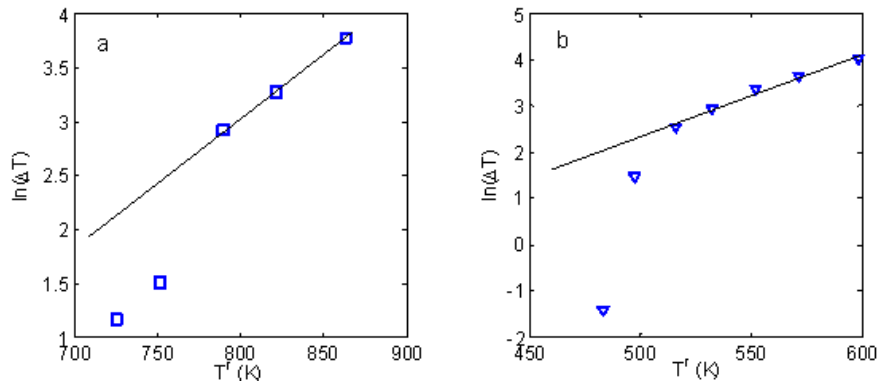
Figure 6.10: Relation between the reaction temperature T^r and the logarithm of the surface temperature excess ΔT: a. Wei's experiment; b. Perry's experiment

At first sight, these are not linear relations in Fig. 6.10. Actually, we did introduce a systematic error in our treatment when we selected the lowest experimental point of the Arrhenius plot as a reference point with $T = T^m = T^r = T^o$. This assumption pulls the plots in Fig. 6.10 down at the low end of the temperature scale. Extrapolating the linear, high temperature, part downwards indicates a $\Delta T = 8.4$ K, instead of 3.2 K, for $T^r = 725.4$ K in the Wei experiment and $\Delta T = 7.4$ K instead of 0.2 K at $T^r = 483.2$ K in Perry's results. Since the effect of this systematic error diminishes when the temperatures in the experiment are higher, the corrected results for the low temperature data points seem more realistic and the correction by extrapolation is then a valid approach. Although we still must allow for a considerable error margin (the correction would really have to be worked out in an iterative way) the plots in Fig. 6.10, after correction or only taking the more restricted number of high temperature, high rate, high ΔT data into account, seem to bear out our assumptions: the logarithm of ΔT is a linear function of the temperature T^r, the real temperature in the 2-dimensional reaction plane - which we have treated as a separate thermo-

dynamic system. That we could derive the functional logarithmic relation between ΔT and T^r from the assumption that the catalytic 2-dimensional system must have a linear Arrhenius plot, lends credibility to our model. In both the experiments by Perry and by Wei we find the expected proof for a really physical thermal effect in the reaction plane, which couples with the chemical conversion and enhances the catalytic reactions.

6.6 Discussion and conclusions

In terms of the above calculations, there is a temperature excess in the 2-dimensional reaction plane. The reason for the higher reaction temperature is the amount of excess energy that must be released after the conversion in the reaction plane.

Energy excesses in product molecules after CO-oxidation have been investigated by Watanabe *et al.* and by Mullins *et al* [84, 85]. They report that CO_2 molecules produced on catalytic Pt-surfaces are ejected into the gas phase with a translational, vibrational, and rotational energy in excess of that expected from the surface temperature. These results are also discussed in the review paper by Nieuwenhuys [86].

The group of King [87] investigated CO oxidation on a Pt (110) catalyst using the technique of single-crystal adsorption microcalorimetry. It was found that when CO was dosed onto a saturated O overlayer, the product CO_2 molecules contained an additional 9 ± 17 kJ/mol of internal energy in excess of the expected energy per mol for thermally accommodated molecules. However, when O_2 molecules were dosed onto a CO overlayer, the product CO_2 molecules had an excess energy of 52 ± 21 kJ/mol.

The essential aspect of all these results is that after the desorption of the product the CO_2 molecules contained more energy in their higher energy levels than would correspond to the thermal equilibrium at the experimental temperature of the catalyst. These results lead, along different lines of reasoning, to the same proposition as ours: that the actual reaction temperature T^r in the 2-D reaction plane is different from the measured catalyst temperature. The real reaction temperature T^r describes how much extra energy is stored temporarily in the CO_2 product molecules. The occupation of higher energy levels gives a heat capacity to these molecules in the reaction plane. The corresponding temperature excess does indeed exist because extra energy must be stored temporarily in the 2-D reacting plane. In that plane the temperature excess ΔT is the driving force for a two-dimensional energy flux while the molecules relax to their ground states, and for the heat flux into the materials behind the catalytically active surface. In both our exothermic model systems, the

temperature excesses are positive and a coupling of the heat flux with the conversion process will speed up the reaction at the catalyst surface.

Chapter 7

Coupling of reaction rates and heat flows in heterogeneous catalysis

In chapter 6 it has been demonstrated that catalytically active surfaces can differ in temperature from the two adjacent bulk phases in heterogeneous catalytic systems. Generally, there are temperature and concentration gradients in heterogeneous gas-solid catalytic reactors. Sometimes these gradients are caused by the transport resistances of heat and matter. In heterogeneous catalytic systems, the heat of the reaction is released in the two-dimensional reaction plane, in the course of the catalytic conversion reaction itself. If the conversion reaction in that plane is rate determining, the rate and the selectivity of the process may be affected by a thermodynamic coupling of the conversion rate and the heat flow in the two-dimensional reaction plane, a coupling which would be forbidden in three-dimensional homogeneous systems by the Curie-Prigogine principle.

The ambient medium itself has the reactor temperature T^g. In a steady state of the conversion reaction the difference $T^m - T^g$ in the temperatures of the active catalyst (a solid) and the ambient medium (a gas or a liquid) is determined by the transfer of the reaction heat from the catalyst material to the medium. That this heat flux can also be coupled to the mass flows of reactants and products has been discussed in Chapter 4. It was demonstrated there, how the coupling of the fluxes can be investigated by calculating the resistance (or conductivity) coefficients which relate the fluxes to the thermodynamic forces that drive them. In a matrix of resistance

coefficients the diagonal terms relate the fluxes (heat flow, mass flow, conversion, electric current) to the corresponding forces (temperature difference, concentration gradient, chemical affinity, electrical potential). The cross terms describe the coupling effects. If a cross term is found to be zero, there is no coupling between the pertinent fluxes in the system.

7.1 Temperature difference between the catalyst surface and the gas phase, $T^m - T^g$

The gas temperature T^g is related to the measured solid surface temperature T^m by the film model for heat transport. The temperature gradient is assumed to exist only in the gas film between the catalyst and the gas phase. In order to investigate if the catalyst and the gas phase have similar temperature, we use a similar force-flux equation

$$\frac{1}{T^m} - \frac{1}{T^g} = r_{qq}^{\mathrm{f}} \; \frac{\Delta_r H \; \Re'}{a} \tag{7.1}$$

as in Chapter 4.

In a steady state, no appreciable temperature gradient is expected between the active site (metal) and the support, in kinetically controlled differential reactors, because of their high thermal conductivities. The whole catalyst particles have a uniform temperature. The thermal conductivity of a catalyst with supporting solid, like SiO_2 or TUD-1, is much larger than that of the gas mixture. The heat released from the surface reaction (normally inside the pores of the catalyst) is assumed to be transferred rapidly to the external surface of the solid. From there, it is carried away by the gases.

There is always some temperature gradient (small or large) in the gas film at external surface of an active catalyst particle. In steady state, all the heat that is released by the surface reaction has to be transported away, through the external surface of the catalyst and finally out of the system. Therefore, the total external surface area of the solid a is used to calculate the heat flux. The conversion rate $\Re'$ has the dimension of mol/s and the reaction heat $Q = \Delta_r H \; \Re'$ that is developed in the conversion has the dimension of J/s, which creates a source for the heat flow through the unit surface area.

In an experiment like Wei's, which we have described as an example of a kinetically controlled conversion process, the heat flow through the catalyst surface is no bottleneck for the reaction rate. The total catalyst volume in the reactor is about 8×10^{-8} m^3 and the diameter of the catalyst spherical particle is about 2×10^{-4} m.

The total external surface area of the catalyst particle is then about 2.4×10^{-3} m^2. Considering the conductivity data for the atmosphere like we did before, when the thickness of the gas films at an external catalyst surface is taken as 1 mm [31], the calculated temperature differences $T^m - T^g$ are in the order of magnitude 10^{-3} K, which is rather small. The reason for that is the low conversion, not more than 5 percent, for this kinetically controlled differential reactor, in combination with the high thermal conductivity of helium, which is the main constituent of the gas in the film. Only this small temperature difference is necessary, under the conditions of this special experiment, as driving force for all the heat transfer from solid surface to gas phase in the steady state.

This calculated result agrees with the general opinion in catalyst research, that the gas temperature can be regarded as the same as the catalyst temperature in kinetically controlled differential reactors.

In this chapter, however, we plan to study the coupling between heat effects and conversion rates in a kinetically controlled catalytic process. The heat and mass transfer at the interface between the catalyst and the medium is not rate limiting step any more. We have seen that in Wei's experiment. The ample capacity for a heat flow follows from the necessary temperature differences at the solid-gas interface ($i.e$, $T^m - T^g$) and the heat transfer resistance at the external catalyst surface. In such a reaction the rate controlling mechanisms operate in the two-dimensional reaction plane, which we have introduced in the previous chapters as a separate thermodynamic system, characterized by excess properties and rates.

A kinetically limited reaction process has, as a result of straightening out the curved Arrhenius plots for CO-oxidation, a reaction temperature T^r for the conversion reaction, which differs from the temperature of the catalyst by $\Delta T = T^r - T^m$. These temperatures and temperature differences affect the conversion rate and the heat effects in the reaction plane in different ways. The higher reaction temperature speeds up the conversion reaction. The temperature excess ΔT is responsible for creating a new type of coupling for two principal fluxes in the two-dimensional system. In a catalytic reaction these fluxes are the chemical conversion of reactants into products and the conversion of the reaction enthalpy into dissipated heat: a transport of the surplus in chemical energy of the reactants that has to be transferred from the locus of the reaction into the ambient.

It is not correct to assume the equality of the temperatures T^r and T^m in a heterogeneous reaction. We still have the rather large temperature difference, $\Delta T = T^r - T^m$, to deal with. This temperature difference is between two connected but autonomous thermodynamic systems: the two-dimensional reaction plane and the

three-dimensional catalyst particle. Temperature excess ΔT is an additional factor in the rate of the conversion reaction according to Arrhenius equation. But it could also be related to the storage and subsequent transfer of energy inside the reaction plane. Our idea is that ΔT describes the difference in local temperature between the excited states of the product molecules just after the conversion and their thermally equilibrated ground state, which can exchange surplus heat with the environment.

7.2 Coupling of two fluxes: heat generation and conversion rate

Coupling of fluxes has been introduced in Chapter 2. The phenomenological force-flux relations tell us that, apart from the (diagonal) principal fluxes in a system, there exist cross-effects. In the mass and heat transfer process that has been discussed in Chapters 3 and 4, the Soret and Dufour effects represent the coupling between these fluxes. This coupling affects their strength in a positive or negative sense, depending on the sign of the coupling resistance coefficients.

To evaluate these coupling effects in kinetically controlled reactions we shall have to follow the similar thermodynamic recipe as before. We shall need the driving forces (*i.e.* the Gibbs free energy of the reaction and the temperature differences in the system), the measured fluxes (*i.e.* the conversion reaction rate and the heat flows) and effects of the individual resistance coefficients on the magnitude of these fluxes. These cross effects tune the entropy production in our particular system (*i.e.* in the two-dimensional reaction plane when the system is a kinetically controlled heterogeneous catalytic chemical reaction in the steady state) to a minimum level for the conditions that are given in the experiments.

We begin this analysis by using the data from the Wei's experiment that has been described in the previous Chapter. In that experiment we know all the necessary parameters for calculating resistance coefficients. Then, after making some necessary assumptions about experimental conditions we shall also study the data from Perry *et al.* Data from Wei's experiments, which we have obtained previously, such as the experimental values of ΔT for different conversion rates, have been summarized in the first table, together with the calculated Gibbs energies for these reaction conditions. These Gibbs free energies and the experimental heat fluxes and conversion rates can be used to calculate the resistance coefficients.

7.2.1 Gibbs free energy of the reaction

The Gibbs free energy of the surface reaction divided by the reaction temperature T^r, which we have introduced as the real temperature in the two-dimensional reaction plane, is the driving force of the surface reaction.

The Gibbs free energy of the surface reaction is introduced in eq. (7.2). It depends on the excess reactant concentrations in the reaction plane and is obtained as

$$\Delta_r G = \Delta_r G^\circ + RT \ln \frac{x_{CO_2}}{x_{CO} \; x_{O_2}^{1/2}} \tag{7.2}$$

where x_i is mole fraction of component i at steady state. It is assumed that these mole fractions of adsorbed molecules are proportional with the mol fractions of the reactants in the reactor gas.

The standard Gibbs free energy $\Delta_r G^\circ$ at temperature $T = T^r$ can be found with the Gibbs-Helmholtz equation

$$\frac{d\left(\Delta_r G^\circ / T\right)}{dT} = -\frac{\Delta_r H^\circ}{T^2} \tag{7.3}$$

According to the handbook [88], the reaction enthalpy for CO oxidation hardly changes in this temperature range. Therefore, here for convenience, we have assumed that the reaction enthalpy has a constant value of -283 kJ/mol in the experimental temperature ranges. The effect of the volume change before and after reaction on the calculated Gibbs free energy is negligible due to the large amount (98.5%) of the carrier gas in the reactor. In such low concentrations of the reactants, we assume each molecule is equally adsorbed and in equilibrium with the molecules close to the surface. Therefore, assuming a linear adsorption regime the adsorbed mole fractions of the reacting components at steady state are given by:

$$x_{co} = x_{co}^\circ \left(1 - conv.\right)$$
$$x_{o_2} = x_{o_2}^\circ - 0.5 \; x_{co}^\circ \; conv. \tag{7.4}$$
$$x_{co_2} = x_{co}^\circ \; conv. \tag{7.5}$$

where x_i° is initial mole fraction of component i and $conv.$ is the reaction conversion. Using specific conditions of the experiment, which are found in table 7.1, the Gibbs free energies for CO oxidation at various temperatures in steady states are calculated. The results are also listed in table 7.1.

Table 7.1: Experimental conditions and calculated reaction Gibbs free energies for experiments by Wei et al.

x_{co}°	0.005				
$x_{o_2}^{\circ}$	0.01				
T^m (K)	722.2	746.7	770.9	794.6	819.7
T^r (K)	726.8	753.5	795.7	829.4	876.5
ΔT (K)	4.6	6.8	24.8	34.8	56.8
$\Re$ (10^{-10} mol/(m^2 s))	0.408	0.497	0.645	0.789	1.005
$conv.$ (%)	1.498	1.819	2.368	2.889	3.690
$\Delta_r G$ (kJ/mol)	-231.0	-227.8	-223.0	-219.0	-213.5

7.2.2 Reaction rates

The conversion rates at different temperatures have been measured experimentally. We have discussed this in the previous chapter and concluded that Arrhenius equation should combine these experimental rates with the corresponding values of the temperature T^r in the reaction plane. We have used the reaction temperatures T^r, in combination with the measured rates $\Re$ from Wei's report. These data for each experiment are also given in Table 7.1. The experimental conversion rates, as fluxes, were then related to the pertinent Gibbs energies, as driving forces for the reaction, and to the temperature T^r. In this way we calculated resistance coefficients for the separate diagonal and cross effects in the reaction plane.

7.2.3 Resistance coefficients

We have learned in Chapter 4 how to calculate driving forces from the resistance coefficients and fluxes. Now we are going to calculate the individual resistance coefficients and the possible coupling coefficients between heat effects and conversion rates in the reaction plane from a set of fluxes and driving forces for a kinetically controlled process. In Wei's experiment the reaction surface with adsorbed molecules is in equilibrium with the reactant gas close to the surface. The effect of chemical potential gradients in the gas film and in the thin surface layer on the catalyst may be neglected: $\Delta(\mu_j/T) = 0$. Couplings of mass fluxes between each reacting component are assumed to be negligible, too. These reasonable approximations are made to simplify the calculations.

Then, rewriting the phenomenological relations for the two-dimensional reaction

surface as a separate thermodynamic system, the linear force-flux equations become:

$$\Delta_{i,s} \left(\frac{1}{T} \right) = r_{qq}^{s,i} J_q^{\prime i} + r_{qr}^{i} \, \Re \tag{7.6}$$

$$\Delta_{s,o} \left(\frac{1}{T} \right) = r_{qq}^{s,o} J_q^{\prime o} + r_{qr}^{o} \Re \tag{7.7}$$

$$-\Delta_{i,s} \left(\frac{\mu_{j,T}}{T^s} \right) = \left(r_{jr} - \nu_j r_{jj}^s \right) \Re \tag{7.8}$$

$$-\frac{\Delta_r G}{T^s} = r_{rq}^{i} J_q^{\prime i} + r_{rq}^{o} J_q^{\prime o} + \left(-\sum_{k=1}^{n} r_{rk} \nu_k + r_{rr} \right) \Re \tag{7.9}$$

where "$\Delta_{i,s}$" means the temperature difference between the reacting surface and gas phase "i". Symbol "o" represents the phase of catalyst. The superscripts "s" mean that the quantities are for the surface and "i" or "o" again corresponds to phase i or o. We used these expressions for obtaining the set of resistance coefficients for the described processes that are given in Table 7.2. The coefficient r_{qq}^s is the diagonal resistance coefficient for the principal process of a heat transfer in the reaction plane, analogous to the heat transfer that is described by Fourier's Law in a three-dimensional medium. But here the thermodynamic effects are two-dimensional by definition and should be modelled accordingly. The coefficient r_{qr} is the coupling resistance coefficient in the reaction plane between the two-dimensional "heat flux" and the conversion rate.

In the reaction plane there is also a mass transfer resistance coefficient for fluxes of reactant molecules. For the component j it is r_{jj}^s. It describes the mobility of reactant and product molecules in the adsorbed state and is related to the turn over number of the active sites. The coefficient r_{jr} is the coupling coefficient between this kind of mass transfer in the reaction plane and the catalytic conversion rate. The coefficient r_{rr} is again a diagonal coefficient in the matrix. It represents the "resistance" to the conversion reaction itself. If this principal flux in the reaction plane is the rate limiting step in the process, we expect that this must be the largest of the resistance coefficients. We suppose that all the resistance coefficients in the reaction plane are still subject to Onsager symmetry relations, like they were in three-dimensional systems.

We can now apply a similar formulism as in Chapter 3 to calculate the heat transfer resistance coefficients for the thermal effects in the reaction surface. Of course, we shall use the reaction temperature T^r in these calculations, and not some other temperatures. Let us, this time, model the catalytic interface as a separate interphase of thickness δ^s, sandwiched between the two (solid and gas) phases of the

system. Such a thin layer interphase would have a heat resistivity:

$$r_{qq}^{\text{s}} = \frac{\delta^{\text{s}}}{\lambda (T^r)^2} \qquad (7.10)$$

The thermal conductivity of the reacting gas mixture enters this equation. It is averaged into the properties of the interphase and used to estimate the heat transfer resistance coefficients r_{qq}^{s}. Since the whole thin surface layer is taken as one layer of adsorbed molecule, about 0.2 nm thick, little is known about the gradients of the properties in the surface phase over its volume. But using available "guestimates" for the material properties one discovers immediately from the calculations that the resistance coefficient multiplifying the heat flux, $r_{qq}^{\text{s}} J_q'$, is of the order of 10^{-20} K^{-1}. This is much smaller than $\Delta(1/T)$. Consequently, such a resistance of a quasi three-dimensional character plays no role in eqs. (7.6) and (7.7).

But we must really consider the two-dimensional version of the parameter $r_{qq}^{\text{s}} J_q'$. Excess heat in a two-dimensional surface can only be stored and transported by the excess amounts of matter in that surface. The excess matter in the reaction surface is the reactants and the product molecules of the components j, which can store surplus energy in the excited state, by the occupation of higher energy levels of the molecules. The dissipative heat flux will then occur during the relaxation of these excited molecules to their ground states. There are different resistances for the different excited states, but one of those is the principal pathway that has the lowest resistance coefficient for this kind of a two-dimensional heat flux. The temperature, which would correspond to the energy distribution in the excited molecules in a three dimensional system is also the real temperature T^r in the reaction plane, whereas the relaxation process to the equilibrium at T^m is cast as a heat flux, driven by the temperature difference $\Delta T = T^r - T^m$. Therefore, the principal heat flux does exist, as witnessed by its driving force ΔT, but the heat is easily transferred in the catalyst material and dissipated into the ambient gas.

Coupling resistance coefficients r_{qr} between heat transfer and reaction rate can be calculated with equation (7.11). Because the gas temperature T^g and catalyst temperature T^m are almost the same, as we have seen in the previous paragraph, we may write $\Delta_{\text{i,s}}(1/T) = -\Delta_{\text{s,o}}(1/T)$. The eqs. (7.6) and (7.7) can then be rewritten as one simple equation:

$$\frac{1}{T^r} - \frac{1}{T^m} = r_{qr}\,\Re, \qquad \text{and} \quad r_{qr} = r_{qr}^{\text{s,i}} = -r_{qr}^{\text{s,o}} \qquad (7.11)$$

From a dimensional analysis of eq. (7.11), it is seen immediately that this coefficient r_{qr} is independent of any surface thickness δ^s, but proportional to the surface

area. The dimension of r_{qr} is $(m^2 \text{ s})/(\text{mol K})$.

The two-dimensional coupling resistance coefficients between mass transfer and reaction rate, r_{jr}, are obtained by using eq. (7.8) and the properties of $\Delta\left(\mu_j/T\right) = 0$:

$$r_{jr} = \nu_j r_{jj}^{\text{s}} \tag{7.12}$$

The dimension of r_{jr} is $(J \text{ m}^2 \text{ s})/(\text{mol}^2 \text{ K})$.

The resistance coefficients r_{jj}^{s} for mass transfer by diffusion in the interphase describe a possible bottleneck in the interface. This type of mass transfer could become a separate rate determining effect when it affects the turnover number (T.O.N.) of an active site that has to be replenished after the conversion has taken place. This resistance coefficient is different for each of the reactant and product components j. It can be calculated by

$$r_{jj}^{\text{s}} = \frac{R^2 \ T}{\DJ_{j,He} \ x_j \ p} \tag{7.13}$$

where $\DJ_{j,He}$ is Maxwell-Stefan diffusion coefficient for component j and p the total pressure for the reaction.

Finally, the force-flux relation for the conversion according to eq (7.9) can be rewritten, using the relation of $r_{qr} = r_{qr}^{\text{s,i}} = -r_{qr}^{\text{s,o}}$

$$-\frac{\Delta_r G}{T^{\text{s}}} = r_{rq}\left(J_q'^{\text{i}} - J_q'^{\text{o}}\right) + \left(-\sum_{k=1}^{n} r_{rk}\nu_k + r_{rr}\right)\Re \tag{7.14}$$

Here, heat fluxes into and out of the surface must remain subject to the steady state requirement, of

$$J_q'^{\text{i}} + \sum_j h_j^{\text{i}} J_j - J_q'^{\text{o}} = 0 \tag{7.15}$$

as described in chapter 2. The molar fluxes of the components can be related to the surface reaction rate by $J_j^{\text{i}} = -\nu_j \Re$ in steady state. This expression can be used to replace J_j in eq. (7.15). As a result, one obtains the excess "heat production" in the reaction plane:

$$J_q'^{\text{i}} - J_q'^{\text{o}} = \Re \Delta_r H \tag{7.16}$$

The surface reaction rate $\Re$ is in the dimension of $\text{mol}/(m^2 \text{ s})$. The eq. (7.14) can finally be written as

$$-\frac{\Delta_r G}{T^{\text{s}}} = \left(r_{rq}\Delta_r H - \sum_{k=1}^{n} r_{rk}\nu_k + r_{rr}\right)\Re \tag{7.17}$$

The resistance coefficients for the catalytic conversion in the surface r_{rr}, in the same dimension as r_{jr}, are calculated by putting the relevant experimental data into eq. (7.17).

The "chemical" resistance coefficients, like r_{jr} and r_{rr} are, of course, independent of the surface thickness. The fluxes in the reaction plane are proportional with the catalytic surface area.

We have collected the calculated resistance coefficients on the basis of Wei's experimental data in Table 7.2.

Table 7.2: Resistance coefficients with temperature for CO oxidation by Wei et al.

T^m (K)	722.2	746.7	770.9	794.6	819.7
T^r (K)	725.4	751.2	789.5	821.0	863.4
ΔT (K)	3.2	4.5	18.6	26.4	43.7
r_{qr} (10^5, m^2 s mol^{-1}K^{-1})	-1.50	-1.61	-4.74	-5.13	-6.14
$r_{jr,CO}$ (10^5, J m^2 s mol^{-2}K^{-1})	1.80	1.77	1.74	1.71	1.69
r_{jr,O_2} (10^4, J m^2 s mol^{-2}K^{-1})	4.34	4.26	4.16	4.09	3.99
r_{jr,CO_2} (10^7, J m^2 s mol^{-2}K^{-1})	-2.04	-1.66	-1.25	-1.00	-0.76
r_{rr} (10^{12}, J m^2 s mol^{-2}K^{-1})	7.77	6.06	4.25	3.25	2.30

Whereas the diagonal coefficient r_{qq}^s for the heat transfer resistance is small and was eliminated from equations (7.6) and (7.7), the coupling of the experimental heat flow through the cross term with the conversion rate is rather large. The coefficient for the chemical reaction rate r_{rr} is the biggest of all the resistances in the table. This is as anticipated: Wei's catalytic oxidation of CO was, after all, a kinetically limited system.

The cross term r_{qr}, which is responsible for the coupling of the conversion rates with thermal effects, turns out to be relatively large. These coupling resistances between a heat flux in the reaction plane and the total reaction rate suggest the possibility of temporary energy storage in the adsorbed reactant molecules (as some sort of latent heat in a heat capacity). This excess energy keeps the reaction plane at the elevated surface reaction temperature T^r.

With increasing the catalyst temperature T^m, the coupling effect of r_{qr} tends to increase too, whereas all the other resistance coefficients tend to become smaller. But in the Wei experiment this is a small effect. The orders of magnitude remain the same over the range of the reaction temperatures.

The temperature excesses $\Delta T = T^r - T^m$ are of the order of 10 K, as is seen in table 7.2. That increase of the reaction temperature is due to the coupling of the conversion rate with thermal effects in the reaction plane. For a constant activation energy E_a, this consequence of the coupling between heat flux and conversion rate

should increase the reaction rate by a factor of 2.

7.3 Analysis of Perry's experiments

We have analyzed the data from Perry's experiment [79] in a similar way. The metal and its supporting material are again regarded as one solid phase. It has a uniform temperature, the measured temperature T^m. All the heat that is produced by the catalytic reaction is transferred to the medium. The reactor temperature T^g is then, as expected, very near to the measured temperature of the catalyst T^m. Temperature differences in the boundary layer at the interface, $T^m - T^g$, are of the order of 10^{-3} K.

A problem for our interpretation of the data is that Perry has not reported the actual conversions, but only the steady state conversion rates at the different temperatures. This introduces some uncertainty about the distribution of the reactants in the medium. Based on general knowledge about the type of his reactor, we estimate that the highest conversion at a temperature of 543 K was 8%. Eight percent conversion is quite high for differential reactors. We have assumed this relatively high conversion, because of the high reaction rates in the experiments and the estimated time interval is then 0.36 s for each measuring point. Combining these conditions in the experiments, we obtained estimates for every conversion, and for the corresponding mole fractions in the steady state. These estimates were used in the calculation of Gibbs free energies for the CO-oxidation. Errors in the estimated conversions will only influence the precise values of the coefficients r_{rr}. But these are the resistances for the principal flux of the conversion rate. The rest of the calculations, which is made to demonstrate the coupling of fluxes ran along the same lines as with Wei's experimental data. The results of these calculations are found in table 7.3.

Table 7.3: Resistance coefficients and Gibbs free energies with temperature for CO oxidation by Perry et al

T^m (K)	483	493	503	513	523	533	543
T^r (K)	483.2	497.3	515.7	532.1	552.0	571.7	598.6
ΔT (K)	0.2	4.3	12.7	19.1	29.0	38.7	55.6
$\Delta_r G$ (kJ/mol)	-255.2	-252.8	-249.7	-246.9	-243.4	-240.0	-235.2
r_{qr} (10^4)	-0.09	-1.04	-1.82	-1.77	-1.63	-1.38	-1.11
$r_{jr,CO}$ (10^4)	1.54	1.52	1.50	1.49	1.48	1.48	1.49
r_{jr,O_2} (10^4)	1.16	1.14	1.13	1.11	1.10	1.10	1.10
r_{jr,CO_2} (10^6)	-4.47	-2.99	-1.86	-1.23	-0.78	-0.51	-0.30
r_{rr} (10^{11})	4.58	2.99	1.75	1.12	0.67	0.42	0.22

7.4 Conclusions

It was found in both experiments that the principal resistance coefficient for the conversion reaction r_{rr} decreases when the temperature is increased. Smaller resistance coefficients imply easier scaling over the rate limiting energy barrier for the conversion process and a faster reaction rate at higher temperatures. Such an effect had to be expected on the basis of the Arrhenius equation. Of course, this elevated temperature itself is a manifestation of the interaction between a two-dimensional heat effect and the conversion rate - which are coupled fluxes in the reaction plane.

On the basis of our interpretation of Wei's and Perry's results one could say, that Perry's is the better catalyst. All its resistances for processes in the reaction plane are smaller, sometimes by one or two orders of magnitude. Such a catalyst is more active. It produces faster conversion rates for the same driving force and can, therefore, operate at lower temperatures.

This performance of the catalyst is enhanced by the stronger coupling of the conversion rate with thermal processes in Perry's experiments. The coupling manifests itself in a larger discrepancy between the measured temperature of the catalyst material (T^m) and the temperature T^r in the two-dimensional reaction plane of the catalyst, which is the real temperature for the conversion. In the eyes of an experimentalist it would seem, that such a catalyst is operating at higher temperatures than expected. In these heterogeneous catalysts the elevated temperature in the reaction plane is not only affecting the conversion rates, but also the selectivity of the catalytic process. In general, reaction temperatures for heterogeneous catalytic conversions should, "after further research" be corrected by $\Delta T = T^r - T^m$. This temperature excess ΔT is due to the coupling of fluxes in the two-dimensional reaction plane. It may acquire positive or negative values, and affect the apparent properties of heterogeneous catalysts accordingly.

An approach along these lines might, eventually, even have solved Soede's selectivity puzzle with his multiphase hydrogenation catalysts. Ballpark calculations [4] of the coupling between heat flow and conversion rate in his catalytic model systems indicate temperatures T^r, exceeding the measured catalyst temperatures T^m by 10 K or more. Such a discrepancy between the measured and the real temperatures would certainly produce the reported selectivity effects. This observation may be generalized! Interfacial temperature excess effects, deriving from the thermodynamic coupling between the fluxes in an active catalyst surface can have a decisive effect for the activity and the selectivity of the catalytic process.

Chapter 8

Theses

Following the custom, which has grown in our Laboratory over the years, we summarize the line of thought in this dissertation by formulating the following theses:

Heterogeneous catalysis can be investigated thermodynamically by introducing the reaction plane as a separate thermodynamic system, to which all the properties and processes in the interface of catalyst and medium are assigned as excess quantities, following the Gibbs convention.

Following Gibbs, the properties of the interface between the catalyst and the medium is described by the Gibbs dividing surface, and assigning excess quantities of heat, energy, entropy, adsorbed components to that plane in the interfacial region. Such a Gibbs dividing surface is a separate, two-dimensional thermodynamic system. All the relations of local equilibrium thermodynamics and of the thermodynamics of irreversible processes are valid in it when these quantities are assigned correctly, following the Gibbs convention. This validity includes the thermodynamics of chemical conversion and the production of the reaction heat, which take place in the reaction plane. The thermodynamics of irreversible processes introduces the possibility, that fluxes in the reaction plane are coupled by novel cross effects in this two-dimensional thermodynamic system, which generally must remain subject to the Onsager symmetry relations.

The temperature T^r of the reaction plane can differ from the measured temperature T^m of the catalyst surface. This is a consequence of the coupling between conversion rates and thermal effects, which is possible

in the catalytically active interface.

Bedeaux and Kjelstrup have shown that the coupling of the (scalar) conversion rate and the (vectorial) heat flux, which is forbidden in three dimensional homogeneous phases by the Curie-Prigogine principle, may be possible in the two-dimensional reaction plane. Calculated resistance coefficients from experimental data for coupled conversion rates and heat fluxes in the reaction plane suggest that the cross effects may be responsible for temperature differences $\Delta T = T^r - T^m$ in kinetically controlled catalytic reactions, which can become of the order of 10 K. That these temperature differences are caused by thermal cross effects follows from their logarithmic dependence on T^r.

Arrhenius plots, of the logarithm of a chemical reaction rate as a function of the inverse temperature, should theoretically be straight lines. Curved Arrhenius plots do not always indicate temperature dependent activation energies. They can also be obtained when the catalyst temperature T^m is, erroneously, used in Arrhenius' law, instead of the real temperature T^r in the reaction plane.

In many catalytical systems the experimental Arrhenius plots are curved. It seems that the activation energy E_a of the catalysed reaction is then a function of the measured temperature at the active interface. However, we believe that there is no general theoretical reason for such a temperature dependence. The measured temperature of the catalyst T^m is not equal to the temperature T^r in the two dimensional reaction plane. For a strongly exothermic process like the catalytic oxidation of CO the difference $\Delta T = T^r - T^m$ increases with the conversion rates. It may reach 56 K in an experimental situation. Such a difference between the temperature of the catalyst and the real reaction temperature causes curved Arrhenius plots. It also leads to unexpected values for temperature dependent catalyst properties, like activity and selectivity. In those cases the catalytic reaction operates at a higher or lower level of temperature than would follow from the measured surface temperature T^m.

Coupling of fluxes is also important in transport limited catalytic reactions. The Soret and the Dufour effects (thermodiffusion and diffusion thermal effects) can couple fluxes of heat and mass in the diffusion boundary layer and reduce their total entropy production to a minimum. This coupling effect is important in the experimental rates of catalytic conversions.

Coupling of fluxes is a general phenomenon in the thermodynamics of irreversible

processes. Cross effects between heat and mass transfer fluxes, like the Soret effect for thermodiffusion have quantitative consequences for the magnitude of the individual transport fluxes in a diffusion boundary layer. A good example is the catalytic oxidation of hydrogen, where analysis indicates that the Soret effect can give about 40 K difference in the catalyst temperature. It may also severely reduce the available amount of the oxygen reactant in the reaction plane of a high temperature (fuel cell) hydrogen electrode. Effects of this magnitude should not be ignored in the technological design of such important processes!

Bibliography

[1] R.I. Masel, "Chemical Kinetics and Catalysis", John Wiley & Sons, p. 18, 2001.

[2] R.S. Berry, S.A. Rice, J. Ross, "Physical and Chemical Kinetics, Part 3", p. 1147, John Wiley & Sons, 1980.

[3] H. Kuhn, H.D. Forsterling, "Principles of Physical Chemistry–Understanding Molecules, Molecular Assemblies, Supramolecular Machines", p. 675, John Wiley & Sons, Ltd, 2000.

[4] M. Soede, "The partial hydrogenation of aromatics", Ph. D Thesis, p. 146-147, TUDelft, Netherlands, 1996.

[5] D. Barten, "Temperature jump at the surface of catalyst particle", Internal report of Faculty of Chemical Technology in Delft University of Technology, 2000.

[6] F. Yoshida, D. Ramaswami, and O.A. Hougen, "Temperatures and partial pressures at the surfaces of catalyst particles", AIChE J., 8 (1), 5-11, 1962.

[7] M.A.A. Cardoso and D. Luss, "Stability of catalytic wires", Chem. Eng. Sci., 24, 1699-1710, 1969.

[8] H. Wu, Q. Yuan and B. Zhu, "An experimental investigation of optimal active catalyst distribution in nonisothermal pellets", Ind. Eng. Chem. Res., 27, 1169-1174, 1988.

[9] H. Wu, Q. Yuan and B. Zhu, "An experimental study of optimal active catalyst distribution in pellets for maximum selectivity", Ind. Eng. Chem. Res., 29, 1771-1776, 1990.

[10] F. Basile, L. Basini, M.D. Amore, G. Fornasari, A. Guarinono, D. Matteuzzi, G.D. Piero, F. Trifiro, and A. Vaccari, "Ni/Mg/Al anionic clay derived catalysts for the catalytic partial oxidation of methane——Residence time dependence of the reactivity features", J. Catal., 173, 247-256, 1998.

[11] F. Basile, G. Fornasari, F. Trifiro, and A. Vaccari, "Partial oxidation of methane effect of reaction parameters and catalyst composition on the thermal profile and heat distribution", Catal. Today, 64, 21-30, 2001.

[12] F.J. Weinberg, "Combustion Temperatures: The Future?", Nature, 233, 239-241, 1971.

[13] S.A. Lloyd and F.J. Weinberg, "A burner for mixtures of very low heat content", Nature, 251, 47-49, 1974.

[14] G.F. Froment and K.B. Bischoff, "Chemical reactor analysis and design", Second edition, 136-139, 467-471 and 477-478, Wiley, 1990.

[15] J.C.M. Lee and D. Luss, "Maximum temperature rise inside catalytic pellets", Ind. Eng. Chem. Fundam., 8 (3), 596-597, 1969.

[16] J.J. Carberry and D. White, "On the role of transport phenomena in catalytic reactor behavior", Ind. Eng. Chem., 61 (7), 27-35, 1969.

[17] J.J. Carberry, "The catalytic effectiveness factor under non-isothermal conditions", AIChE J., 7 (2), 350-351, 1961.

[18] J.A. Moulijn, A. Tarfaoui and F. Kapteijn, Catal. Today, 11, 1-12, 1991.

[19] D.E. Mears, "Diagnostic criteria for heat transport limitations in fixed bed reactors", J. Catal., 20, 127-131, 1971.

[20] S. Kjelstrup, D. Bedeaux, "Jumps in electric potential and in temperature at the electrode surfaces of the solid oxide fuel cell", Physica A, 244, 213-226, 1997.

[21] D. Bedeaux and S. Kjelstrup, "The dissipated energy of electrode surfaces: temperature jumps from coupled transport processes", J. Electrochem. Soc., 143 (3), 767-779, 1996.

[22] E. M. Hansen and S. Kjelstrup. "Application of nonequilibrium thermodynamics to the electrode surfaces of aluminum electrolysis cells", J. Electrochem. Soc., 143 (11), 3440-3447, 1996.

[23] D. Bedeaux and S. Kjelstrup, "Irreversible thermodynamics–a tool to describe phase transitions far from global equilibrium", Chem. Eng. Sci., 59, 109-118, 2004.

[24] I. Chorkendorff, J.W. Niemantsverdriet, "Concepts of Modern Catalysis and Kinetics", WILEY-VCH Verlag Gmbh & Co. KGaA, Weiheim, 2003.

[25] J.A. Moulijn, F. Kapteijn, A.E. van Diepen, M.T. Kreutzer and J.C. Jansen, "Catalysis Engineering", Delft University of Technology, March, 2001.

[26] S.W. Benson, "Thermochemical Kinetics–Methods for the Estimation of Thermochemical Data and Rate Parameters", John Wiley & Sons, pp. 10, 1976.

[27] S. Glasstone, K.J. Laidler and H. Eyring, "The theory of rate processes: the kinetics of chemical reactions, viscosity, diffusion and electrochemical phenomena", New York, McGraw-Hill, 1941.

[28] D. Bedeaux, A.M. Albano and P.Mazur, "Boundary conditions and nonequilibrium thermodynamics", Physica A, 82 (3), 438-462, 1975.

[29] D. Bedeaux, "Nonequilibrium thermodynamics and statistical physics of surface", Adv. Chem. Phys. 64, 47-109, 1986.

[30] A.M. Albano and D. Bedeaux, "Nonequilibrium electro-thermodynamics of polarizable multicomponent fluids with an interface", Physica A, 147 (1-2), 407-435, 1987.

[31] R. Taylor and R. Krishna, "Multicomponent Mass Transfer", Wiley, New York, 1993.

[32] H. Kubota, Y. Yamanaka and I.G. Dalla Lana, "Effective Diffusivity of multicomponent gaseous reaction system", J. Chem. Eng. Jpn., 2, 71-75, 1969.

[33] S. Kjelstrup and D. Bedeaux, "Elements of Irreversible Thermodynamics for Engineers", Int. Centre of Applied Thermodynamics, Instanbul, Turkey, 2001.

[34] J.W. Gibbs, "The Scientific Papers of J.W. Gibbs, Vol. one: Thermodynamics", Dover, London, unabridged republication of 1st (1906) edition, 1961.

[35] A. Røsjorde, D.W. Fossmo, S. Kjelstrup, D. Bedeaux and B. Hafskjold, "Nonequilibrium molecular simulations of steady state heat and mass transport in condensation, I. Local equilibrium", J. Colloid Interf. Sci., 232, 178-185, 2000.

[36] S.R. de Groot and P. Mazur, "Non-Equilibrium Thermodynamics", Dover, London, 1984.

[37] Y.P. Pao, "Temperature and density jumps in kinetic theory of gases and vapors", Phys. Fluids, 14 (7), 1340, 1971.

[38] J.W. Cipolla Jr., H. Lang and S.K. Loyalka, "Kinetic theory of condensation and evaporation, 2.", J. Chem. Phys. 61 (1), 69-77, 1974.

[39] D. Bedeaux, L.F.J. Hermans and T. Ytrehus, " Slow evaporation and condensation", Physica A, 169, 263-280, 1990.

[40] D. Bedeaux, J.A.M. Smit, L.F.J. Hermans and T. Ytrehus, " Slow evaporation and condensation. 2. A dilute mixture", Physica A, 182, 388-418, 1992.

[41] G.D.C. Kuiken, "Thermodynamics of irreversible processes: Applications to diffusion and rheology", Wiley, Chichester, U.K., 1994.

[42] J.A. Maymo and J.M. Smith, "Catalytic oxidation of hydrogen—Intropellet heat and mass transfer", AIChE J., 12 (5), 845-854, 1966.

[43] R.J. Bearman, F.H. Horne, "Comparison of theories of heat of transport and thermal diffusion with experiments on cyclohexane-carbon tetrachloride system", J. Chem. Phys., 42 (6), 2015, 1965.

[44] M. Sugisaki, "Soret coefficients and heat of transport of polyvalent electrolytes in an aqueous solution", Bullet. Chem. Soc. Japan, 48 (10), 2751-2754, 1975.

[45] J. Demichowiczpigoniowa, "Temperature and concentration dependence of soret coefficient for aqueous copper-sulfate solutions. 1. Soret coefficient and heat of transport at 25 degrees", Electrochemica ACTA, 22 (9), 1031-1033, 1977.

[46] R.L. Rowley, F.H. Horne, "Dufour effect. 3. Direct experimental determination of the heat of transport of carbon tetrachloride-cyclohexane liquid mixtures", J. Chem. Phys., 72 (1), 131-139, 1980.

[47] R.L. Rowley, S.C. Yi, V. Gubler, J.M. Stoker, "Mutul diffusivity, thermal conductivity and heat of transport in binary liquid mixtures of alkanes in carbon tetrachloride", Fluid Phase Equilib., 36, 219-233, 1987.

[48] A.R. Allnatt, "Corrected expression for the heat of transport", Mol. Phys., 82 (4), 781-785, 1994.

[49] T. M. Clinton, L.B. David, C. Piergiorgio and F.P. Leon, "Onsager heat of transport measured at the n-heptanol liquid-vapor interface", J. Phys. Chem. B, 108, 2681-2685, 2004.

[50] V.I. Rudakov, V.V. Ovcharov, "Mathematical description of the diffusion in a temperature field and measuring the heat of transport", Intern. J. Heat Mass Transfer, 45, 743-753, 2002.

[51] B.L. Sawford, T.H. Spurling and D.S. Thurley, "The diffusion thermoeffect (Dufour effect) in gaseous mixtures of hydrogen and carbon dioxide", Aust. J. Chem., 23, 1311-1320, 1970.

[52] W. Hort, S.J. Linz and M. Lucke, "Onset of convection in binary gas mixtures: Role of the Dufour effect", Phys. Rev. A, 45 (6), 3737-3748, 1992.

[53] S.J. Linz, "Binary mixtures: Onset of Dufour driven convection", Phys. Rev. A, 40 (12), 7175-7181, 1989.

[54] A. Boushehri and A. Abbaspour, "Diffusion thermoeffect in gases (the Dufour effect), Bullet. Chem. Soc. Japan, 52 (7), 2097-2098, 1979.

[55] R.P. Rastogi and G.L. Madan, "Cross-phenomenological coefficients, Part 6– Dufour effect in gases", Trans. Faraday Soc. 62, 3325-3330, 1966.

[56] S.R. de Groot, thesis, 1945, Amsterdam.

[57] C.C. Tanner, "The Soret effect", Nature, 170 (4314), 34-35, 1952.

[58] C.C. Tanner, "The Soret effect. 2", Trans. Faraday Soc., 49 (6), 611-619, 1953.

[59] H.J.V. Tyrrell and R. Colledge, "Thermal diffusion potential and the Soret effect", Nature, 173 (4397), 264-265, 1954.

[60] J.N. Agar and W.G. Breck, "Thermal diffusion potentials and the Soret effect", Nature, 175 (4450), 298-299, 1955.

[61] O. Lhost and J.K. Platten, "Large-scale convection induced by the Soret effect", Phys. Rev. A, 40 (11), 6415-6420, 1989.

[62] L. Hao and D.G. Leaist, "Large Soret effect for silicotungstic acid in a supporting electrolyte-9-percent change in concentration per degree", J. Phys. Chem. 98 (51), 13741-13744, 1994.

[63] J. Liu and G. Ahlers, "Rayleigh-Benard convection in binary-gas mixtures: Thermophysical properties and the onset of convection", Phys. Rev. E, 55 (6), 6950-6968, 1997.

[64] J.P. Jenkinson and R. Pollard, "Thermal diffusion effects in chemical vapor deposition reactors", J. Electrochem. Soc.: Solid-State Science and Technology", 131 (12), 2911-2917, 1984.

[65] C.L. Leakeas and M.A.R. Sharif, "Effects of thermal diffusion and substrate temperature on silicon deposition in an impinging-jet CVD reactor", Numer. Heat Transfer A, 44 (2), 127-147, 2003.

[66] R. Krishna and J.A. Wesselingh, "Review article number 50—The Maxwell-Stefan approach to mass transfer", Chem. Eng. Sci., 52 (6), 861-911, 1997.

[67] J.O. Hirschfelder, C.F. Curtiss, R.B. Bird, "Molecular theory of gases and liquids", Wiley, 4th edition, 1967, Chapters 7 & 8.

[68] J.A. Wesselingh and R. Krishna, "Mass transfer in multicomponent mixtures", P. 95, Delft University Press, 2000, P.O. Box 98, 2600 MG Delft, The Netherlands.

[69] C.R. Kleijn, "Chemical vapor deposition processes", In M. Meyyappan (Ed.), Computational modeling in semiconductor processing, Chapter 4, p. 97-229, Boston: Artech House, 1995.

[70] Y.S. Touloukian, "Thermophysical properties of matter, Vol. 3, Thermal conductivity, nonmetallic liquids and gases", IFI/Plenum Pres., New York, 1970.

[71] B.K. Hodnett, "Heterogeneous Catalytic Oxidation–Fundamental and Technological Aspects of the Selective and Total Oxidation of Organic Compounds", John Weley & Sons, Ltd.,2000.

[72] F. Kapteijn, J.A. Moulijn, and R.A. van Santen, "Chemical Kinetics of Catalysed Reactions, in Catalysis, An integrated Approach to Homogeneous, Heterogeneous and Industrial Catalysis", 2nd ed. Elsevier, Amsterdam, 1999.

[73] I.M. Kolesnikov, S.I. Kolesnikov, V.A. Vinokurov, I.M. Gubkin, "Kinetics and Catalysis in Homogeneous and Heterogeneous Systems", Nova Science Publishers, Inc., Huntington, New York, 2001.

[74] H. Liu, G.D. Lei, and W.M.H. Sachtler, "Alkane Isomerization over Solid Acid Catalysts Effects of One-dimensional Micropores", Appl. Catal. A: General, 137, 167-177, 1996.

[75] G.D. Lei, B.T. Carvill, and W.M.H. Sachtler, "Single File Diffusion in Mordenite Channels: Neopentane Conversion and H/D Exchange as Catalytic Probes", Appl. Catal. A: General 142, 347-359, 1996.

[76] A. van de Runstraat, J. van Grondelle and R.A. van Santen, "On the Temperature Dependence of the Arrhenius Activation Energy for Hydroisomerization Catalyzed by Pt/Mordenite", J. Catal., 167, 460-463, 1997.

[77] V.C. Belessi, P.N. Trikalitis, A.K. Ladavos, T.V. Bakas, P.J. Pomonis, "Structure and Catalytic Activity of $La_{1-x}FeO_3$ System (x=0.00, 0.05, 0.10, 0.15, 0.20, 0.25, 0.35) for the NO+CO reaction", Appl. Catal. A: General 177, 53-68, 1999.

[78] G.F. Froment and K.B. Bischoff, "Chemical Reactor Analysis and Design, 2nd edition, Wiley, New York, 1991.

[79] W.L. Perry, J.D. Katz, D. Rees, et al., "Kinetics of the Microwave-Heated CO Oxidation Reaction over Alumina-Supported Pd and Pt Catalysts", J. Catal., 171, 431-438, 1997.

[80] K.I. Choi and M.A. Vannice, "CO Oxidation over Pd and Cu Catalysts, III. Reduced Al_2O_3-Supported Pd", J. Catal., 131, 1-21, 1991.

[81] P.J. Berlowitz, C.H.F. Peden and D.W. Goodman, "Kinetics of CO Oxidation on Single-Crystal Pd, Pt, and Ir", J. Phys. Chem., 92, 5213-5221, 1988.

[82] N.W. Cant, P.C. Hicks and B.S. Lennon, "Steady-State Oxidation of Carbon Monoxide over Supported Noble Metals with Particular Reference to Platinum", J. Catal., 54, 372-383, 1978.

[83] W. Wei, G. Mul, F. Kapteijn and J.A. Moulijn, Reactor & Catalysis Engineering, Julianalaan 136, 2628 BL, Delft, Delft University of Technology.

[84] K. Watanabe, H. Uetsuka, H. Ohnuma and K. Kunimori, "The dynamics of CO oxidation on Pt (110) studied by infrared chemiluminescence of the product CO_2: effect of CO coverage", Catal. Lett., 47, 17-20, 1997.

[85] C.B. Mullins, C.T. Rettner, and D.J. Auerbach, "Dynamics of the oxidation of CO on Pt (111) by an atomic oxygen beam", J. Chem. Phys., 95 (11), 8649-8651, 1991.

[86] B.E. Nieuwenhuys, "The surface science approach toward understanding automotive exhaust conversion catalysis at the atomic level", Adv. Catal., 44, 259-328, 2000.

[87] C.E. Wartnaby, A. Stuck, Y.Y. Yeo, and D.A. King, "Calorimetric measurement of catalytic surface reaction heat: CO oxidation on Pt (110)", J. Chem. Phys. 102 (4), 1855-1858, 1995.

[88] D.R. Lide (editor-in-chief), "Handbook of chemistry and physics", 81st edition, CRC Press, 2000-2001.

Summary

Surface Temperature Excess in Heterogeneous Catalysis

In this dissertation we study the surface temperature excess in heterogeneous catalysis. For heterogeneous reactions, such as gas-solid catalytic reactions, the reactions take place at the interfaces between the two phases: the gas and the solid catalyst. Large amount of reaction heats are released at the interface for strong exothermic reactions, which makes it possible that the catalyst surface temperatures are higher than those in the gas phases due to poor thermal conductivities of gases. These are very often the case for transport limited reactions based on the literature and the temperature differences can be a few hundred degrees.

It is often found in kinetic studies that Arrhenius plots are gradually curved when measured catalyst temperatures or gas temperatures are applied. It seems that the activation energy changes gradually with increasing temperature. However, according to Arrhenius, the activation energies should be constant. Therefore, there is a possibility that the real reaction temperature in a 2-D reacting surface differs from the measured catalyst temperature or gas temperature and that the real reaction temperature T^r should be used in the Arrhenius plot.

Using irreversible thermodynamics three distinct temperatures, gas temperature, solid catalyst surface temperature and reaction temperature in a 2-dimensional Gibbs surface, are modelled for two oxidation reactions. They are one transport limited reaction: hydrogen oxidation, and one kinetically controlled reactions: CO oxidation, respectively.

In Chapter 1 a brief introduction to catalysis, especially heterogeneous catalysis and a short literature review on the temperature related studies are given first. Three distinct temperatures, T^g, T^m and T^r may exist in heterogeneous catalysis. Arrhenius equation and transition state theory are described to remind people for further reading. Concept on irreversible thermodynamics, a good potential tool to model the

three temperatures, is introduced.

The theory on irreversible thermodynamics is described in details in Chapter 2. Two sets of reciprocal phenomenological equations which include conductivity coefficients and resistance coefficients, respectively, are presented. An expression of effective conductivity coefficients for mass transfer is given to simplify the equations. Starting from the entropy production the force-flux equations for a reaction surface, which is regarded as a separate thermodynamic system, and for the gas film around a catalyst particle are given. These equations are the basis for the calculations in later chapters.

Heat of transfer and resistance coefficients in the coupled processes are investigated in Chapter 3. Hydrogen oxidation on Pt/Al_2O_3 catalyst is used as the model system. Heat of transfer in the coupling process Q_i^* is expressed either by the ratio of two resistance coefficients or by the ratio of two conductivity coefficients. In terms of these relations the coupling coefficients, l_{qi} and r_{qi}, can be calculated, which is the key to the investigation on coupling processes.

Temperature and concentration dependences of heats of transfer are investigated and discussed. Approximately, linear relations hold between heats of transfer for each of the three gases and the mole fractions of oxygen. Heats of transfer change linearly as well with temperature. Oxygen and water vapour are found to thermally diffuse from the hot catalyst surface to the cold gas phase but hydrogen thermally diffuses to the surface. Using method given by Bedeaux *et al.* the resistance coefficients are calculated, which are used for the calculations in Chapter 4.

In Chapter 4 the catalyst surface temperature T^m is calculated for a transport limited hydrogen oxidation reaction. Two sets of reciprocal flux-force equations are used and the same results are obtained. This shows that there is a sufficient internal consistency of the experimental data which we used. The Dufour effect is found negligible but the Soret effect is significant for the surface temperature prediction. The calculated surface temperature T^m is lowered by 39 K as a result of the negative Soret effect. An interesting phenomenon is observed that the mole fraction of hydrogen near the surface is a little bit higher than that in the gas bulk phase although the hydrogen is consumed by the surface reaction. The reason is that the pure mass transfer rate plus the thermal diffusion rate is higher than the consumption rate by the surface reaction. The effective conductivity coefficients for mass transfer are sufficient to be used to obtain a rather accurate prediction.

From Chapter 5 we focus on kinetically controlled reactions. A brief introduction on kinetic models for heterogeneous catalysis which include the relation between temperature and reaction mechanisms, is given first in Chapter 5. Then we introduce

our new concept: surface temperature excess in the 2-D reacting surface and related heat storage in the 2-D surface shaping the Arrhenius plots. Excess enthalpy is stored in the excited molecules in the 2-D reaction surface, which corresponds to a higher reaction temperature T^r.

In Chapter 6, we calculate the surface reaction temperature excess using experimental data. The idea is that the reaction activation energy is constant and the gradually curved Arrhenius plots are straightened by the temperature excesses. Two kinetically controlled CO oxidation reactions in differential reactors are used as model systems. The real reaction temperatures in 2-D surface are calculated using the Arrhenius equation in which the surface reaction rate functions as a kind of temperature sensor. The surface temperature excesses, $\Delta T = T^r - T^m$, are then calculated. They increase with increasing temperature and reaction rates and the maximum value is 56 K. Of course, such a discrepancy of more than 10 K in the reaction temperature has a big influence on the reaction rate, and therefore, on the apparent activity of the catalyst.

Using irreversible thermodynamics analyses are performed in Chapter 7 in order to understand why there are temperature excesses in the 2-D reaction surfaces. Calculations demonstrate that there are small temperature differences between the gas phase and the catalyst surface, which is consistent with the general opinion. These small temperature differences are the driving forces for the heat fluxes between catalyst particles and gas phases. The coupling between surface reaction rates and heat fluxes in the 2-D surfaces are found responsible for temperature excesses in the 2-D reacting surfaces. The temperature excess can be positive or negative, big or small depending on the reactions and conditions. The reaction temperatures for heterogeneous catalytic reactions should be corrected by the temperature excess $\Delta T = T^r - T^m$.

Following the tradition of this laboratory, theses are written in Chapter 8 to summarize our scientific conclusions on temperature excess in heterogeneous catalysis.

ZHU, Lianjie

Page: 105

Samenvatting

Temperatuur Exces in het Reactievlak by de Heterogene Katalyse

In deze dissertatie wordt het temperatuur exces aan het oppervlak van een actieve heterogene katalysator bestudeerd. Een heterogene reactie, zoals een katalytische gasreactie aan een vast katalysatoroppervlak, verloopt op het grensvlak van de twee fasen, het gas en de vaste stof. Bij sterk exotherme reacties komen dan in het grensvlak grote hoeveelheden reactiewarmte vrij. Daardoor bestaat, alleen al vanwege de slechte warmtegeleiding van de gasfase, de mogelijkheid dat de oppervlaktetemperatuur T van de katalysator hoger ligt dan de temperatuur van het gas.

Bij een door transport gelimiteerde reactie wordt de snelheid bepaald door de overdracht van het grensvlak naar het medium. Dan is de temperatuurgradient die zich instelt de snelheidsbepalende factor. Er kan een temperatuurverschil van honderden graden ontstaan tussen het actieve (hete) katalysatoroppervlak en de (koele) gasatmosfeer waarin de reactanten gedoseerd zijn.

Bij reacties waar de chemische kinetiek de snelheid bepaalt treden soms ook onverwachte temperatuureffecten op. Dikwijls lijkt de Arhenius-plot voor zo'n reactie, die volgens de theorieën van Arrhenius en Eyring een rechte zou opleveren, opwaarts of neerwaarts gekromd te zijn. Dat zou dan betekenen dat de activeringsenergie van de reactie (namelijk de helling van de plot) toeneemt of afneemt met de temperatuur. Of dat er concurrerende mechanismen zijn die samen de effectieve reactiesnelheid bepalen.

In de plaats van dergelijke, breed gegeven, maar moeilijk experimenteel te staven, ad hoc verklaringen opperen wij in dit proefschrift de mogelijkheid, dat de werkelijke reactietemperatuur T^r in het twee-dimensionale reactievlak van een actieve heterogene katalysator kan afwijken van zowel de gemeten oppervlaktetemperatuur T^m van de katalysator zelf als van de ingestelde temperatuur T^g van het medium. In de

Arrhenius-vergelijking moet natuurlijk deze 2D-reactietemperatuur T^r worden ingevuld om de theoretisch verwachte temperatuur-onafhankelijke activeringsenergie van de reactie te krijgen. Eén of andere daarvan verschillende temperatuurwaarde, die ergens in de reactor of de katalysator is gemeten, resulteert in de kromming van de "experimentele" Arrhenius-plot.

De basis voor ons voorstel ligt in de thermodynamica van irreversibele processen. In de beschrijving van een katalytische reactie aan een grensvlak komen de drie verschillende temperaturen T^g, T^m en T^r naar voren. Elk daarvan heeft een eigen functie in het proces.

T^g is de temperatuur van het medium. Deze wordt van buiten af ingesteld, door de reactorcondities, om het proces te beheersen en legt het temperatuurniveau in het proces vast. De geleiding in het medium bepaalt via het temperatuurverschil $T^m - T^g$ de afvoer van reactiewarmte naar de omgeving. Dit wordt een bepalende factor als de reactiesnelheid door het warmtetransport gelimiteerd is.

De temperatuur T^r is de temperatuur die heerst in het tweedimensionale reactieoppervlak waar de omzetting zich afspeelt. Met behulp van de Gibbs conventie kan het reactievlak worden opgevat als een onafhankelijk systeem met eigen thermodynamische eigenschappen. De thermodynamica van de irreversibele processen in dit 2D-reactieoppervlak beschrijft de snelheid van de chemische conversie als één van de processtromen, met de chemische affiniteit als drijvende kracht.

Voorbeelden van door transport en door kinetiek gelimiteerde heterogeen-katalytische vast/gasreacties die in dit proefschrift behandeld worden zijn, respectievelijk, de oxidatie van waterstof en van koolmonoxide aan verschillende typen katalysatoren.

Hoofdstuk 1 heeft een inleidend karakter, met een introductie over heterogene en homogene katalyse en een kort overzicht van literatuur over temperatuureffecten in katalytische processen. Het onderscheid tussen de drie verschillende temperaturen T^r, T^m en T^g wordt toegelicht. In een twee-dimensionaal thermodynamisch systeem blijkt een koppeling mogelijk tussen de warmtestroom en de chemische conversiesnelheid. Daardoor kan de reactietemperatuur T^r afwijken van katalysatortemperatuur T^m.

De temperatuur T^r speelt haar rol in de Arrhenius vergelijking. Uit de verklaring van dit verband tussen temperatuur en reactiesnelheid blijkt waarom een experimenteel bepaalde Arrhenius plot voor een eenduidige heterogene katalytische reactie eigenlijk lineair hoort te wezen.

In Hoofdstuk 2 wordt gedetailleerd ingegaan op de relaties tussen processtromen en hun drijvende krachten, zoals die volgen uit de thermodynamica van irreversibele processen in chemisch actieve grensvlakken. Twee (reciproke) stelsels van fenomenol-

ogische vergelijkingen worden gepresenteerd om geleidings- en weerstandscoefficienten te beschrijven. Bovendien wordt toegelicht hoe het resulterende mathematische model van het totale proces zich laat vereenvoudigen door het introduceren van effectieve geleidingscoefficienten voor het massatransport.

Stroom/kracht ("flux/force") relaties worden stelselmatig opgeschreven voor het reactievlak (dat als een apart thermodynamisch systeem opgevat wordt) en voor de dunne film waarin de uitwisseling van warmte en reactanten tussen medium en katalysator verloopt. Deze relaties vormen de grondslag voor de berekeningen aan experimentele systemen in de volgende hoofdstukken.

Het thema van Hoofdstuk 3 is de koppeling van processtromen. Deze berust op de minimalisering van de totale entropieproductie in een proces. De warmteontwikkeling ("heat of transfer") in de processtromen houdt verband met de verhouding van twee weerstands- of twee geleidingscoefficienten. Uit experimentele gegevens over reactiewarmten kunnen dus de koppelingscoefficienten tussen processtromen worden berekend. Als voorbeeld worden in dit hoofdstuk koppelingscoefficienten van massa- en warmtetransport in de grenslaag bij het katalysatoroppervlak berekend uit literatuurgegevens over de waterstofoxidatie op Pt/Al_2O_3- katalysatoren.

Onderzocht werd hoe in deze reactiecondities de warmteontwikkeling afhangt van de temperatuur en van reactant concentraties. Er was een nagenoeg lineair verband tussen het aandeel van elk der drie reactanten in het warmte-effect en de molfractie van het zuurstofgas in het reactiemengsel. De thermische diffusie van water en van zuurstof in de gasfase is ván het warme katalysatoroppervlak náár het koude gas, terwijl de waterstof in de omgekeerde richting, naar het oppervlak toe, getransporteerd wordt. Met de methode van Bedeaux et al. werden de weerstandcoefficienten voor de gekoppelde massa- en warmtestromen uitgerekend, die bij de berekeningen in het volgende hoofdstuk gebruikt worden.

In Hoofdstuk 4 wordt namelijk de invloed berekend van de koppeling tussen processtromen op de katalysator-temperatuur T^m. Bij de waterstofoxidatie is de reactiesnelheid gelimiteerd door transportprocessen in de gasfase. De koppelingen tussen de afzonderlijke transportstromen, bijvoorbeeld door thermodiffusie van reactanten, worden in de traditionele theorie verwaarloosd. Maar die koppelingen zijn de thermodynamische consequentie van het algemene theorema der minimale entropieproductie.

Beide reciproke verzamelingen van de stroom/kracht-relaties werden gebruikt in de interpretatie van experimentele literatuurgegevens over de reactiesnelheden. Beide gaven, berekend langs de eigen weg, ook overeenkomstige resultaten. Dit duidt op voldoende interne consistentie van de gebruikte data.

Het Dufour-effekt (warmtetransport van de reactantstromen) bleek slechts ver-

waarloosbare invloed te hebben op de temperatuur van het katalysatoroppervlak. Het Soret-effekt daarentegen, (thermodiffusie), bleek van significante invloed op de voorspelde temperatuur T^m, die uiteindelijk de transport-gelimiteerde reactiesnelheden bepaalt. Wanneer de koppeling tussen de separate processtromen door het (negatieve) Soret effekt in de berekeningen meegenomen wordt, valt de berekende katalysatortemperatuur 39 K lager uit.

Het model laat ook nog zien dat de molfractie van waterstof aan het katalysatoroppervlak hoger is dan in de omringende gasatmosfeer. Waterstof wordt als reactant verbruikt door de oxidatiereactie in het oppervlak. Maar nu blijkt dat gewone diffusie en thermodiffusie (als processtroom) samen een groter transport aankunnen dan het netto verbruik door de chemische conversie aan het katalysatoroppervlak bij de lagere temperatuur T^m en de zich daar aan aanpassende molfracties van de reactanten.

Bij een berekening met behulp van de "effectieve geleidingscoefficiënten", die met de reactiesnelheid variëren en eveneens uit de experimentele gegevens zijn af te leiden, werd overigens vrij accuraat dezelfde waarde voor de temperatuur T^m voorspeld als met het complete model van de gekoppelde processtromen.

In het vervolg van de dissertatie, vanaf Hoofdstuk 5, richten we de aandacht op katalytische processen waarbij de snelheid van de chemische conversie zelf gelimiteerd wordt door de kinetiek. Dit hoofdstuk begint met een korte uiteenzetting over de kinetische modellering van heterogene katalytische reacties en hoe de temperatuur het snelheidsbepalende mechanisme van de reactie beïnvloeden kan. Op dit katalysator-model wordt ons nieuwe concept toegepast van een reactievlak waarin de chemische omzetting zich voltrekt. Het reactievlak wordt, in overeenstemming met de Gibbs conventie, opgevat als een tweedimensionaal thermodynamisch systeem. Het heeft dan eigen waarden voor de extensieve thermodynamische (exces)grootheden zoals concentratie of enthalpie en in dit systeem gelden de gebruikelijke relaties tussen thermodynamische grootheden. Omdat het reactievlak geadsorbeerde en thermisch exciteerbare reactantmoleculen bevat moet het ook een bepaalde warmtecapaciteit bezitten. Er is daarmee dus sprake van een eigen temperatuur T^r van de moleculen in het tweedimensionale systeem, die niet gelijk hoeft te zijn aan T^m of T^g. Die temperatuur T^r is nu, per definitie, de temperatuur waarbij zich de katalytische conversie voltrekt. Aangezien het reactievlak tweedimensionaal is, kan een temperatuur-exces $\Delta T (= T^r - T^m)$ in dat vlak in principe aanleiding geven tot koppeling tussen de chemische conversiesnelheid en thermische stromen in het reactievlak die aangedreven worden door het temperatuur-exces. In gewone, drie-dimensionale thermodynamische systemen is deze koppeling verboden vanwege het Curie-Prigogine principe.

In Hoofdstuk 6 wordt onderzocht of er experimentele gegevens zijn, die kunnen

wijzen op zo'n koppeling tussen chemische en thermische processtromen in het reactievlak. Een voorbeeld blijkt de kromming van de Arrhenius-plot die bij sommige reacties experimenteel waargenomen wordt. Ons idee is, dat de Arrhenius-plot, die de invloed van de temperatuur op de reactiesnelheid beschrijft, eigenlijk lineair zou moeten zijn. Bij een gekromde Arrhenius plot zijn de gegevens over de reactiesnelheid gewoon uitgezet tegen verkeerde waarden van de temperatuur bij het proces van de chemische conversie. De geplotte temperatuur had T^r moeten zijn, de temperatuur in het reactievlak, en niet één of andere temperatuurwaarde ergens in het systeem, zoals T^m of T^g.

Met deze aanname – waarin de reactiesnelheid dus gebruikt wordt als een indicator voor de werkelijke temperatuur in het reactievlak - berekenen we voor verschillende reactieomstandigheden het oppervlakte-temperatuurexces $\Delta T = T^r - T^m$ dat nodig is om de Arrhenius-plot recht te trekken. Dit berekende exces blijkt, geheel volgens onze verwachting, toe te nemen met de ingestelde reactortemperatuur - ofwel met de gemeten reactiesnelheid. Bij een door de kinetiek gelimiteerde reactie als de oxidatie van koolmonoxide was het maximale door ons gevonden temperatuur-exces 56 K. Uiteraard is zo'n afwijking van tientallen graden in de reactietemperatuur van grote invloed op de reactiesnelheid, en dus op de schijnbare activiteit van de katalysator.

Analoog met de procedure die we in de vorige gevallen gebruikt hebben voor het berekenen van gekoppelde processtromen in experimentele modelsystemen wordt dan, in Hoofdstuk 7, de koppeling onderzocht tussen de chemische conversiesnelheid en een thermische flux die aangedreven wordt door het temperatuurexces ΔT in het reactievlak. Dit is namelijk de koppeling die alléén in oppervlakken, en niet in volumes toegestaan zou zijn.

Zoals verwacht blijken bij kinetisch gelimiteerde katalytische reacties de verschillen in temperatuur tussen het katalysatoroppervlak en de gasfase zeer klein te zijn. Alle thermische invloeden, zoals een koppeling van processtromen, spelen dus binnen het reactievlak van de actieve katalysator. De koppeling van de katalytische reactiesnelheid met een warmtestroom veroorzaakt verschillen tussen T^r en T^m. Het resulterende temperatuur-exces kan positieve of negatieve waarden aannemen en het kan groot zijn of klein, al naar gelang de bestudeerde reacties of condities.

Hiermee is aangetoond dat bij de interpretatie van activiteit of selectiviteit in heterogene katalytische reacties de mogelijkheid moet worden meegenomen dat de conversiesnelheid gekoppeld is met de thermische effecten in het reactievlak. Dat deze koppeling bestaan kan hebben we afgeleid uit de thermodynamica van irreversibele processen. Chemische reacties verlopen bij de temperatuur T^r in het (tweedimensionale) reactievlak. Ten opzichte van de katalysatortemperatuur T^m moet bij het

construeren van een Arrhenius-plot gecorrigeerd worden met het temperatuurexces $\Delta T = T^r - T^m$, om daardoor een lineair verband te krijgen tussen de logarithme van de reactiesnelheidsconstante en de reciproke temperatuur. Met behulp van deze correctie wordt het effect van de koppeling tussen de conversiesnelheid en de thermische effecten in het reactievlak adequaat beschreven.

Volgens de tradities van ons Laboratorium worden, aan het eind van de dissertatie, in Hoofdstuk 8, de ontwikkelde inzichten gecondenseerd tot een paar gemotiveerde Stellingen ("Theses") over het temperatuur-exces van het 2D-reactievlak in de heterogene katalyse.

ZHU, Lianjie

Acknowledgements

I would like first to thank my promotor, Prof. G. Frens, for bringing me here to start my Ph.D study. Although he is retired now, he put so much effort to help me finish this challenging project and my thesis writing. I learned so much from him, not only science itself, but also the idea, the methodology and the manner as an educator. I admire him on his intelligence, zeal, selflessness, confidence and responsibility. I also very appreciate him for translating the "proposition" and the "summary" into Dutch. Thanks for the illuminating discussions!

I would like to thank my supervisor Dr. G. Koper, who guides me to the field of theoretical research and help me with the calculation software. Many thanks for his always finding time for helpful discussions and all help during last four years.

I will never forget the helps from Prof. D. Bedeaux and Prof. S. Kjelstrup, who introduce and teach me the "irreversible thermodynamics". Prof. Kjelstrup is always so patient and enthusiasm on discussions with me even though my English speaking was so poor when I just started. I am appreciated so much! Thanks Prof. Bedeaux for correcting the Chapter 2 and all helpful discussions! It is a pity that he could not officially be my co-promotor because of the rule from Delft University.

Thanks a lot, Wei Wei and his co-workers for offering me some experimental data in Chapter 6! Professor C.R. Klein is gratefully acknowledged for the programme to calculate the thermal diffusion coefficient. Many thanks are to Dr. X. Xu for a lot of helps in the beginning of my Ph.D study. I would like also to thank Prof. Coppens and Prof. Kapteijn for helpful discussions and advice on my thesis.

Many thanks to my nice colleagues who offer me various kinds of helps, advice or friendship: Nico, Mieke, Pilar, Christophe, Veronica, Antonia, Sander, Steven, Urjan, Stefan, Kourosh, Jouke, Peggy, Wang jia.... I thank all my friends that I do not mention here! Thank you all for making me a wonderful time here.

At last, I thank my dear parent and sisters who give me so much love and support. I am very grateful to my dear husband Bai Zhaomin for his love, encouragement and great support.

Curriculum Vitae

Zhu, Lianjie was born on February 28, 1971 in Beizhen (liaoning province), P.R. China. From 1990 to1994, she was studying in Jilin University (China), Department of Chemistry. She obtained her Bachelor Degree in inorganic chemistry with a thesis title of "Hydrothermal Synthesis and Characterization of $InPO_4$ Zeolite".

During the years of 1994-1998, she worked in the key lab of inorganic synthesis & preparative chemistry of Jilin University, Department of Chemistry.

She started her Master Degree study from 1998 in the same department. In 2001, she obtained her Master Degree in physical chemistry with a thesis "Studies of Photovoltaic Properties and the Dipole Inductivity for Functional Materials".

From 2001 to 2005, she studies in Delft University of Technology (the Netherlands), Department of Chemical Technology for her Ph.D Degree. She managed to carry out the challenging project "Surface temperature excess in heterogeneous catalysis" under the supervision of Prof. G. Frens, Dr. G. Koper and Prof. D. Bedeaux.

Notation

a	external surface area of a catalyst pellet, m^2
A	pre-exponential factor, dimension depending on the reaction order
c_i	molar concentration, mol/m^3
$conv.$	conversion of a reaction, dimensionless
$D_{i,eff}$	Fick's effective diffusion coefficient of the component i, m^2/s
D_i^T	thermal diffusion coefficient of the component i, kg/(m s)
$Đ_{ij}$	Maxwell-Stefan diffusion coefficient, m^2/s
d	diameter of the molecule, m
d_c	diameter of the catalyst pellet, m
E_a	activation energy, kJ/mol
$H_i(h_i)$	(partial) molar enthalpy of the component i, J/mol
h	Planck's constant, J s
J	molar flux, and $J = \Re'/a$, mol/(m^2 s)
J_e	energy flux, J/(m^2 s)
J_i	molar flux of the component i, mol/(m^2 s)
J_i^T	molar flux due to the thermal diffusion for component i, mol/(m^2 s)
J_q'	measurable heat flux, J/(m^2 s)
J_s	entropy flux, J/(m^2 s K)
$\mathbf{k}$	Boltzmann constant, J/K
K	equilibrium constant of a chemical reaction, dimensionless
$K^{\#}$	equilibrium constant for formation of activated complex, dimensionless
$k^{\#}$	rate constant, dimension depending on the reaction order
k	overall reaction rate constant, dimension depending on reaction order
k_f	rate constant of a forward chemical reaction, dimension depends
k_r	rate constant of a reward chemical reaction, dimension depends
k_f'	rate constant of a forward catalytic reaction, dimension depends
k_r'	rate constant of a reward catalytic reaction, dimension depends
l_{ij}	conductivity coefficient for mass transfer, mol^2 K/(J m s)
$l_{i,eff}$	effective conductivity coefficient for mass transfer, mol^2 K/(J m s)

l_{qq}	conductivity coefficient for heat transfer, J K/(m s)
l_{qi}	coupling conductivity coefficient, mol K/(m s)
M	molar mass, kg/mol
N_A	Avogadro constant, 6.02×10^{23} mol^{-1}
N_i^s	total excess number of moles of compoent i, dimensionless
p	total pressure of the gas mixture, Pa
p_i	partial pressure of component i, Pa
Q	heat released by a surface reaction, J/mol
Q_i^*	heat of transfer by component i in coupling processes, J/mol
R	gas constant, J/(mol K)
R_{ij}	resistance coefficient for mass transfer at a constant T, J m^2 s/(mol^2 K)
$\Re$	reaction rate, mol/(m^2 s)
$\Re^{'}$	reation rate, mole/s
$\Re^{''}$	reaction rate, mol/(s g$_{cat.}$)
r$_i$	radius of the molecule i, m
r_{ij}	mass transfer resistance coefficient, J m^2 s/(mol^2 K)
r_{jj}^s	mass transfer resistance coefficient of component j in the 2-D surface, J m^2 s/(mol^2 K)
r_{qi}	coupling resistance coefficient, m^2 s/(mol K)
r_{qq}	heat transfer resistance coefficient in the gas film, m^2 s/(J K)
r_{qq}^s	heat transfer resistance coefficient in the 2-D surface, m^2 s/(J K)
r_{qr}	coupling resistance coefficient between heat transfer and surface reaction rate, m^2 s/(mol K)
r_{jr}	coupling resistance coefficient between mass transfer and surface reaction rate, J m^2 s/(mol^2 K)
r_{rr}	resistance coefficient of the surface reaction, J m^2 s/(mol^2 K)
S^s	total excess entropy, kJ/(mol K)
s^s	excess entropy density, kJ/(mol K m^2)
T	temperature, K
T°	temperature of the reactor, K

Page: 118

T^g	temperature in the bulk of gas phase, K
T^m	measured catalyst temperature, K
T^r	reaction temperature at a 2-D surface, K
T^s	surface temperature, K
U^s	total excess internal energy, kJ/mol
u	excess internal energy density, kJ/(mol m^2)
u_i	velocity of the diffusing component i, m/s
u_i^T	augmented species velocity including the contribution due to the thermal diffusion, m/s
x_i	mole fraction of the component i, dimensionless
x_i^s	mole fraction near the catalyst surface, dimensionless
x_i^g	mole fraction in the bulk of gas phase, dimensionless

Greek letters

λ_i	thermal conductivity of the component i, mW/(m K)
λ_m	thermal conductivity of the gas mixture, mW/(m K)
σ	entropy production rate, Jm^{-2}s^{-1}K^{-1}
ρ_i	density of the component i, kg/m^3
δ	thickness of the gas film, m
δ^s	thickness of the hypothetic surface layer, m
Ω	interface area, m^2
Γ_i	adsorption amount of component i, m^{-2}
ν_j	stochiometric coefficient, dimensionless
μ_i	chemical potential of component i, kJ/mol
μ_i^0	chemical potential of component i at standard state, kJ/mol
$\mu_{i,T}$	chemical potential of component i at constant temperature, kJ/mol
Δ	differences across the gas film or in a 2-D surface
$\Delta G^{\circ\#}$	standard Gibbs free energy of the transition state, kJ/mol
$\Delta_r G$	Gibbs free energy of a reaction, kJ/mol
$\Delta_r H$	reaction enthalpy, kJ/mol
$\Delta H^{\circ\#}$	standard reaction enthalpy of the transition state, kJ/mol
$\Delta S^{\circ\#}$	standard reaction entropy of the transition state, kJ/(mol K)

Superscripts

f	in a gas film

f,e	in the surrounding gas film and an energy flux J_e is used
f,q	in the surrounding gas film and a heat flux J_q' is used
i	into the surface from the phase i (gas phase)
m,s	interface between a metal catalyst and it's support
o	out of the surface to the phase o (phase of the catalyst)
s	surface
s,i	in the surface on the side of phase i
s,o	in the surface on the side of phase o
s,e	in the surface and an energy flux J_e is used
s,q	in the surface and a heat flux J_q' is used

Subscripts

H	hydrogen
O	oxygen
W	water gas
He	helium
i,s	thin surface layer from the boundary of bulk phase i to the surface plane
j	component j
m,s	interface between a metal catalyst and it's support
s,o	thin surface layer from the surface plane to the boundary of bulk phase o
T	at constant temperature T